LOW LYSOSOMAL ACID LIPASE ACTIVITY IN SMOOTH MUSCLE CELLS RELATIVE TO MACROPHAGES PROVIDES NEW INSIGHTS INTO FOAM CELL FORMATION IN ATHEROSCLEROSIS

by

Joshua Andrew Dubland

B.Sc., Simon Fraser University, 2008

M.Sc., University of Toronto, 2010

A THESIS SUBMITTED IN PARTIAL FULFILLMENT OF

THE REQUIREMENTS FOR THE DEGREE OF

DOCTOR OF PHILOSOPHY

in

THE FACULTY OF GRADUATE AND POSTDOCTORAL STUDIES

(Experimental Medicine)

THE UNIVERSITY OF BRITISH COLUMBIA

(Vancouver)

July 2018

The following individuals certify that they have read, and recommend to the Faculty of Graduate and Postdoctoral Studies for acceptance, the dissertation entitled:

LOW LYSOSOMAL ACID LIPASE ACTIVITY IN SMOOTH MUSCLE CELLS RELATIVE TO MACROPHAGES PROVIDES NEW INSIGHTS INTO FOAM CELL FORMATION IN ATHEROSCLEROSIS

submitted by Joshua A. Dubland in partial fulfillment of the requirements for the degree of Doctor of Philosophy

in The Faculty of Graduate and Postdoctoral Studies (Experimental Medicine)

Examining Committee:

Gordon A. Francis, Department of Medicine
Supervisor

Sharon Gorski, Department of Medical Genetics
Supervisory Committee Member

Daniel Holmes, Department of Pathology and Laboratory Medicine
Supervisory Committee Member

Pascal Bernatchez, Department of Anesthesiology, Pharmacology, and Therapeutics
University Examiner

Honglin Luo, Department of Pathology and Laboratory Medicine
University Examiner

Thomas Lagace, Department of Biochemistry, Microbiology, and Immunology
External Examiner (University of Ottawa)

Abstract

Smooth muscle cells (SMCs) are the predominant cell type in the intima of human atherosclerosis-prone arteries and promote initial retention of atherogenic lipoproteins in the deep intima. We previously found that ≥50% of foam cells in intermediate coronary atheromas are of SMC origin and that intimal SMCs have reduced expression of the cholesterol exporter protein ATP-binding cassette transporter A1 (ABCA1). ABCA1 expression is dependent on the flux of cholesterol out of lysosomes, generated via the hydrolysis of lipoprotein-derived cholesteryl esters (CEs) to cholesterol by lysosomal acid lipase (LAL), and subsequent generation of oxysterols such as 27-hydroxycholesterol by CYP27A1 for promotion of gene transcription via the nuclear liver X receptor (LXR). **In the present studies we tested the hypothesis that SMCs have reduced lysosomal function that contributes to foam cell formation.** Chapter 2 investigates and defines the role of lysosomal function in cholesterol metabolism using a mouse LAL KO peritoneal macrophage model. Chapter 3 investigates lysosomal function and cholesterol metabolism differences between human monocyte-derived macrophages (HMMs) and arterial SMCs treated with aggregated LDL (agLDL). Unlike HMMs, lipid loading of SMCs did not significantly increase 27-hydroxycholesterol or ABCA1 levels and did not decrease new cholesterol synthesis. Microscopy revealed sequestration of CEs in lysosomes of SMCs, while HMMs displayed mostly cytosolic CE accumulations. We did not find evidence of a lysosomal functional defect from lipid induced loss of acidity or loss of lysosomal proteolytic function in SMCs. Instead, LAL levels were markedly higher in macrophages compared to SMCs (LAL activity 23.4-times higher in agLDL loaded HMMs compared to SMCs, $p<0.001$). Treatment of SMCs with LAL containing medium decreased lysosomal lipid accumulation, decreased new cholesterol synthesis, and

increased cholesterol efflux. Persistent reduction of ABCA1 response to LAL treatment in SMCs was potentially attributable to low CYP27A1 and LXR expression relative to macrophages. Overall, we find that arterial SMCs have a relative deficiency in LAL and associated defects in downstream sterol regulatory events compared to macrophages. Our results indicate low LAL activity in SMCs as a novel reason for foam cell formation and a potential target to reduce atherosclerosis development and promote regression therapeutically.

Lay Summary

Lysosomes are cellular compartments critical to the breakdown of the cholesterol-containing particles LDL, and are important for both generating cholesterol-overloaded “foam cells” in atherosclerosis, the main cause of heart attacks and strokes, and the removal of excess cellular cholesterol. We previously found that arterial smooth muscle cells (SMCs) have reduced expression of the key cell exporter of cholesterol, ATP-binding cassette transporter A1 (ABCA1). Gene expression of ABCA1 is dependent on the flux of cholesterol out of lysosomes. Here we tested the theory that SMCs have a defect in lysosomal function resulting in cholesterol overload. We find a deficiency in lysosomal acid lipase, the key enzyme lysosomes use to break down fats, and also further defects in SMC cholesterol metabolism. These discoveries are a breakthrough in understanding how arterial SMCs accumulate excess cholesterol, and identify a potential new target to reduce heart attacks and strokes, the leading cause of death worldwide.

Preface

Chapter 1: Introduction

Section 1.2 contains a previously published review article written by Joshua Dubland and Gordon Francis. Joshua Dubland performed the literature review, drafted and assisted with editing the article, and generated all figures.

Dubland JA, and Francis GA. Lysosomal acid lipase: at the crossroads of normal and atherogenic cholesterol metabolism. *Frontiers in cell and developmental biology.* 2015; 3(3).

Section 1.3 contains a previously published review article written by Joshua Dubland and Gordon Francis. Joshua Dubland performed the literature review, drafted and assisted with editing the article, and generated all figures.

Dubland JA, and Francis GA. So Much Cholesterol: the unrecognized importance of smooth muscle cells in atherosclerotic foam cell formation. *Current opinion in lipidology.* 2016; 27(2): 155-61.

Chapter 2: Recombinant LAL treatment rescues cellular cholesterol metabolism pathways in LAL knockout macrophages

Data and accompanying text in Chapter 2 are derived from portions of a published research article from the laboratory of Gordon Francis that Joshua Dubland is a co-first author on, with exception to ***Figure 2.1 & Figure 2.7*** *and associated text, which were not published but are the sole work of Joshua Dubland. The original publication manuscript was drafted by Kristin Bowden under the supervision of Gordon Francis. Joshua Dubland performed extensive experiments for the revision, wrote sections of text, edited text, performed data and statistical analysis, and generated and edited figures for the publication. Approximately 80% of all aspects of the work presented here was performed by Joshua Dubland. Experimental design, acquisition, initial figure presentation, and initial data analysis/statistical analysis for* ***Figure 2.2 & Figure***

2.3 *were performed by Kristin Bowden, with portions of each experiment (~30%) repeated by Joshua Dubland, who also performed the final statistical analysis and final figure editing. Experimental design, acquisition, data analysis, statistical analysis, and figure generation for* ***Figure 2.4***, ***Figure 2.5***, *and* ***Figure 2.6*** *was 95% the work of Joshua Dubland with technical assistance on* ***Figure 2.6 B*** *from Teddy Chan. Joshua Dubland also adapted and developed the LC/MS/MS assay for 27-hydroxycholesterol analysis shown in* ***Figure 2.6 A*** *and used in Chapter 3.* ***Figure 2.8*** *was designed by Joshua Dubland and Gordon Francis with graphical creation by Josephine Francis. In vivo experiments described in the discussion section in association with* ***Figure 2.8*** *were conducted by Kristin Bowden.*

Bowden KL*, **Dubland JA***, Chan T, Xu Y-H, Grabowski GA, Du H, and Francis GA. LAL (Lysosomal Acid Lipase) Promotes Reverse Cholesterol Transport In Vitro and In Vivo. *Arteriosclerosis, thrombosis, and vascular biology.* 2018; 38(5): 1191-201.
***Equal contribution**

Animal work in the publication was performed under approval by the UBC Animal Care Committee (Certificate #A12-0067).

Chapter 3: Arterial SMCs express low levels of LAL relative to macrophages leading to deficiencies in cholesterol metabolism pathways

Experimental design, data acquisition, results analysis, text, and figure presentation in Chapter 3 are derived from Joshua Dubland's main project work. Approximately 95% of all the work presented here was done by Joshua Dubland. Joshua Dubland also adapted and developed the LC/MS/MS assay for cholesterol and cholesteryl ester analysis.

Additional notes:

Figure 3.9 *was primarily the work of Kamel Boukais. Joshua Dubland adapted and developed the lysosomal acid lipase assay used for analysis of mouse macrophages and SMCs in* ***Figure 3.9*** *and assisted with running the samples and data analysis/statistical analysis for these experiments (~30%). Joshua Dubland performed the final data analysis/statistical analysis on the mouse macrophage and SMC LIPA mRNA in Figure 3.9 and generated the final figure (30%). Teddy Chan provided technical assistance for data acquisition in* ***Figure 3.2*** *and* ***Figure 3.10*** *(~10%). Teddy Chan also designed the primers for RNA analysis in* ***Figure 3.2***, ***Figure 3.3***, ***Figure 3.8***, *and* ***Figure 3.9***. *RNA for primary SMCs in* ***Figure 3.12*** *was obtained from the laboratory of a collaborator Jean-Baptiste Michel located at the French Institute of Health and Medical Research,* Paris *Inserm. Human macrophage and SMC cell line RNA experiments in* ***Figure 3.12***, ***Figure 3.13***, *and* ***Figure 3.14*** *were conducted by Joshua Dubland (95%) with data analysis and figure generation 95% by Joshua Dubland.*

Approval for use of human tissues was by UBC-PHC Research Ethics Board (#H09-00442).

Table of Contents

Abstract ..... **iii**

Lay Summary ..... **v**

Preface ..... **vi**

Table of Contents ..... **ix**

List of Tables ..... **xiv**

List of Figures ..... **xv**

List of Abbreviations ..... **xvii**

Acknowledgements ..... **xx**

Dedication ..... **xxi**

Chapter 1: Introduction **1**

1.1 Overview 1

1.2 The role of lysosomal acid lipase (LAL) in normal and atherogenic cholesterol metabolism 4

1.2.1 Lysosomal acid lipase (LAL) 5

1.2.1.1 Gene expression and mutation 5

1.2.1.2 Transcriptional regulation 5

1.2.1.3 Regulatory role of lysosomally-derived cholesterol 8

1.2.2 Lipoprotein uptake and lipid accumulation 9

1.2.3 Overaccumulation of cholesterol in lysosomes 11

1.2.3.1 Extracellular modification of low-density lipoprotein (LDL) by LAL 11

1.2.3.2 Oxidative modification of LDL 12

1.2.3.3 Aggregation of LDL 13

1.2.4 Effects of excess modified LDL uptake on lysosomal hydrolytic function 14

1.2.5 Lysosomal cholesterol accumulation in atherosclerosis 18

1.2.6 Indications of a lysosomal cholesterol trafficking defect 20

1.2.7 LAL augmentation in atherosclerosis 21

1.2.8 Conclusion 22

1.3 Importance of SMCs in atherosclerotic foam cell formation 24

1.3.1 Appearance of intimal SMCs early in life 25

1.3.2 Diffuse intimal thickening promotes plaque formation in atherosclerosis 26

1.3.3 Phenotypic modulation of SMCs 27

1.3.4 SMC foam cell formation 29

1.3.5 Cholesterol efflux from SMC foam cells 31

1.3.6 Conclusion 33

1.4 Rational, hypothesis and specific aims 34

Chapter 2: Recombinant LAL treatment rescues cellular cholesterol metabolism pathways in LAL knockout macrophages 36

2.1 Summary 36

2.2 Introduction 36

2.3 Materials and methods 38

2.3.1 Materials 38

2.3.2 Preparation of ^{3}H-cholesteryl-oleate labeled acetylated LDL and isolation of apolipoprotein A-1 from plasma 39

2.3.3 Cell culture 39

2.3.4 Lysosomal acid lipase enzyme activity assay 39

2.3.5 Western blot 40

2.3.6 mRNA analysis 40

2.3.7 Cholesterol efflux assay 41

2.3.8 ApoE ELISA 41

2.3.9 Measurement of 27-hydroxycholesterol production 42

2.3.10 Mevalonolactone incorporation assay 42

2.3.11 ACAT activity assay 43

2.3.12 Statistical analysis 43

2.4 Results 44

2.4.1 ABCA1 expression and cholesterol efflux are impaired in macrophages lacking LAL and corrected by addition of exogenous LAL. 44

2.4.2 Dysregulation of post-lysosomal cholesterol metabolism in lal$^{-/-}$ macrophages and correction by exogenous LAL. 51

2.5 Discussion 55

2.6 Conclusion 59

Chapter 3: Arterial SMCs express low levels of LAL relative to macrophages leading to defects in cholesterol metabolism pathways 61

3.1 Summary 61

3.2 Introduction 62

3.3 Materials and methods 64

3.3.1 Materials 64

3.3.2 Isolation, radiolabeling, and modification of LDL 66

3.3.3 Cell culture of human SMCs and mouse SMCs 67

3.3.4 Isolation and differentiation of human monocytes 67

3.3.5 Lipid loading of macrophages and SMCs 67

3.3.6 LC/MS/MS analysis of total cholesterol, free cholesterol, and cholesteryl esters 68

3.3.7 LC/MS/MS analysis of 27-hydroxycholesterol production 70

3.3.8 Mevalonolactone incorporation assay 72

3.3.9 ACAT activity 72

3.3.10 Reverse transcription-PCR analysis of ABCA1, ABCG1, and LIPA mRNA 73

3.3.11 High throughput RNA analysis 74

3.3.12 Western blot analysis of ABCA1 and LAL protein 75

3.3.13 Lysosensor Yellow/Blue DND-160 Assay 76

3.3.14 DQ-bovine serum albumin assay 76

3.3.15 Lysosomal acid lipase enzyme activity assay 77

3.3.16 LAMP1 and BODIPY fluorescent cellular staining 78

3.3.17 Lysotracker red and BODIPY fluorescent cellular staining 79

3.3.18 Lysotracker red and filipin fluorescent cellular staining 79

3.3.19 LAMP1 and filipin fluorescent cellular staining 80

3.3.20 LAL and CD45 fluorescent staining of human coronary artery sections 80

3.3.21 Microscopy 81

3.3.22 Statistical analysis 82

3.4 Results 82

3.4.1 Defective SMC ABCA1 expression is associated with impaired cellular cholesterol metabolism 82

3.4.2 SMCs tend to sequester lipoprotein derived CE in lysosomes 88

3.4.3 SMCs do not display an affinity for losing lysosomal acidity from excess lipid loading 91

3.4.4 Lysosomal CE accumulation in SMCs is a result of low LAL expression 94

3.4.5 SMC uptake of LAL leads to rescue of lysosomal CE accumulation 99

3.4.6 SMCs display differences compared to macrophages in cholesterol metabolism gene expression 104

3.5 Discussion 110

Chapter 4: Concluding remarks 117

4.1 Summary and conclusions 117

4.2 Future directions 120

References 122

List of Tables

Table 3.1 NanoString Custom Codeset for RNA analysis...... 75

List of Figures

Figure 1.1 Cholesterol metabolism in atherosclerotic lesion foam cells. 10

Figure 1.2 Human monocyte derived macrophage foam cells. 14

Figure 1.3 Loss of lysosomal function with excess lipid loading. 19

Figure 1.4 The major role of smooth muscle cells in diffuse intimal thickening and atherosclerotic foam cell formation. 26

Figure 2.1 LAL activity in lal+/+ and lal-/- mouse peritoneal macrophages 44

Figure 2.2 ABCA1 mRNA and protein are reduced in $lal^{-/-}$ mouse peritoneal macrophages and partially rescued by rhLAL. 46

Figure 2.3 Rescue of impaired apoA-I-dependent cholesterol efflux in $lal^{-/-}$ macrophages by treatment with rhLAL. 48

Figure 2.4 Inhibition of $lal^{+/+}$ macrophage lysosomal function with chloroquine recapitulates cholesterol distribution of $lal^{-/-}$ macrophages. 49

Figure 2.5 ApoE is secreted into medium by $lal^{+/+}$ and $lal^{-/-}$ macrophages 50

Figure 2.6 Impaired regulation of oxysterol production and cholesterol synthesis in $lal^{-/-}$ macrophages and correction with rhLAL. 52

Figure 2.7 Impaired cholesterol esterification in lal-/- macrophages and correction with rhLAL. 54

Figure 2.8 LAL promotes reverse cholesterol transport 58

Figure 3.1 Excess lipid accumulation in HMMs and SMCs with agLDL treatment. 83

Figure 3.2 SMCs display absence of ABCA1 response and defects in sterol regulatory events downstream of lysosomal processing. 85

Figure 3.3 SMCs display absence of ABCG1 response to lipid loading. 86

Figure 3.4 Neutral lipid staining patterns are cytosolic in HMMs and lysosomal in SMCs with agLDL loading. 89
Figure 3.5 Neutral lipid staining patterns are significantly more localized to lysosomes in mouse SMCs compared to mouse macrophages. 90
Figure 3.6 SMCs do not display a functional defect in control of lysosomal acidity with excess agLDL loading. 92
Figure 3.7 Macrophages have elevated lysosomal FC accumulation relative to SMCs. 93
Figure 3.8 LAL expression is reduced in SMCs compared to macrophages. 96
Figure 3.9 LAL expression is reduced in mouse SMCs compared to mouse macrophages. 97
Figure 3.10 Treatment with LAL is able to reduce lysosomal lipid accumulation and increase cholesterol efflux in SMCs. 101
Figure 3.11 HMM conditioned medium and 27-OHC treatment does not up regulate ABCA1. 103
Figure 3.12 Primary intimal and medial SMCs display similar reduced response to agLDL treatment in comparison to HMMs in gene expression changes associated with lysosomal cholesterol processing, cholesterol synthesis & uptake, and cholesterol removal. 105
Figure 3.13 Primary intimal and medial SMCs display markedly reduced expression of several lysosomal and post-lysosomal genes important for ABCA1 regulation in comparison to macrophages. 108
Figure 3.14 Effect of 3 day chronic LAL treatment on SMCs cholesterol metabolism genes. .. 109

List of Abbreviations

ABCA1	ATP-binding cassette transporter A1
ABCG1	ATP-binding cassette transporter A1
ACAT	acyl-coenzyme A:cholesterol acyltransferase
agLDL	aggregated low density lipoprotein
apoA1	apolipoprotein A1
apoB	apolipoprotein B
apoE	apolipoprotein E
ATP	adenosine triphosphate
CE	cholesteryl esters
CESD	cholesteryl ester storage disorder
CYP27A1	sterol 27-hydroxylase
CYP51A1	lanosterol 14-α demethylase
DHCR7	7-dehydrocholesterol reductase
DHCR24	24-dehydrocholesterol reductase
ER	endoplasmic reticulum
FAFA	fatty acid free albumin
FC	free cholesterol
HDL	high density lipoprotein
HPLC	high performance liquid chromatography
HMGCR	3-hydroxy-3-methylglutaryl-coenzyme A reductase
HMM	human monocyte derived macrophage

LAL	lysosomal acid lipase
LAMP1	lysosomal-associated membrane protein 1
LDL	low density lipoprotein
LDL-R	low density lipoprotein receptor
LPDS	lipoprotein deficient serum
LRP1	LDL receptor-related protein-1
LSC	liquid scintillation counting
LXRα	liver X receptor alpha
nCEH	neutral cholesteryl ester hydrolase
MVK	mevalonate kinase
NPC	Niemann Pick type C
OCT	optimal cutting temperature
oxLDL	oxidized low density lipoprotein
PBMC	peripheral blood monocyte
PDGF	platelet-derived growth factor
RCT	reverse cholesterol transport
rhLAL	recombinant human lysosomal acid lipase
SMC	smooth muscle cell
STARD3	StAR-related lipid transfer domain protein 3
TC	total cholesterol
TLC	thin layer chromatography
TFEB	transcription factor EB
UC	unesterified cholesterol

v-ATPase	vacuolar H^+-ATPase
VLDL	very low density lipoprotein

Acknowledgements

First, I would like to sincerely thank Dr. Gordon Francis for taking me on as PhD student in his research group, for his advice and encouragement during my studies, and the freedom to pursue my own ideas in the research laboratory.

I would next like to thank my supervisory committee (Drs. David Granville, Daniel Holmes, and Sharon Gorski) for their insightful suggestions and advice for both my project and research in general.

To all past and present members of the Francis Laboratory I express appreciation and gratitude. Teddy Chan, Dr. Sima Allahverdian, Dr. Ying Wang, Collin Pryma, Dr. Kamel Boukais, and Dr. Kristin Bowden, it has been a pleasure working and learning together with you in the laboratory.

Lastly I would like to thank all the faculty, staff, and students at the Centre for Heart Lung Innovation (HLI) at St. Paul's Hospital. Many different people provided helpful input and assistance during various stages of this work.

Dedication

I would like to dedicate this thesis to my wife Stephanie for her unwavering support during my PhD, also to my daughter Georgia, and my son Benjamin. I would also like to thank my parents Edward and Pennie and my sister Elysia for all their encouragement and support during my studies.

Chapter 1: Introduction

1.1 Overview

Cardiovascular disease (CVD) remains the leading cause of mortality globally, primarily from heart attacks strokes (1). A combination of population aging and growth worldwide has resulted in an increase (~41%) in cardiovascular mortality despite a decrease (~39%) in the age specific death rate between 1990 and 2013 as indicated in a recent study by Roth, *et al*. (2). In 2013 CVD deaths accounted for ~31% of mortality worldwide (3) with approximately 70% of CVD deaths occurring in low- and middle-income (LMIC) countries (4, 5). The global economic burden of CVD is predicted to rise from USD $863 billion in 2010 to USD $1,044 billion by 2030 (6). By 2030 the American Heart Association has projected that ~43.9% of the US population alone will have some form of CVD with ~60.5% of total direct medical expenditures from CVD being a result of hospital costs (5). The worldwide burden of cardiovascular disease remains very high and as such, development of new therapeutic and preventive strategies will be required to meet the growing needs of the global community.

The principal driving force behind heart attacks and strokes is the development of atherosclerosis caused by accumulation of cholesterol in susceptible arteries such as the coronary, aortic, carotid and femoral arteries. Although generally thought of as a modern day disease, atherosclerosis was also present in ancient cultures as determined by computed tomography analysis of mummies (7, 8). It is only within the last century though that the fundamental role of cholesterol in the development of atherosclerosis has been determined. The composition of arterial atheromas, cholesterol rich and containing calcified connective tissue, was described in 1910 by the German chemist Adolf Windaus (9, 10) followed by the first experimental description by Nikolai Nikolaevich Anichkov in 1913 using a cholesterol-fed rabbit

model to induce atherosclerosis (11). The finding by Anichkov about the role of cholesterol in the development of atherosclerosis is considered to be one of the greatest discoveries in medicine of the 20th century (12, 13). A less recognized fact about Anichkov is that he is also considered to be the first person to describe the presence of lipid overloaded cells in atherosclerosis called "cholesterinesterphagozyten" or today known as "foam cells" (14). By investigation of plaque progression and histology Anichkov also identified the presence of smooth muscle cells (SMCs), macrophages, and lymphocytes in atheromas (14). Although SMCs have been reported to be the main cell type present in the human atherosclerotic intima (~90%) (15, 16), the majority of literature reports have focused on the role of macrophages in cholesterol accumulation and removal during atherosclerosis. Early reports, however indicated that lipid-overloaded SMCs are present, making up a significant portion of the foam cell population found in atherosclerosis (17-22). Building on these initial indications, our laboratory has found that intimal SMCs have reduced expression of the key cholesterol exporter protein ATP-binding cassette transporter A1 (ABCA1) compared to medial SMCs (23), a finding suggesting that SMCs would make up a large portion of the foam cells found in atherosclerosis. Subsequently our laboratory made the original observation that SMCs make up >50% of the foam cells found in intermediate human coronary atheromas and additionally reported that SMCs relative to macrophages have reduced expression of ABCA1 in advanced atherosclerotic lesions (24). As processing of cholesterol taken up by cells has a critical role in the regulation of ABCA1 expression (25-27), this finding suggested the presence of key cholesterol metabolism differences between SMCs and macrophages. Although much has been reported in the literature about cholesterol metabolism in macrophages, relatively little is known about SMCs. A more comprehensive understanding of

the pathogenesis of atherosclerosis in all relevant cell types is critical for developing new therapeutic strategies for reducing the global burden of cardiovascular disease.

Foam cell formation is primarily driven by cellular uptake of low density lipoprotein (LDL), the "bad cholesterol" and its modified forms (described in detail later in this Chapter). LDL was initially isolated from serum in 1950 by Oncley, *et al.* (28) and based on percentage of dry mass is composed of the following: 22% β-globulin apolipoprotein B100 (apoB100), 22% phospholipids, 8% cholesterol, 42% cholesteryl esters, and 6% triglycerides (29). The association of elevated blood cholesterol levels with CVD was initially reported by Carl Müller (30) by investigation of patients with familial hypercholesterolemia (FH). The mechanism resulting in very high levels of circulating LDL in FH was determined by Joseph L. Goldstein and Michael S. Brown (1985 Nobel Prize in Physiology or Medicine) with the formal report of the LDL receptor in 1974 (31) stemming from experiments with skin fibroblasts isolated from patients with homozygous FH (32). Following endocytosis of LDL via the LDL receptor the first critical LDL processing event occurs in the lysosome with hydrolysis of cholesteryl esters to free cholesterol through the actions of lysosomal acid lipase (LAL) (33, 34). Previous studies in our laboratory using fibroblasts isolated from patients deficient in LAL, known as Cholesteryl Ester Storage Disease (CESD), showed that failure of lysosomes to process and release LDL-derived cholesterol has significant detrimental effects on both upregulation of ABCA1 and cellular cholesterol removal (25). Building on our previous *in vivo* observation that ABCA1 expression is reduced in SMCs relative to macrophages found in atherosclerosis (24) and our prior report showing that ABCA1 expression is acutely dependent on lysosomal flux of cholesterol generated through the actions of LAL (25), we now investigate the role of LAL and reduced lysosomal function in SMC foam cell formation.

Section 1.2 in this Chapter provides detailed background information on LAL and reduced lysosomal function. Section 1.3 describes SMC foam cell formation.

1.2 The role of lysosomal acid lipase (LAL) in normal and atherogenic cholesterol metabolism

Atherosclerosis is characterized biochemically by the accumulation of excess cholesterol in the artery wall. This process is initiated by migration of low density lipoproteins (LDL) and other apolipoprotein B (apoB)-containing lipoproteins across an injured artery endothelium, where they are retained through a charge-charge interaction with matrix proteoglycans in the subendothelial space (35). Within this space the trapped lipoproteins are subject to modification including oxidation and aggregation, converting them to ligands for scavenger receptors on intimal macrophages and SMCs. Excessive scavenger receptor-mediated uptake of modified lipoproteins leads to accumulation of cytosolic cholesteryl ester (CE) droplets in these cells, giving them a “foamy” appearance microscopically, hence their name foam cells. There is also evidence that at later stages of atherosclerosis, both free cholesterol (FC) and CE droplets accumulate within the lysosome itself (36). LAL plays the central role in hydrolyzing lipoprotein CE to generate FC, which after leaving the lysosome can be re-esterified in the endoplasmic reticulum to form cytosolic lipid droplets. If excess FC is retained in the lysosome it can inhibit lysosomal activity including that of LAL. Therefore, in addition to the relative expression level of LAL in cells found in atherosclerotic lesions, the physiologic role of LAL may lead to eventual inhibition of LAL activity in the presence of excess atherogenic lipoprotein uptake, contributing further to the progression of atherosclerosis.

1.2.1 Lysosomal acid lipase (LAL)

1.2.1.1 Gene expression and mutation

LAL is the enzyme with primary responsibility for hydrolysis of CE and triglycerides in lipoproteins taken up by receptor-mediated endocytosis. LAL has been called by several names, including lipase A, acid cholesteryl ester hydrolase, acid cholesterol esterase, and acid cholesteryl esterase. LAL is a 46 kDa glycoprotein whose gene *LIPA* is found on chromosome 10q23.2-23.3 (37). Human LAL cDNA encodes a 372-amino acid mature protein and a 27-amino acid signaling sequence (38). After undergoing co-translational glycosylation in the endoplasmic reticulum and attachment of mannose-6-phosphate residues in the Golgi apparatus, LAL is targeted to pre-lysosomal compartments (39, 40). Mutations of *LIPA* can result in complete deficiency of LAL in patients with Wolman disease, which is fatal in the first year of life without LAL replacement, or near-total and non-fatal deficiency known as Cholesteryl Ester Storage Disease (CESD). The most common mutation seen in CESD patients is a splice junction mutation at exon 8 of *LIPA,* which leads to approximately 3-5% of normally spliced LAL protein and LAL activity (41, 42). In addition to having fatty liver and spleen enlargement, individuals with CESD have elevated LDL-Cholesterol, low HDL-Cholesterol, and develop premature atherosclerosis, indicating the critical role LAL plays in cellular cholesterol and lipoprotein metabolism (43, 44).

1.2.1.2 Transcriptional regulation

Several reports have demonstrated an increase in LAL mRNA and protein in the artery wall during the progression of atherosclerosis. Ries, et al. (45) reported that LAL mRNA is increased as human blood monocytes differentiate to macrophages, and that increases in LAL mRNA resulted in higher amounts of LAL enzyme within differentiated macrophages.

Therefore, macrophages expressing increased levels of LAL may contribute to the increased LAL activity in the atherosclerotic relative to normal artery wall.

LAL has been shown to be regulated by transcription factors involved in the autophagy pathway. The transcription factor forkhead homeobox type protein O1 (FOXO1) is upregulated in response to nutrient restriction (Sandri, 2012), and has been shown to upregulate *LIPA* in adipocytes as part of the autophagy response (46). It has also been reported that the basic helix-loop-helix (bHLH) transcription factor EB (TFEB), described as a master regulator of autophagy and lysosomal biogenesis, targets the *LIPA* gene (47). When cellular nutrient conditions are plentiful TFEB is phosphorylated by mammalian target of Rapamycin complex 1 (mTORC1) and is located in the cytosol on the lysosomal membrane (48). More detailed descriptions of the upstream mechanisms of autophagy through mTORC1 can be found in (49, 50, 51, 52). Under conditions of starvation and lysosomal stress TFEB is dephosphorylated and translocates to the nucleus for upregulation of genes involved in the lysosomal-autophagic pathway (53). Recently it has been reported that overexpression of TFEB led to a 2.5-fold increase in *LIPA* mRNA in mouse peritoneal macrophages (54). Whether such an upregulation occurs in response to more physiologic excursions of TFEB expression is not yet known. Translocation of TFEB to the nucleus and a modest (1.2-fold) upregulation of *LIPA* also occurred after a 12 hour incubation of peritoneal macrophages with oxidized LDL (oxLDL); the TFEB nuclear localization was reduced at 24 hours of oxLDL incubation, however, indicating this response of *LIPA* is likely mild and transient (55). Heltianu et al. (2011) reported no change in *LIPA* expression in SMCs and a 20% reduction in *LIPA* expression in endothelial cells incubated with oxLDL for 24 hrs. Further studies are required to confirm the importance and cell specificity of TFEB-dependent

upregulation of *LIPA* in response to modified forms of LDL and cellular stress induced by excess cell cholesterol.

It has also been demonstrated by Heltianu, et al. (56) that in some cell types *LIPA* expression increases with liver-X-receptor (LXR) and peroxisome proliferator-activated receptor (PPAR) agonists. *LIPA* is not known to contain an LXR or PPAR response element in its promoter region. Bowden, et al. (25) demonstrated in CESD fibroblasts that the LXR agonist TO901317 failed to correct LDL-CE hydrolysis and cholesterol efflux to apolipoprotein A1 (apoA1), indicating the residual expression of LAL in CESD cells was not increased by the LXR agonist. *LIPA* response to LXR and PPARγ agonist may be cell type specific and involve stimulation of the autophagy pathway. LXR is not a known target of TFEB, whereas peroxisome proliferator-activated receptor gamma coactivator 1-alpha (PGC-1α), which interacts with PPARγ, is a transcriptional target of TFEB (47).

Our understanding of the transcriptional regulation of *LIPA* in the artery wall during the progression of atherosclerosis is far from complete. Initially it was hypothesized by de Duve (22) that a deficiency in LAL was the cause of intracellular accumulations of lipids in atherosclerosis. Supporting this hypothesis was the observation of lipid-engorged lysosomes in post-mortem liver tissue samples from Wolman disease patients having complete absence of LAL (57, 58) and premature atherosclerosis seen in the near-total LAL deficiency CESD (59). Several groups subsequently reported that LAL activity was increased in atherosclerotic tissue (60, 61, 62). Haley, et al. (63) indicated a 2-fold increase in LAL activity in lipid-laden lysosomes isolated by density centrifugation from atherosclerotic tissue homogenates. Davis, et al. (64) reported that increased LAL activity in human aortic lesions at various stages of disease correlated with increased macrophage infiltration. These studies do not support the LAL deficiency hypothesis

of atherosclerosis. It is not yet clear whether increased LAL in atherosclerotic tissue is a result of upregulation of LAL within cells or simply a higher number of LAL-expressing cells being present in the lesion.

1.2.1.3 Regulatory role of lysosomally-derived cholesterol

Cholesterol is a component of all cell membranes, and is the precursor for oxysterol, steroid hormone, bile acid, and vitamin D synthesis. FC released by lysosomes from lipoprotein and membrane turnover is an important substrate pool for these metabolites. In addition the lysosomally-derived cholesterol pool has multiple regulatory roles through inhibition of sterol regulatory element binding protein (SREBP) cleavage activating protein (SCAP) in the endoplasmic reticulum, and downregulation of SREBP-dependent new cholesterol synthesis and LDL receptor expression by the cell (65). In this way cholesterol released from lysosomes is a critical regulator of overall cell cholesterol homeostasis. When flux of FC from lysosomes is high, oxysterol levels including 27-hydroxycholesterol are increased and bind to the nuclear receptor liver X receptor (LXR), which activates transcription of several genes involved in the removal of cholesterol from cells and other steps in reverse cholesterol transport (66). One of these genes encodes the ATP-binding cassette transporter A1 (ABCA1), a plasma membrane protein that promotes cholesterol efflux to apoA1, the rate-limiting step in the formation of high density lipoproteins (HDL) (67). The importance of lysosomally-derived cholesterol in, and the inability of increased de novo synthesis of cholesterol (68, 69) to correct, ABCA1 expression has been demonstrated in the lysosomal cholesterol storage disorders Niemann Pick Disease type C (NPC) and CESD (25, 27). In both cases the reduced flux of FC out of lysosomes leads to reduced 27-hydroxycholesterol production and reduced ABCA1 expression, the likely cause of low plasma HDL-Cholesterol in both these disorders (43, 70). Delivery of exogenous oxysterols

to NPC fibroblasts (26) and recombinant human LAL to CESD fibroblasts (25) were both able to correct ABCA1 expression and cholesterol efflux to apoA1. This indicates that the rate of release of FC from the lysosome after both LAL-dependent CE hydrolysis and the action of Niemann Pick type C1 (NPC1) protein in the lysosomal membrane is a critical determinant of cholesterol-dependent gene regulation. As hydrolysis of CE derived from both LDL and modified LDL in the lysosome is also likely to be a key regulator of ABCA1 expression in cells in atherosclerotic lesions, a defect in LAL activity could result in impaired ABCA1-dependent cholesterol efflux from macrophage and SMC foam cells.

1.2.2 Lipoprotein uptake and lipid accumulation

Uptake of LDL through cell surface LDL-receptors is tightly regulated and therefore insufficient to explain intimal foam cell formation (34, 71). Within the artery wall LDL and other apoB-containing particles become oxidized, aggregated, or enzymatically-modified (72, 73, 74, 75, 76) (**Figure 1.1**). These altered forms of LDL are no longer recognized by the LDL receptor but are recognized and taken up by scavenger receptors expressed on macrophages and SMCs, a cellular process that is not feedback regulated and can lead to massive accumulation of cholesterol in these cells (77, 78, 79). Scavenger receptors as well as the LDL receptor utilize the endocytic pathway for delivery of cargo to lysosomes. Lipoprotein cholesterol is primarily in the form of CE, which is hydrolyzed within lysosomes by LAL, the only lysosomal lipase known to perform this function (33, 71, 74, 80, 81, 82). LAL in the lysosome is most catalytically active at pH 3.5-4.5 (63, 83). The FC released from lipoprotein CE is transported out of the lysosome by the concerted actions of the Niemann-Pick Type C2 (NPC2) and NPC1 lysosomal proteins, with one fate of the FC then being re-esterification in the endoplasmic reticulum by acyl-coenzyme A:cholesterol acyltransferase (ACAT) (84). Re-esterification is a protective

mechanism to prevent the toxicity of excess FC in membranes (85), particularly in the endoplasmic reticulum, with the reformed CE then stored in the cytoplasm as benign lipid droplets (77). CE in foam cell cytosolic lipid droplets can be transported back to lysosomes through the autophagic process termed "lipophagy" (86); cholesterol derived from this process appears to form a large part of the substrate pool of ABCA1 for efflux from cells (87).

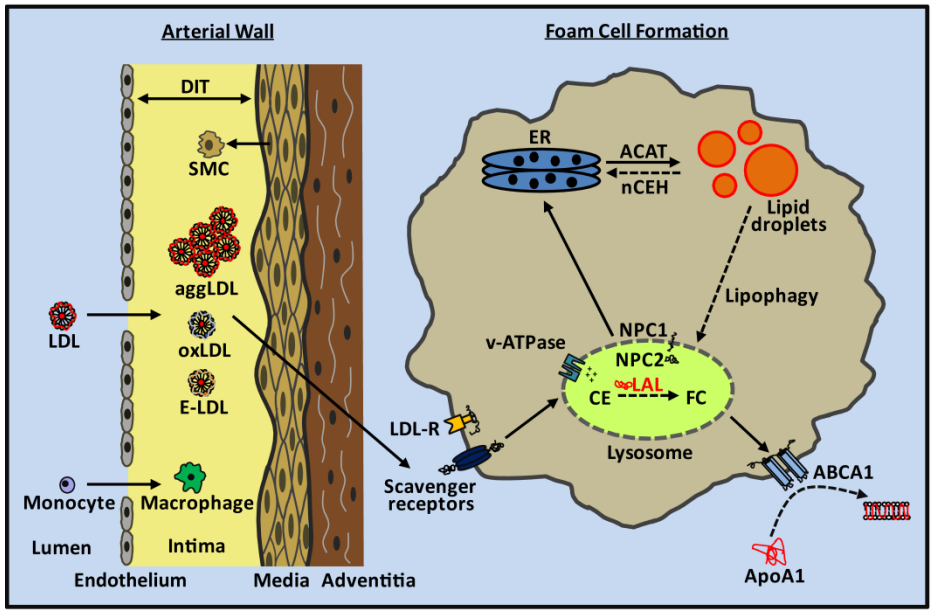

Figure 1.1 Cholesterol metabolism in atherosclerotic lesion foam cells.
LDL and other apoB-containing lipoproteins pass through the damaged endothelium and undergo aggregation, oxidation, and enzymatic modification within the intima of the arterial wall. SMCs from the media migrate to the intima and contribute to diffuse intimal thickening (DIT). Monocytes enter through the damaged endothelium and differentiate into macrophages. SMCs and macrophages take up agLDL, oxLDL, and enzymatically-modified LDL (E-LDL) through scavenger receptors in an unregulated manner, and deliver their cargo to the lysosome through the endocytic pathway. Within the lysosome, lipoprotein cholesteryl esters (CE) are hydrolyzed by LAL to generate free cholesterol (FC). The pH of the lysosome is acidified by the proton pumping action of v-ATPases. FC leaves the lysosome through the concerted action of NPC2 and NPC1 proteins and is transported within the cell including to the endoplasmic reticulum (ER) where it is re-esterified by ACAT and accumulates as lipid droplets within the cytosol. CE in lipid droplets can be hydrolyzed by nCEH and used for cellular functions or removed from the cell along with phospholipids by the actions of ABCA1 to create new HDL particles. CE in lipid droplets can also be transported back to the lysosome through the lipophagy pathway for hydrolysis by LAL and cellular removal of FC via ABCA1. Early atherosclerotic lesion foam cell lipid droplets are primarily cytosolic whereas later stage lesion foam cells contain a mixture of ACAT-derived lipid droplets and lysosomal lipid droplets.

During early stages of atherosclerosis foam cells appear as visible fatty streaks in the intima of the artery wall (88). In addition to the presence of macrophage derived foam cells, SMCs present in the intima beginning in the pre-atherosclerotic diffuse intimal thickening stage also take up modified forms of LDL via scavenger receptors to become smooth muscle derived foam cells (89, 90). It has been previously thought macrophages were the major contributors to foam cells in the intima, however recent studies from our lab suggest SMCs are the source of more than 50 % of the total foam cell population in human coronary artery atherosclerotic lesions (24).

1.2.3 Overaccumulation of cholesterol in lysosomes

Retention of LDL and other apoB-containing lipoproteins in the arterial intima by matrix proteoglycans, as a result of charge-charge interactions (91, 92), means these lipoproteins are susceptible to modification to more atherogenic forms. This modification, either by enzymes, oxidants, or through aggregation converts these lipoproteins to ligands for scavenger receptors and allows for the formation of cholesterol-overloaded foam cells (73, 75). Within the intima LDL has been demonstrated to undergo both extracellular and intracellular modifications (72, 74, 75, 76, 93, 94, 95, 96). LAL and lysosomal enzymes have also been implicated in the modification of LDL, and, conversely, modified forms of LDL have been shown to affect lysosomal function and lead to changes in LAL activity.

1.2.3.1 Extracellular modification of low-density lipoprotein (LDL) by LAL

LAL is present within the extracellular space of atherosclerotic intima (97), and there are indications that LAL may actively participate in the modification of retained LDL. Secretion of lysosomal enzymes by macrophages is known to occur without stimuli, and increase under inflammatory conditions (98). Catalytic activity of LAL would require conditions of at least

localized reduced pH in the extracellular space. Naghavi, et al. (99) reported that pH heterogeneity exists within atherosclerotic lesions with increased acidity in lipid-rich, macrophage-containing areas compared to calcified areas of human and rabbit atherosclerotic plaque. Micro-environments with much lower pH supportive of LAL activity may exist within lesions, as macrophages can acidify their pericellular space through the action of proton pumps (100) and by secreting lactic acid (101). Buton, et al. (102) reported that CE present in matrix-retained aggregated LDL (agLDL) may be hydrolyzed by LAL during extensive cell-surface contact with cultured macrophages. Fluorescence microscopy was utilized to indicate that the matrix-retained agLDL was present on the cell surface during CE hydrolysis; definitive proof that the observed CE hydrolysis is extracellular is still needed. Thus, LAL might be present in a catalytically active form in the pericellular space of macrophages within lesions, which could contribute to extracellular CE hydrolysis and atherogenic modification of apoB containing particles. In support of CE hydrolysis of LDL increasing the atherogenicity of LDL, human macrophages have been shown to take up LDL modified by hydrolysis with neutral cholesteryl ester hydrolase (nCEH) at a rate exceeding that of oxLDL or acLDL (76). Further evidence is required to know whether extracellular hydrolysis of LDL CE by LAL increases uptake of the modified LDL by scavenger receptors.

1.2.3.2 Oxidative modification of LDL

Oxidation of LDL is proposed to contribute to foam cell formation by virtue of oxLDL being a ligand for scavenger receptors. The presence of oxLDL within atherosclerotic lesions has been demonstrated by immunostaining using antibodies generated against oxLDL epitopes (103). Within the artery wall, oxidation of LDL may occur by a number of concurrent mechanisms involving enzymes (e.g. myeloperoxidase, NADPH oxidase, lipoxygenase, and xanthine

oxidase), peroxynitrite-generators, superoxide, low levels of metal ions, and thiols (104, 105, 106), and is thought to occur mainly within the interstitial fluid of atherosclerotic lesions.

The presence of oxidized sterols within human atherosclerotic tissue and lesion LDL has been reported. Steinbrecher and Lougheed (107) found 7-ketocholesterol, 7-hydroxycholesterol, and 5,6-epoxycholesterol in LDL isolated from atherosclerotic but not healthy aortas. Significant accumulations of oxysterols are present in atherosclerotic lesions (108). Quantitative comparison of in vitro studies conducted using oxLDL is difficult due to the variety of methods by which LDL is oxidized and the degree of oxidation induced (81, 109). Oxidative modification of apolipoprotein B by oxidized lipids reduces recognition of LDL by the LDL receptor and increases its affinity for scavenger receptors, making oxLDL a potent promoter of foam cell formation *in vitro* (110). *In vitro* studies show a significant fraction of the sterols present in oxLDL are retained within the lysosome and that oxidized CE are resistant to hydrolysis by LAL (111, 112). Of note, LDL isolated from human atherosclerotic plaques was found to be largely aggregated and only mildly oxidized (107, 113).

1.2.3.3 Aggregation of LDL

Isolated aortic LDL fractions from human lesions are potent inducers of macrophage CE accumulation relative to normal aortic LDL fractions and plasma LDL (114, 115). Steinbrecher and Lougheed (107) demonstrated that this affect was due primarily to agLDL isolated from human atheromas. The presence of agLDL in the extracellular space of human atherosclerotic tissue was also reported using electron microscopy (116). *In vivo*, aggregation of LDL may be a result of a variety of stimuli including oxidation, extracellular matrix interactions, phospholipase A_2 and C, sphingomyelinase, and glycosylation (117, 118, 119, 120, 121, 122, 123, 124). As oxidation is known to cause aggregation of LDL it may be difficult to separate the relative

contributions of oxLDL and agLDL to foam cell (**Figure 1.2**) formation in the atherosclerotic intima.

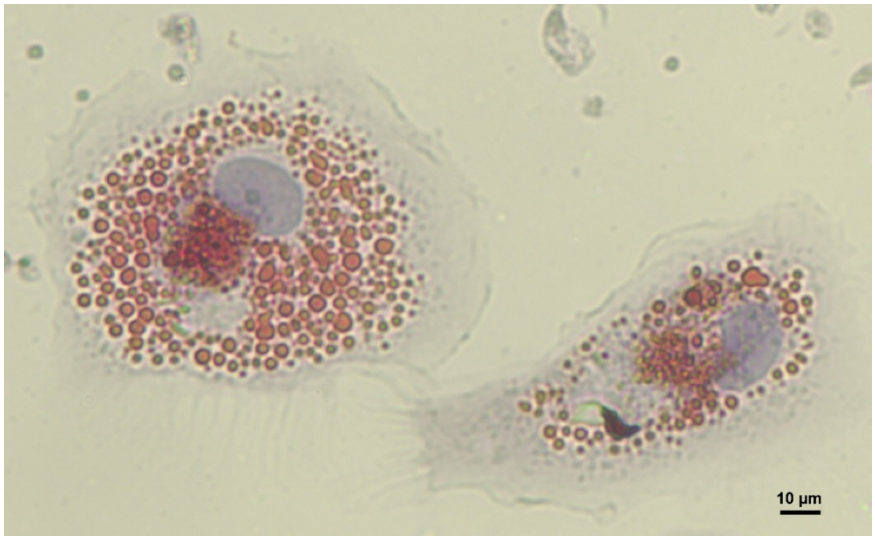

Figure 1.2 Human monocyte derived macrophage foam cells.
Foam cells were generated by incubation of macrophages with 100µg/mL agLDL for 48h. Cells were then fixed and intracellular lipids stained using Oil Red O.

1.2.4 Effects of excess modified LDL uptake on lysosomal hydrolytic function

Previous studies have reported variable effects of different forms of modified LDL on accumulation of cholesterol either in the cytosol alone or also in lysosomes, with oxLDL and agLDL causing accumulation of cholesterol in lysosomes, while enzymatically-modified and acetylated LDL cause mainly cytosolic accumulations (80, 81, 109). Treatment of THP-1 macrophages in culture with mildly oxLDL or agLDL shows similar trends in loss of lysosomal hydrolysis (80, 81). Initially CE hydrolysis is not inhibited but lysosomal sequestration of FC occurs. After prolonged exposure to mildly oxLDL or agLDL (48 hours or more) increasing inhibition of CE hydrolysis occurs and lysosomal accumulation switches to mainly CE (80, 81).

Some variability between species has been observed (80). Yancey and Jerome (111) reported that THP-1 human macrophages and pigeon macrophages store FC and CE derived

from mildly oxLDL within lysosomal compartments, whereas mouse macrophages stored most of the cholesterol in cytosolic lipid droplets. Interestingly, acLDL was efficiently hydrolyzed in macrophages regardless of the species and led to cytosolic lipid droplet accumulation (111). Maor and Aviram (125) reported that the addition of oxysterols isolated from oxLDL to medium when loading J-774 mouse macrophages with acLDL led to significant lysosomal FC accumulations.

Cox, et al. (126) have reported a general loss of lysosomal function including reduction in LAL-dependent CE hydrolysis over time following incubation of THP-1 human macrophages with mildly oxLDL or agLDL. The similar effects using unoxidized agLDL and oxLDL suggest this inhibition of lysosomal function is not specific to the effects of oxidized lipids. Increasing levels of lysosomal membrane FC during lipid loading were shown to inhibit lysosomal acidification (126). It was demonstrated using fluorescence quenching studies that excess FC in the lysosomal membrane leads to loss of acidity as a result of inhibition of vacuolar H^+-ATPase (v-ATPase) proton pumping activity in the lysosomal membrane, without a change in the amount of v-ATPase protein. The resultant increase in pH within the lysosome corresponded with a time-dependent inhibition of CE hydrolysis and accumulation of apoB, indicating a general decline in lysosomal hydrolytic activity. After 7 days of incubation with mildly oxLDL or agLDL, the majority of lysosomal vesicles within THP-1 macrophages had pH >4.8. Vacuolar ATPase activity could be partially recovered if isolated lysosomes were treated with cyclodextrins in order to remove membrane cholesterol. As LAL is only active at acidic pH, with maximal activity ~pH 4 and very little activity above pH 4.5 (63, 127), this loss of v-ATPase activity in response to cholesterol loading of the lysosomal membrane may be the main cause of loss of hydrolytic activity of LAL, and hence lead to lysosomal lipid droplet accumulations.

In contrast to oxLDL and agLDL, incubation of THP-1 macrophages with acLDL, an experimental rather than physiologic form of modified LDL, did not result in an increase in lysosomal membrane FC or an increase in lysosomal pH (126). The reasons for the differential effects of acLDL and oxLDL or agLDL on sequestration of FC in lysosomal membranes following hydrolysis by LAL are unknown. In order to investigate if the observed neutralization of lysosomal pH and inactivation of LAL following oxLDL uptake could be reversed by acLDL, THP-1 macrophages were incubated for 3 days in the presence of oxLDL to accumulate lysosomal CE and then chase incubated with acLDL for an additional 3 days (128). Hydrolysis of CE in the chase acLDL incubation was inhibited and the loss of acidic pH from the initial loading with oxLDL was maintained, indicating lysosomal dysfunction was not readily reversible. Similar results were found in human monocyte derived macrophages. This data indicates that inhibition of LAL activity is the result of a long-lived alteration in lysosomal function under excess lipid loading.

Emanuel, et al. (55) also found a loss of lysosomal acidity occurred in mouse peritoneal macrophages at 72 hrs of oxLDL treatment and in isolated macrophages from atherosclerotic aortic tissue of $ApoE^{-/-}$ mice. This group also reported that overexpression of TFEB in mouse peritoneal macrophages was able to preserve lysosomal acidity, by mechanisms that are not yet clear.

An interesting study by Ullery-Ricewick, et al. (129) demonstrated that in THP-1 human macrophages lysosomal CE accumulations from agLDL could be reduced by 50% by chase incubation with triglyceride (TG)-rich lipid dispersions or VLDL. It was shown that TG treatment reestablished acidic pH by restoring proton pumping by v-ATPases in the lysosomal membrane (129). TGs also increased LAL activity, with no change in LAL expression. The exact

mechanism by which TG-containing particles restore lysosomal function in foam cells remains to be determined; however, it was demonstrated to not be a result of competitive uptake of TG-rich vs. CE-rich particles (129). This is further evidence that inhibition of v-ATPase proton pumping in the lysosomal membrane leads to loss of LAL activity and lysosomal CE accumulations, but may be reversible under some conditions. Further investigation is needed to evaluate the role of TGs in lysosomes of arterial wall foam cells, including the signaling role of TG-derived fatty acids on the LXR and PPAR metabolic pathways.

An alternative or additional reason for the increase in lysosomal pH is that excess membrane FC and oxidized FC can cause lysosomal leakiness, leading to a loss of the proton gradient. Li, et al. (130) reported that incubation of J-744 macrophages with oxLDL resulted in leakage of lysosomal enzymes into the cytosol. Yuan, et al. (131) found that a mixture of cholesterol oxidation products found in oxLDL were also able to induce damage to lysosomes and leakage of lysosomal contents into the cytosol, and eventual macrophage cell death. Although leakiness was not implicated in the studies by Cox, et al. (126) using mildly oxLDL or agLDL, as apoptosis was not observed, it may be a long term contributing factor *in vivo*. The presence of free cholesterol crystals has been reported in J774 macrophage foam cells by Tangirala, et al. (132), and treatment of mouse peritoneal macrophages with free cholesterol was shown to induce lysosomal membrane leakiness by Emanuel, et al. (55). An increase in lysosomal pH has also been shown to increase extracellular excretion of lysosomal enzymes (133), which may contribute to the extracellular LAL observed in atherosclerotic lesions (97). Overall it appears that increases in lysosomal FC induce both defects in lysosome acidification and leakiness of the lysosomal membrane.

Oxidation of apoB-100 has been reported to increase its resistance to degradation by cathepsin D in mouse peritoneal macrophages and its accumulation in lysosomal compartments (134, 135, 136, 137, 138). Decreased apoB-100 protein degradation may also limit LAL mediated hydrolysis of the CE lipid core of oxLDL. Oxidized phospholipids in oxLDL can inhibit cathepsin D, which may explain the reduced ability to degrade apoB (139). Oxidized phosphatidylcholine-apoB complexes have been found in human atherosclerotic lesions and also in lysosomes of cultured mouse macrophages incubated with oxLDL (140). Brown, et al. (112) found that oxidized CE from heavily oxidized LDL loading are resistant to hydrolysis by LAL and accumulate in lysosomal compartments. Therefore, oxidative modifications to apoB containing particles may lead to impaired lysosomal clearance for reasons additional to those induced by non-oxidized agLDL.

1.2.5 Lysosomal cholesterol accumulation in atherosclerosis

In the absence of genetic deficiency in LAL, *in vivo* studies including electron microscopy have indicated that, in addition to storage of CE droplets in the cytoplasm, there are substantial accumulations of FC and CE within the lysosomes of foam cells (141). This phenomenon has been previously reported for both human (142) and animal (19, 20, 21, 143, 144, 145) atherosclerosis. It has been indicated that as atherosclerosis progresses there is initially an increasing amount of FC retained in lysosomes, and at later disease stages also retention of lysosomal CE (36). A possible conclusion that can be drawn from this is that there is a general loss of lysosomal function due to cholesterol overload following unregulated cellular uptake of modified forms of LDL within artery wall cells. As LAL hydrolyzes lipoprotein CE, the loss of LAL function due to excess FC within the lysosome contributes to the formation of

foam cells and the altered distribution of lipid stores within these cells. Therefore, atherosclerosis has been proposed as a type of lysosomal storage disorder (21, 142, 143, 144, 146, 147).

As indicated above, the reason for the loss of lysosomal hydrolytic function may not be a result of deficiency in LAL expression as atherosclerosis progresses but rather a decrease in the catalytic activity of LAL as a result of excess lysosomal cholesterol accumulation from modified forms of LDL (**Figure 1.3**). LAL remains catalytically active initially but over time FC in the lysosomal membrane increases and inhibits the proton pumping ability of the v-ATPases. As a result, the pH of the lysosome increases and renders LAL catalytically inactivate. Lysosomal CE accumulation then occurs in addition to cytosolic accumulation in later stage atherosclerotic lesions.

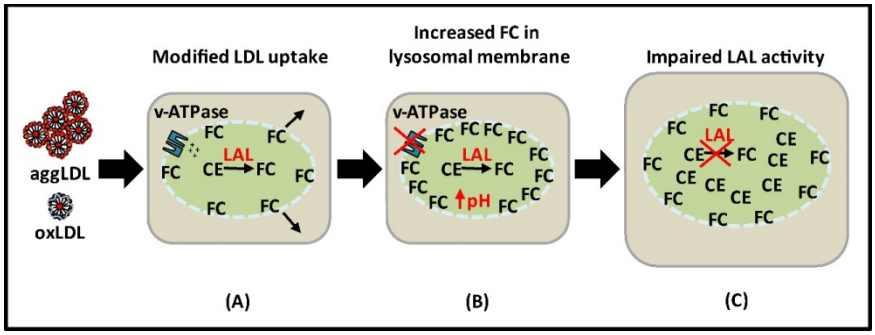

Figure 1.3 Loss of lysosomal function with excess lipid loading.
(**A**) CE from excess modified LDL is hydrolyzed by LAL to produce FC. (**B**) Sequestration of FC in lysosomal membrane leading to increase in pH as a result of inhibition of ATPase proton pumping ability. (**C**) Impairment of LAL activity as a result of increased pH leading to CE accumulation in lysosomes.

Previous studies in atherosclerotic tissue have indicated that LAL activity is increased relative to non-atherosclerotic arteries (60, 61, 62, 63, 64). The analytical procedures for those studies, however, involved *ex vivo* acidic pH adjustment and therefore reflects the total amount of potentially active LAL present, but not what may be actually active *in vivo* within intact cells

under the influence of excess lipids and altered lysosomal pH. As activity is also reflective of protein amount, these studies may indicate that LAL expression increases to deal with the increased cellular influx of apoB containing particles within the artery wall. It can be proposed that LAL activity and protein amount in arterial cells increases with lipid challenge up to a certain point, either from increased LAL expression per cell or an increase in total LAL-expressing cells, after which the lysosome is overwhelmed with lipids and the activity of LAL decreases due to increased pH caused by excess lysosomal membrane cholesterol and leakiness.

1.2.6 Indications of a lysosomal cholesterol trafficking defect

The question then arises what is responsible for the elevation of lysosomal FC in response to the excess lipoprotein load in the intima. As NPC1 and NPC2 facilitate the release of FC from the lysosome, investigation of the expression and activity of these proteins may provide useful insight in this area. Previous studies in fibroblasts have suggested that retention of cholesterol within lysosomal compartments may serve to protect cells from endoplasmic reticulum (ER) stress caused by an excess of FC in the ER membrane. Garver, et al. (148) and Jelinek, et al. (149) found that loading normal human fibroblasts with LDL results in reduced SREBP-dependent expression of NPC1 and NPC2. Jelinek, et al. (150) reported that in a mouse model of diet induced obesity, dietary fatty acids but not cholesterol induced down regulation of NPC1 in both hepatic cells and peritoneal fibroblasts via feedback inhibition of the SREBP pathway. In THP-1 macrophages it has been reported that oxLDL treatment for 3 days leads to a buildup of NPC1 protein in the Golgi apparatus (151). Differential responses to cholesterol-dependent manipulations of NPC1 and NPC2 expression have been indicated in the literature. Rigamonti, et al. (152) demonstrated that expression of NPC1 and NPC2 increased in the presence of LXR agonists in human but not mouse macrophages. It has also been demonstrated

that treatment of human macrophages with oxLDL leads to increases in NPC1 and NPC2 expression via PPARα- and mitogen-activated protein kinase (MAPK)-dependent pathways (153, 154). These results indicate that the expression of NPC1 and NPC2 with lipid overload varies between cell types and species. Further investigation is needed to elucidate the reason for FC overload in the lysosomes of atherosclerotic foam cells.

As the rate of release of FC from the lysosome is a regulator of ABCA1 expression, lysosomal dysfunction in atherosclerosis may also lead to decreased expression of ABCA1 in artery wall cells. Choi, et al. (23) have reported that model human intimal SMCs as well as human coronary artery intimal SMCs express lower levels of ABCA1 than medial SMCs. More recently, Allahverdian, et al. (24) reported that intimal SMCs but not myeloid lineage cells express lower levels of ABCA1 in late vs. early stage human atherosclerotic lesions. Further studies are required to determine whether decreased LAL catalytic activity as a result of lysosomal dysfunction is responsible for this defect in ABCA1 expression, and hence further contributing to the overaccumulation of cholesterol in intimal SMC foam cells.

1.2.7 LAL augmentation in atherosclerosis

Recombinant human LAL (rhLAL) is commercially available for the treatment of LAL deficiency with phase 3 clinical trials conducted for both Wolman disease (155) and CESD (156). This treatment is potentially life-saving in Wolman disease. Phase 2 clinical trials in patients with CESD using rhLAL previously had demonstrated safety and improvements in serum lipid profiles (157, 158). Long-term follow up will be needed in CESD patients to determine outcomes in terms of cardiovascular events. Several studies in mice have indicated that rhLAL may be beneficial in reversing atherosclerosis. Studies by Du, et al. (159) and Sun, et al. (160) demonstrated that injection of rhLAL into $LAL^{-/-}$ mice was able to reverse the

pathogenic storage of lipids in multiple tissues. Du, et al. (161) also showed that administration of repeat doses of rhLAL to LDL-receptor-deficient mice fed a high fat/cholesterol diet resulted in complete regression of early stage lesions in coronary and aortic tissue and a significant reduction in late stage lesions.

Although rhLAL treatment seems to be a viable therapeutic strategy for premature atherosclerosis in CESD patients, it is unclear what the effects would be of rhLAL treatment in patients having atherosclerosis unrelated to a deficiency in LAL. The lysosomal acid lipase A (*LIPA*) gene has been identified as a susceptibility gene for coronary artery disease by several genome-wide association studies (162, 163, 164). For the reasons outlined here, increasing the activity of LAL beyond the normal cellular response may not be an effective strategy. As scavenger receptor mediated uptake of modified forms of LDL in both macrophages and SMCs occurs in atherosclerotic lesions, it is conceivable that rhLAL treatment might increase lysosomal membrane FC in these cells by increasing the rate of lipoprotein CE hydrolysis, and thereby exacerbate lysosomal dysfunction. Reducing the level of atherogenic lipoproteins in plasma and their initial influx into the artery wall, therefore, remains of paramount importance.

1.2.8 Conclusion

The role of LAL in the progression of atherosclerosis is complex. Modified forms of LDL such as oxLDL and agLDL lead to lysosomal accumulations of first FC and later CE, indicating an acquired loss of LAL hydrolytic activity. In agreement with this observation, tissue studies have indicated increased lysosomal lipid accumulations in addition to cytosolic lipid droplets at later stages of atherosclerosis. Activity assays of atherosclerotic tissue homogenates have indicated an increase in LAL and also other lysosomal enzymes. As these studies are conducted *ex vivo* using acidic pH adjustment, they are representative of potentially functional

LAL present *in vivo* but not necessarily actual LAL activity. Therefore, although the amount of artery wall LAL may increase in response to increased cellular influx of apoB-100 containing lipoproteins, the hydrolytic activity of LAL may decrease over time as lysosomal function is impaired. Sequestration of cholesterol in the lysosomal membrane has been implicated as a cause of lysosomal dysfunction, specifically through the inhibition of v-ATPase proton pumping. Increasing lysosomal pH reduces the activity of LAL. The result of this is a time dependent switch of lysosomal accumulation of FC to CE. Early stage atherosclerosis may involve normal and perhaps increased LAL activity leading to cytosolic lipid droplet accumulation, whereas later stages of atherosclerosis may have an acquired dysfunction in LAL hydrolytic activity leading to lysosomal lipid sequestration. Therefore, later stages of atherosclerosis, where LAL function is inhibited, may be considered to be morphologically similar to Wolman disease and CESD, albeit for an entirely different reason.

Outside of alleviating premature onset of atherosclerosis associated with genetic deficiency in LAL, it is hard to predict whether augmentation of LAL is a good therapeutic strategy. There are suggestions that selective upregulation of the autophagic-lysosomal pathway may be able to recover lysosomal function and LAL hydrolysis (55, 87). It is unclear, however, whether induction of this pathway beyond normal response is a viable *in vivo* strategy. Further research is necessary to know whether manipulation of arterial cell LAL activity is likely to alleviate or aggravate the consequences of cholesterol accumulation in the artery wall. As SMCs are the dominant cell type present during atherosclerosis (16) and display reduced ABCA1 levels compared to macrophages (24) these cells may display a tendency for lysosomal dysfunction, either a result of loss of lysosomal acidity or low LAL levels, compared to macrophages provide a specific cellular therapeutic target.

In Section 1.3 we discuss what is known regarding the role of SMCs in the deposition of cholesterol in atherosclerotic plaque providing further background information and setting the stage for the studies conducted in the subsequent Chapters.

1.3 Importance of SMCs in atherosclerotic foam cell formation

Cholesterol deposition from atherogenic lipoproteins in the artery wall is the principal driver of atherosclerotic plaque formation and the associated inflammation in coronary heart disease, and its removal is the primary predictor of lesion regression and clinical benefit from lipid-lowering therapies (165-167). Awareness of the primary cell types accumulating cholesterol and their mechanisms of taking up and releasing cholesterol is critical to our understanding of the pathogenesis and treatment approaches to preventing this leading cause of death worldwide. The lipid overloaded "foam cell" population in atherosclerotic lesions has been generally assumed to be made up of cells of leukocyte origin, primarily monocyte-derived macrophages. Earlier studies using human tissues, however, had suggested the majority of foam cells in early atherosclerosis are smooth muscle cell-derived (17, 18, 168). We recently reported that more than 50% of foam cells in intermediate human coronary artery atherosclerosis are smooth muscle cell-rather than leukocyte-derived (24). In contrast to animal models, which have appeared to lack a major contribution of SMCs to the developing intima and foam cell population (169), these findings in human arteries provide a basis for intensified research into the role of SMC foam cells in the pathogenesis and as a treatment target in atherosclerosis. The focus of Section 1.3 is on our current understanding of intimal SMC cholesterol metabolism and the role these resident cells play in the progression of atherosclerosis.

1.3.1 Appearance of intimal SMCs early in life

SMCs are the major cell type numerically in most if not all stages of human atherosclerosis (16). The conditions for this are initiated *in utero* (**Figure 1.4**). Development of a circumferential layer of intimal SMCs in atherosclerosis-prone arteries begins in late gestation, and is present in 100% of humans by the age of 2 years (170). This process, known as diffuse intimal thickening (DIT), is considered a pre-atherosclerotic stage and part of normal arterial anatomy due to its consistent appearance in susceptible vessels including the coronary arteries and aorta. DIT occurs in arterial regions of low sheer stress (171) and is localized in non-branching segments of arteries, with contiguous eccentric intimal thickening occurring around arterial branches (172). Formation of the DIT layer precedes the appearance of lipid or inflammatory cell infiltration by years (170, 173-175). DIT is composed almost entirely of SMCs and their product proteoglycans and elastin, with no CD68-positive (leukocyte or SMC) cells found at this stage (170, 176).

The exact reasons for the appearance of non-atherosclerotic DIT are unknown. Evidence suggests medial SMCs with altered phenotype migrate from the media and expand monoclonally in the intima (177, 178). Even in the DIT stage, intimal SMCs exhibit differences from medial SMCs including decreased myosin heavy chain production (179) and increased expression of genes that play a role in atherogenesis including αvβ3 integrin (SMC migration and angiogenesis) (180), heparin-binding epidermal growth factor-like growth factor (mitogen and chemoattractant) (181), and transforming growth factor (TGF)-β (stimulation of proteoglycan synthesis) (182).

The degree of DIT in infants has been found to correlate with the presence of coronary disease in families (183), and in coronary arteries (*e.g.*, left anterior descending) DIT correlates

directly to their propensity to develop plaque (173, 184). Of note, DIT is not found in common mouse or other animal models of early or later stage atherosclerosis (169, 185). Absence of DIT is therefore suggested as a reason SMCs play less of a role in atheroma development in animal as compared to human atherosclerosis.

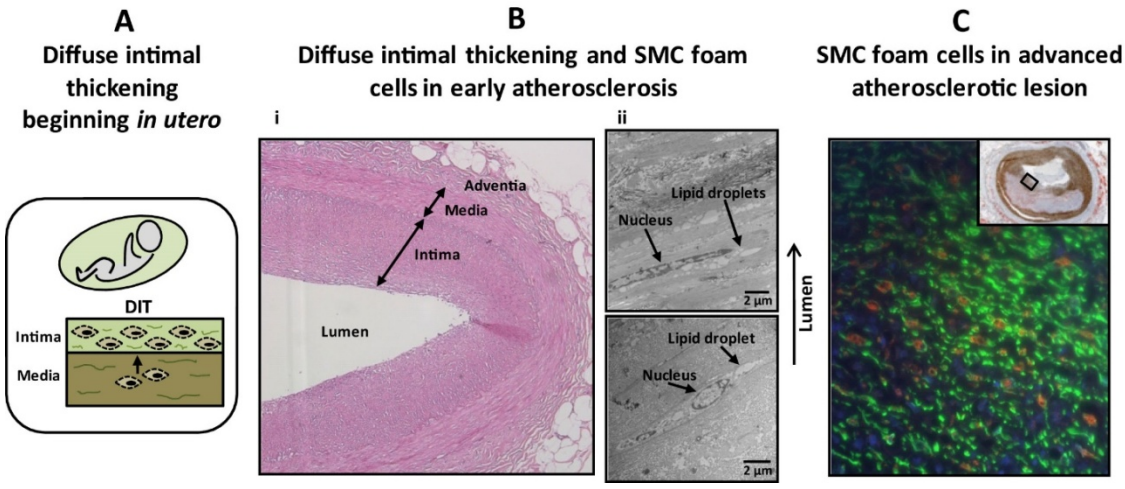

Figure 1.4 The major role of smooth muscle cells in diffuse intimal thickening and atherosclerotic foam cell formation.
(**A**) Migration and proliferation of SMCs forming a thickened intimal layer begins in early life, preceding retention of apoB-containing lipoproteins and infiltration of inflammatory cells. (**B, i**) Over decades of life, a large increase in the intimal-to-medial ratio occurs, as shown in a hematoxylin and eosin-stained human coronary artery from a 50-year old female with early atherosclerosis. (**B, ii**) Electron micrographs showing SMC foam cells in the deep intima in an adjacent section of the same artery in (**B, i**). (**C**) Confocal microscopy of SMC foam cells in an advanced human coronary lesion. Green indicates smooth muscle a-actin, red indicates neutral lipids stained with Oil Red O, and blue indicates DAPI-stained nuclei. Inset shows the region of artery used for the confocal microscopy. Adapted with permission from (24).

1.3.2 Diffuse intimal thickening promotes plaque formation in atherosclerosis

As initially characterized in studies by Stary (186), fatty streaks in human coronary arteries arise in an artery wall already affected by DIT or eccentric intimal thickening composed primarily of SMCs (18). In the earliest stages of atherosclerosis, extracellular deposits of unmodified and modified forms of LDL are found in the deep intima (96, 187), forming the

initial fatty streak (175). These lipid deposits are contiguous with SMCs in the DIT layer, and independent of macrophage infiltration, which at this stage is minimal and confined to the area just beneath the endothelium and away from the lipid deposits (175). Retention of apolipoprotein B (apoB)-containing lipoproteins in the deep intima is due to an interaction with proteoglycans synthesized by SMCs, and possibly promoted by lipoprotein lipase (188), with positively-charged segments of apoB binding to negatively-charged proteoglycans (189). Elegant studies by Nakashima and colleagues demonstrated deposition of lipids in the early fatty streak stage primarily in the deep intima, the region with highest concentration of SMC-secreted proteoglycans including biglycan (175). The colocalization of lipids in this SMC and proteoglycan-rich region away from the endothelium and sparse macrophage infiltration suggests strongly that the retention of apoB-containing lipoproteins is primarily a SMC-dependent event. Intimal SMCs contribute further to lipoprotein retention by increasing the production and chain length of proteoglycans in response to growth factors including TGF-β (190, 191), and oxidized LDL (192). SMC-produced proteoglycans in the deep intima therefore induce the critical step considered to drive atherosclerosis development, the retention of apoB-containing lipoproteins, as first proposed in the "response to retention" hypothesis (91).

1.3.3 Phenotypic modulation of SMCs

While the main factors inducing SMC migration into the intima and DIT formation are not well known, a very large body of work has characterized differences between medial and intimal SMC phenotypes. Arterial SMCs are not terminally differentiated and retain flexibility to alter their phenotype in response to environmental cues (193). Medial SMCs have a contractile phenotype and regulate the diameter of the blood vessel through contraction and relaxation. Within the intima SMCs change to a synthetic phenotype including loss of contractile properties

and increases in proliferation and proteoglycan secretion to increase extracellular matrix synthesis, designed to be reparative and stabilize the artery in vulnerable locations (194, 195). In atherosclerosis, exposure of intimal SMCs to atherogenic lipids, cytokines, and growth factors promotes switching to the de-differentiated synthetic state (193, 196). A key driver towards the synthetic phenotype is platelet-derived growth factor (PDGF)-BB expressed by multiple cell types in the developing lesion (197, 198). Both PDGF-BB and TGF-β exposure have also been shown to increase scavenger receptor expression and activity in arterial SMCs, promoting their conversion to foam cells (199).

Earlier studies had indicated a loss of classic markers of SMC lineage including smooth muscle α-actin in intimal compared to medial SMCs (200). More recent studies suggest this may be largely a consequence of cholesterol loading. In cultured mouse aortic SMCs exposure to cholesterol complexed to cyclodextrins resulted in reduced expression of the smooth muscle markers α-actin, α-tropomyosin, myosin heavy chain, and calponin H1 (201). A more recent study showed cholesterol loading downregulates miR-143/145, a positive regulator of the master SMC differentiation transcription factor myocardin (202). Cholesterol loading was also found to induce expression of macrophage markers CD68, Mac-2 (201), and Lgals3 (202), as well as pro-inflammatory markers including chemokine ligands 2 and 7and toll-like receptor 4 by SMCs (202). A previous study had also found exposure to enzymatically-modified LDL induced expression of monocyte chemotactic protein-1 and interleukin 6 by human SMCs (203). Despite expression of macrophage markers, cholesterol-loaded SMCs were relatively deficient in phagocytosis and efferocytosis, the uptake of apoptotic cells, when compared macrophages (202), suggesting expression of macrophage markers by SMCs does not equate to conversion to full macrophage function (204). These combined findings indicate that the phenotypic switch of

SMCs in the intima is at least in part a consequence of cholesterol loading, and results in reduced expression of SMC markers while increasing expression of macrophage markers and pro-inflammatory mediators by SMCs.

Recent lineage tracing studies using mice (205) or both mice and human coronary tissues (206) have also indicated de-differentiation of intimal SMCs leads to a loss of many SMC markers such as smooth muscle α-actin and myosin heavy chain, and activation of macrophage markers Lgals3 and CD68. Krüppel-like factor 4 (Klf4) has been identified as a key regulator of SMC modulation towards a macrophage-like phenotype and has been demonstrated to be upregulated by PDGF-BB (207) and oxidized phospholipids (208). The loss of typical SMC protein markers in mouse models of atherosclerosis is the apparent reason SMCs have escaped recognition as a major cell type in histologic studies of lesions in these animals, while expression of macrophage markers by SMCs has likely contributed to their mis-identification as macrophages (206). In contrast to the predominant role of SMCs numerically in human atherosclerotic plaque, however, these lineage tracing studies indicated that SMCs form at most about 36% of all cells in advanced lesions of these animals (206).

1.3.4 SMC foam cell formation

Despite evidence that SMCs make up the vast majority (~90%) of cells in human atherosclerotic intima (15), most interest has focused on monocyte-derived macrophage foam cells in studies of atherosclerosis progression and regression. Early studies from autopsies of children and young adults had indicated the majority of foam cells in early human atheromas were SMC- rather than macrophage-derived (17), and located predominantly in the deep intima rather than immediate subendothelial space (18). We recently reported that cells co-staining strongly for smooth muscle α-actin and Oil Red O made up at least 50% of the foam cell

population in intermediate to advanced human coronary atheromas (24). Given the known reduction and loss of smooth muscle α-actin expression by some intimal SMCs, this likely represents an underestimate of the contribution of SMCs to total foam cells in human lesions. The potential exists for smooth muscle α-actin expression by bone-marrow derived hematopoietic stem cells (209, 210), however the importance of this in native human atherosclerosis is likely minor. The contribution of SMCs to total cellularity in human atheromas and these combined studies using autopsy and explanted heart specimens suggest the contribution of SMCs to the total foam cell population has been vastly underestimated, and exceeds that of foam cells derived from leukocyte origin.

Foam cells are formed through the unregulated uptake of modified forms of LDL, as well as phagocytosis of apoptotic cells and free cholesterol crystals (211). The mechanisms by which macrophages take up excess lipids in the form of oxidized, enzymatically-modified or agLDL have been well described, and include the scavenger receptors class A type I/II (SR-AI/II), CD68, CD36, and lectin-like oxidized LDL receptor (LOX-1) (212, 213). Processes by which SMCs, which are not designed to be scavenger cells, become foam cells are less well described and controversial, possibly related to phenotypic variation in the cultured SMCs used or species studied. An example of this is SR-AI/II, which has been found to be reliably expressed by macrophages in atherosclerosis (214), but has shown variable expression by SMCs *in vitro* and *in vivo* (215-218). Scavenger receptor upregulation in SMCs may also be a function of exposure to growth factors and cytokines such as tumor necrosis factor-α (TNF-α) and interferon-γ (INF-γ) (89). Oleic acid uptake via CD36 has been implicated in foam cell formation in SMCs (219). Additionally, macropinocytosis has been demonstrated in the uptake of serum lipids by SMCs (220).

In macrophages, agLDL has been shown to be taken up endocytically via pinocytosis or phagocytosis (117). Processes involving acidic extracellular compartmental uptake of agLDL have been demonstrated in macrophages (221) and dendritic cells (222). In SMCs, the LDL receptor-related protein-1 (LRP1) has been demonstrated *in vitro* to be involved with agLDL uptake, which further increases LRP1 expression and promotes foam cell formation (223). SMC foam cell formation via LRP-1 with agLDL treatment has been indicated to bypass endocytic processing and lead directly to cholesteryl ester lipid droplet formation (224). This may indicate quite different uptake and storage mechanisms of agLDL in SMCs versus macrophages. While cultured medial-type SMCs can be converted to foam cells using cholesterol bound to cyclodextrin (201), it isn't yet known whether an additional phenotypic switch in intimal SMCs *in vivo* is first required for them to take up sufficient lipids to become foam cells.

1.3.5 Cholesterol efflux from SMC foam cells

Prevention and treatment of atherosclerosis depends largely on reduction of cholesterol and its associated inflammatory response in atherosclerotic plaque. This is achieved by reducing plasma levels of LDL including with statin medications, and also expected with proprotein convertase subtilisin/kexin type-9 (PCSK9) inhibitors (167), thereby decreasing LDL retention in the intima, or by enhancing the removal of cholesterol already deposited in the plaque. Efflux of cholesterol is based on the actions of ATP-binding cassette transporter A1 (ABCA1) to deliver cellular cholesterol and phospholipids to lipid-poor apolipoprotein A1 for HDL particle formation, and subsequent removal of more cholesterol by preformed HDL (225). We found that ABCA1 expression is reduced in cultured intimal- compared to medial-type rat SMCs, and in human coronary intimal compared to medial SMCs (23). Further analysis of human coronary arteries indicated expression of ABCA1 decreases in intimal SMCs with advancing lesion stage,

while no reduction in ABCA1 expression was seen in macrophage or other leukocyte-lineage cells (24). Potential reasons for this reduction of ABCA1 include PDGF-BB-stimulated activation of phosphatidylinositol 3-kinase/protein kinase B (PI3K) and downstream phosphorylation of Akt, with inhibitory effects on the ABCA1 gene promoter (226). Whether this activity of PDGF-BB would selectively reduce ABCA1 expression in intimal SMCs but not macrophages is unclear. Alternatively, a SMC-specific defect in lysosomal processing of lipoprotein-derived cholesterol may lead to impaired upregulation of ABCA1 (227), as we previously demonstrated in the lysosomal cholesterol trafficking disorders Niemann Pick Disease Type C (27) and cholesteryl ester storage disease (25). Our finding of reduced ABCA1 expression in intimal SMCs is in contrast to the increased ABCA1 expression in cultured SMCs loaded with free cholesterol using cyclodextrin (201, 202). This difference may be due to phenotypic differences of cultured compared to intimal SMCs *in vivo*, or to differential processing of cyclodextrin-derived compared to lipoprotein-derived cholesterol.

Cholesterol loading of SMCs leads to a loss of expression of markers of contractile SMCs including smooth muscle α-actin and myocardin and expression of macrophage markers (201, 202), while cholesterol efflux by apoA-I and HDL reverses these changes (202). In addition, uptake of excess cholesterol from lipoproteins inhibits assembly of fibronectin and type I collagen (228), required for plaque stabilization, while depletion of excess cholesterol by apoA-I and HDL restores this extracellular matrix production (229). These findings indicate the ability of intimal SMCs to release excess cholesterol via the ABCA1/apoA-I/HDL pathway is critical to the stability and regression of atheromas, as has also been proposed for macrophages (230). The ability of reduced ABCA1 expression in intimal SMCs to be corrected would therefore be required to reverse these plaque destabilizing effects of excess SMC cholesterol *in vivo*. We also

found reduced binding of apoA-I to cultured intimal-type rat SMCs, and failure of overexpression of ABCA1 to correct apoA-I binding or cholesterol efflux from these cells (23). If impaired apoA-I binding is also a feature of intimal SMCs *in vivo*, the mobilization of cholesterol from these cells might be resistant to enhancement of the ABCA1 pathway, and require development of a non-ABCA1-dependent treatment to mobilize cholesterol from this large reservoir of excess cholesterol in SMC foam cells.

1.3.6 Conclusion

SMCs are the predominant cell type in human arterial intima in atherosclerosis-prone arteries well before the onset of atherosclerosis and contribute in a pivotal way to lipoprotein retention and lesion progression. Phenotypic modulation likely plays a key role in the tendency of these SMCs to become foam cells, but may not be an initial requirement as indicated by *in vitro* studies. In the absence of cholesterol storage mechanisms, in the developing lesion SMCs may act as a cholesterol sink, taking up atherogenic lipids in an attempt to prevent further arterial damage. While lipid loading appears responsible for converting SMCs to a macrophage-like and pro-inflammatory state, this may not affect all SMCs in the intima including those forming the protective fibrous cap. In contrast to commonly used animal models, recent studies using human tissues indicate SMCs are the source of the majority of foam cells in atherosclerotic plaque. While animal models have been hugely important for our understanding of the pathogenesis and treatment of atherosclerosis, these results suggest a renaissance of studies using human tissues or animal models more closely mimicking human arterial structure are needed to understand fully the importance of SMCs as compared to macrophages in lesion development and regression. Removal of the cholesterol in SMC foam cells may require approaches different from those applied to macrophages in order to deplete this large reservoir of excess cholesterol from

atherosclerotic lesions, and to make the next leap forward in atherosclerosis treatment and prevention.

1.4 Rational, hypothesis and specific aims

SMCs are the main cell type within the intima of human atherosclerosis-prone arteries and promote initial retention of atherogenic lipoproteins in the deep intima. We previously found that ≥50% of foam cells in intermediate coronary atheromas are of SMC origin and that intimal SMCs have reduced expression of ABCA1. Previously we also found that ABCA1 expression is acutely dependent on the flux of cholesterol out of lysosomes and subsequent generation of oxysterols for promotion of gene transcription by the nuclear liver X receptor (LXR). **In the present studies we tested the hypothesis that SMCs have reduced lysosomal function that contributes to foam cell formation.**

Specific aims:

***Aim 1* - Lysosomal acid lipase is crucial for normal lysosomal processing of lipoprotein-derived cholesteryl esters. We investigate the role of LAL in cellular cholesterol metabolism downstream of lysosomes and efflux using LAL knockout ($lal^{-/-}$) and wild type ($lal^{+/+}$) mouse peritoneal macrophages (Chapter 2).**

***Aim 2* - To develop an in vitro model of excess lipid overloaded human arterial SMCs and monocyte derived macrophages using a modified form of LDL. We investigate whether or not reduced ABCA1 response to lipid loading is associated with defects in cholesterol metabolism pathways in SMCs compared to macrophages (Chapter 3).**

***Aim 3** - To determine if lysosomal lipid accumulation preferentially occurs in human SMCs relative to macrophages. We hypothesize that lysosomal lipid accumulation in SMCs is a result of reduced lysosomal function, either the result of a loss of lysosomal acidity from lysosomal free cholesterol accumulations or a cellular phenotypic deficiency in LAL (Chapter 3).*

***Aim 4**: To investigate if lysosomal lipid accumulation preferentially occurs in mouse arterial SMCs compared to macrophages and determine if LAL deficiency is a feature of mouse arterial SMCs (Chapter 3).*

***Aim 5**: To evaluate if LAL treatment will rescue lysosomal cholesteryl ester accumulation and have beneficial effects on cholesterol trafficking and efflux (Chapter 3).*

Chapter 2: Recombinant LAL treatment rescues cellular cholesterol metabolism pathways in LAL knockout macrophages

2.1 Summary

The objective of this chapter is to investigate the role of LAL in cellular cholesterol metabolism and efflux. For the studies described, we utilized both wild-type ($lal^{+/+}$) and LAL knockout ($lal^{-/-}$) mouse peritoneal macrophages. $Lal^{-/-}$ macrophages showed reduced expression of ABCA1, reduced production of the regulatory oxysterol 27-hydroxycholesterol, and impaired suppression of cholesterol synthesis upon exposure to acetylated LDL (acLDL) when compared to $lal^{+/+}$ macrophages. LAL-deficient macrophages loaded with [^{3}H]-cholesteryl oleate-labeled acLDL showed impaired efflux of released [^{3}H]-cholesterol to apolipoprotein A-I (apoA-I), with normalization of [^{3}H]-cholesteryl ester levels and partial correction of ABCA1 expression and cholesterol efflux to apoA-I when treated with exogenous recombinant human LAL. These results indicate a critical role for LAL in both the regulation of cellular cholesterol metabolism and the removal of excess cholesterol in atherosclerosis. The experimental investigations described in Chapter 2 form the fundamental basis for our investigation of cellular cholesterol metabolism differences between macrophages and arterial SMCs described in Chapter 3.

2.2 Introduction

Retention and uptake of low density (LDL) and other apolipoprotein B-containing lipoproteins by cells in the artery wall is the key driver of atherosclerosis development (35). Lipoprotein cholesterol ingested by artery wall cells including macrophages is primarily in the ester form, which must be hydrolyzed in and released from lysosomes to allow eventual removal

of the excess cholesterol from cells. The sole lysosomal enzyme known to carry out this function is lysosomal acid lipase (LAL), encoded by the gene *LIPA* (227). The critical importance of LAL is indicated by the lethality of complete LAL deficiency (Wolman disease), and by the liver disease, lipoprotein abnormalities and premature atherosclerosis seen individuals with subtotal LAL deficiency (Cholesteryl Ester Storage Disease, CESD) (43, 231). Lysosomal sequestration of LDL-derived cholesteryl esters in CESD results in impaired suppression of new cholesterol synthesis and reduced acyl-CoA cholesterol acyltransferase (ACAT) mediated cholesteryl ester formation (68). Modification of LAL by mannose-6-phosphate allows the uptake of exogenous LAL by cells and targeting to lysosomes (232), where it has been shown to correct the consequences of LAL deficiency at the cellular level (25, 233). Recombinant human LAL delivered intravenously to humans is lifesaving in Wolman Disease (155), and has been shown to rapidly correct the liver and lipoprotein abnormalities in individuals with CESD (156), indicating its efficient uptake in tissues from the circulation.

We previously reported that LAL deficiency in human skin fibroblasts leads to impaired upregulation of ABCA1 and ABCG1, two mediators of cholesterol efflux and high density lipoprotein (HDL) formation, following cholesterol loading, and correction of these defects following delivery of exogenous LAL to the cells (25). Although there is some suggestion of benefit of delivery of exogenous LAL in reducing atherosclerosis (161), the mechanism of this is not understood, including the role of LAL in promoting cholesterol efflux from macrophages. Different from our results using LAL-deficient fibroblasts, a recent study reported macrophages generated from human pluripotent stem cells and lacking *LIPA* expression had a similar upregulation of ABCA1 in response to acetylated LDL loading as cells expressing *LIPA* (234). In the current studies we have utilized immortalized peritoneal macrophages previously isolated

from $lal^{+/+}$ and $lal^{-/-}$ mice to study the effect of LAL deficiency and replacement on cholesterol metabolism in cultured macrophages. Our results indicate a major role for LAL in the regulation of cholesterol metabolism pathways downstream of lysosomal processing of lipoprotein derived cholesteryl esters and the ability of supplemental LAL to correct these defects in LAL deficiency.

2.3 Materials and methods

2.3.1 Materials

Dulbecco's Modified Eagle Medium (SH3024301) and RPMI 1640 media (SH3002701) were from HyClone (Logan, Utah). Fetal bovine serum (12483020) was from Invitrogen. Complete Mini Protease Inhibitor tablets (1836153) were from Roche Applied Science. Nitrocellulose membranes (162-0115) and SDS-PAGE supplies, were purchased from Bio-Rad. Pre-stained protein molecular mass markers (P77032) were from New England Biolabs. The antibody against ABCA1 (NB400-105) was from Novus Biologicals. The primary antibody against protein disulfide isomerase (PDI) (SPA-890F) was from Enzo Life Sciences. Super Signal West Femto chemiluminescence substrate (PI-34096) was from Pierce. PerfeCTa SYBR Supermix (CA101414-148) was from Quanta, VWR. GelRed (41003-BT) nucleic acid stain was from Biotium. The anti-rabbit IgG horseradish peroxidase-conjugated secondary antibody (A0545) was from Sigma. [Cholesteryl –1,2-^{3}H (N)] cholesteryl oleate (NET746L) was from Perkin Elmer (Waltham, Massachusetts). Whatman pre-SIL G plastic-backed flexible plates (05-713-161) used for thin layer chromatography analysis were from Fisher. Purified recombinant human LAL enzyme (rhLAL) was by donated by Shire (Lexington, MA).

2.3.2 Preparation of ^{3}H-cholesteryl-oleate labeled acetylated LDL and isolation of apolipoprotein A-1 from plasma

LDL was isolated from pooled plasma from fasting, healthy donors by density gradient ultracentrifugation (235). Radiolabeling of LDL with ^{3}H-cholesteryl oleate was performed as previously described, (236) then acetylated according to the methods of Basu *et al* (237). Briefly, an equal volume of ^{3}H-cholesteryl-oleate labeled LDL in saline solution (typically 4-5 ml) was mixed with an equal volume of a saturated sodium acetate solution and 1.5µl acetic anhydride per mg acLDL protein was added in 1µl aliquots over 1 hour, while stirring on ice and then dialyzed extensively in a saline-EDTA solution. Apolipoprotein A-1 (apoA-I) was purified from human plasma using Q-Sepharose Fast Flow chromatography as described (238).

2.3.3 Cell culture

Mouse immortalized peritoneal macrophage cell lines were created by isolation of cells following peritoneal lavage of mice that were generated by crossing wild-type ($lal^{+/+}$) or LAL knockout mice ($lal^{-/-}$) with Immortomouse® (Charles River laboratories), engineered to have temperature-sensitive expression of SV40 large T-antigen under an IFN-γ inducible promoter, using methods described in Castoreno *et al* (239). The isolated cells were then grown in monolayer in continuous culture at 33°C and 8% CO_2 in RPMI 1640 medium supplemented with 10% fetal bovine serum, antibiotics and 5 units/ml IFN-γ (growth medium) for the first 10 passages only.

2.3.4 Lysosomal acid lipase enzyme activity assay

$Lal^{+/+}$ and $lal^{-/-}$ mouse immortalized peritoneal macrophages were grown to confluence and then treated with medium containing 2 mg/ml fatty acid free albumin for 24 hrs. Cells were collected on ice in PBS and analyzed for LAL enzymatic activity by the fluorescence increase

after cleavage of the substrate 4-methylumbelliferyl oleate (4-MUO) to 4-methylumbelliferone (4-MU) by kinetic measurement using a plate reader. Refer to Chapter 3 materials and methods for further details.

2.3.5 Western blot

Cells were collected on ice using lysis buffer containing 20 mM Tris, 5 mM EDTA, 5 mM EGTA, 0.5% maltoside and 1X protease inhibitor (25) and homogenized using a glass mortar and Teflon pestle. Proteins were separated by 7.5% (top half) and 12% (bottom half) SDS-PAGE and transferred to nitrocellulose overnight at 35 V. Immunoblotting was performed using polyclonal antibodies against ABCA1 (2 µg/mL) or protein disulfide isomerase (PDI) (1 µg/mL) and anti-rabbit IgG horseradish peroxidase-conjugated secondary antibody (0.4 µg/mL), detected using chemiluminescence substrate.

2.3.6 mRNA analysis

Total RNA was extracted from cell monolayers using 1 ml TRIzol extraction reagent (Invitrogen), and cDNA libraries were constructed by reverse transcription as previously described (25). DNA amplification was performed following initial denaturation at 95°C for 3 min, 40 cycles [denaturation at 95°C for 20 seconds, annealing for 20 seconds, extension at 72°C for 40 seconds] with SYBR Green to detect PCR products in real-time using a Realplex^2 Mastercycler thermocycler (Eppendorf). The annealing temperatures and sequences of primers used were: m-cyclophilin, 58°C, 5'-ACCCAAAGGGAACTGCAGCGAGAGC-3' (forward) and 5'-CCGCGTCTCCTTTGAGCTGTTTGCAG-3' (reverse); ABCA1, 58°C, 5'-GACATCCT GAAGCCAATCCTG-3' (forward), and 5'-CCTTGTGGCTCCACTGTCAGGT-3' (reverse). The mRNA levels for ABCA1 was the mean cycle times, $C_{T,}$ corrected relative to the housekeeping gene m-cyclophilin (m-cyc) and expressed as a ratio relative to untreated controls.

2.3.7 Cholesterol efflux assay

A preparation of ^{3}H-cholesteryl oleate – labeled acetylated LDL (^{3}H-CE – acLDL) was generated by incubation of native LDL with ^{3}H-cholesteryl oleate in the presence of CETP-containing plasma and then acetylated by incubation with concentrated sodium acetate with intermittent addition of acetic anhydride as described above. Macrophage cell monolayers were grown to confluence and incubated with 50 µg/ml ^{3}H-CE – acLDL for 24 hours followed by incubation with 10 µg/ml apoA-I in RPMI 1640 medium for a further 24 hours. For some samples 20 µg/ml rhLAL was added 1 hour prior to and during acLDL loading. Medium was removed and centrifuged for 10 minutes at 3000 rpm to precipitate cell debris and ^{3}H-sterol in medium was quantified by liquid scintillation counting (LSC). Cell monolayers were washed extensively with cold PBS, 1 mg/ml BSA and PBS on ice and cellular lipids were isolated by Folch extraction as previously described (240). Cellular lipids were separated by thin layer chromatography. Unesterified cholesterol (UC) and cholesteryl ester (CE) spots were located on plates using unlabeled carrier lipids stained with iodine gas, and radioactivity was quantified by LSC (241) as previously described (25, 242). Medium UC and cell UC and CE were calculated as percent of total ^{3}H-sterol (cell + medium).

2.3.8 ApoE ELISA

Lal$^{+/+}$ and lal$^{-/-}$ macrophages were grown to confluence and loaded with 50 µg/ml acLDL for 24 hrs followed by incubated medium alone for 24 hrs. Medium was then collected, centrifuged at 2000 rpm for 10 min and frozen at -80 ^{o}C until analysis. Total apoE secreted into medium was measured using an ELISA kit (AB215086, Abcam) as per the manufactures protocol and normalized to cell proteins measured using reagents from Bio Rad.

2.3.9 Measurement of 27-hydroxycholesterol production

Macrophage cell monolayers were grown to confluence in 60 mm dishes and then incubated with RPMI 1640 medium containing 50 µg/ml acLDL for 24 hours. $Lal^{-/-}$ macrophages were also pretreated with 10 µg/ml rhLAL1 hour prior to and during acLDL loading. Cell monolayers were then extensively washed and equilibrated for 24 hours in medium containing 1 mg/ml fatty acid free albumin. Cell lysates and media were combined and 50 µl of 50 ng/ml 27-hydroxycholesterol-d6 (Avanti Polar Lipids, Inc.; Alabaster, Alabama) added as an internal standard. Lipids were extracted with hexanes. The organic extracts were then evaporated under a stream of nitrogen gas and the residues reconstituted in 100 µl of methanol. The mass of 27-hydroxycholesterol (ng) was determined by HPLC tandem mass spectrometry by modification of a previously described method (243). Refer to the material and methods section in Chapter 3 for detailed analytical methodology. The mass of 27-hydroxycholesterol measured was normalized to cell proteins (mg) as determined using reagents from Bio Rad.

2.3.10 Mevalonolactone incorporation assay

Macrophage cell monolayers were grown to confluence in 12-well plates and then incubated with RPMI 1640 medium containing 0.5 µCi/ml ^{3}H-mevalonolactone ± 50 µg/ml acLDL for 24 hours. $Lal^{-/-}$ macrophages were also pretreated with 10 µg/mL rhLAL1 hour prior to and during acLDL loading. Cell monolayers were then washed extensively with cold PBS containing 1 mg/ml BSA, followed by PBS. Lipids were then extracted and separated by thin layer chromatography. Radioactivity of new cholesterol synthesized was quantified by liquid scintillation counting as previously described (244) and normalized to cell proteins (mg) by the method of Lowry (245).

2.3.11 ACAT activity assay

Macrophage cell monolayers were grown to confluence in 24-well plates and then incubated with RPMI 1640 medium containing 50 µg/ml acLDL and for 24 hours. $Lal^{-/-}$ macrophages were also pretreated with 10 µg/ml rhLAL1 hour prior to and during acLDL loading. After extensive washing with PBS containing 1 mg/mL FAFA and cells were then incubated for 1 hr at 37 °C with medium containing 9 µM [^{14}C]oleate bound to 3 µM FAFA (246). Cells were then placed on ice, washed with cold PBS containing 1 mg/mL FAFA followed by cold PBS alone and extracted using hexanes:isopropanol (3:2) (247). Separation of lipid species by thin-layer chromatography was done as previously described (246) and cholesteryl [^{14}C]oleate radioactivity was determined by liquid scintillation counting. The amount of [^{14}C]-labeled cholesteryl ester was normalized to amount of cell protein as determined by the method of Lowry (245).

2.3.12 Statistical analysis

Results were analyzed using GraphPad Prism version 5.0 for statistical significance between treatment groups. The normality of data for figures was determined by performing a D'Agostino & Pearson omnibus normality test (alpha=0.05) and by visual inspection of normality using Q-Q plots. Normally distributed data was analyzed using parametric tests, either a one-way ANOVA with Bonferroni post-hoc comparisons or a Students T-test, as indicated in the figure legends. Data not normally distributed was analyzed using non-parametric tests, either a Kruskal-Wallis test with Dunn's comparisons or a Mann Whitney test, as indicated in the figure legends. A p-value <0.05 was considered significant.

2.4 Results

2.4.1 ABCA1 expression and cholesterol efflux are impaired in macrophages lacking LAL and corrected by addition of exogenous LAL.

Macrophages are a primary site of cholesterol deposition in atherosclerotic plaque, and the level of ABCA1 expression is the rate-limiting determinant of removal of excess cholesterol by apolipoprotein A-I (apoA-I) from these cells (248). To determine the role of LAL in regulating ABCA1 expression and other determinants of macrophage cholesterol efflux, we used immortalized peritoneal macrophages obtained from wild type ($lal^{+/+}$) and LAL-deficient ($lal^{-/-}$) mice. LAL-deficiency was confirmed using an LAL enzyme activity assay based on the increase in fluorescence following cleavage of 4-methylumbelliferyl oleate (4-MUO) to 4-methylumbelliferone (4-MU) (**Figure 2.1**) (40, 249). Similar to a prior report by Schlager *et al*. (250) we found significantly higher 4-MUO cleavage to 4-MU (~22.2-fold higher) in the $lal^{+/+}$ macrophages compared to $lal^{-/-}$ macrophages at pH 4.0.

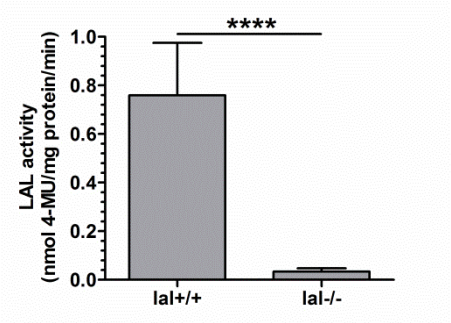

Figure 2.1 LAL activity in lal+/+ and lal-/- mouse peritoneal macrophages.
$Lal^{+/+}$ and $lal^{-/-}$ mouse immortalized peritoneal macrophages were grown to confluence and then treated with medium containing 2 mg/ml fatty acid free albumin for 24 hrs. Cells were collected on ice in PBS and analyzed for LAL enzymatic activity by the fluorescence increase after cleavage of the substrate 4-methylumbelliferyl oleate (4-MUO) to 4-methylumbelliferone (4-MU) by kinetic measurement using a plate reader. Results are mean±SEM (3 experiments with n=4-6 replicates each). Statistical analysis was done using Mann-Whitney test, ****$p<0.0001$.

In contrast to the robust increase in ABCA1 expression in response to incubating $lal^{+/+}$ macrophages with acLDL, $lal^{-/-}$ macrophages exhibited significantly reduced basal and acLDL-stimulated increase in ABCA1 mRNA and protein levels (**Figure 2.2 A-C**). Incubation with recombinant human LAL (rhLAL) 1 hr prior to and during acLDL loading for 24 hours resulted in a significant increase in ABCA1 mRNA and protein levels in $lal^{-/-}$ macrophages (**Figure 2.2 A-C**). This is consistent with the role of LAL in hydrolyzing lipoprotein cholesteryl esters and the subsequent release of this cholesterol from lysosomes driving ABCA1 expression (25). In contrast, addition of supplemental rhLAL to $lal^{+/+}$ macrophages stimulated no further increase in ABCA1 mRNA (**Figure 2.2 A**) or protein (**Figure 2.2 C**).

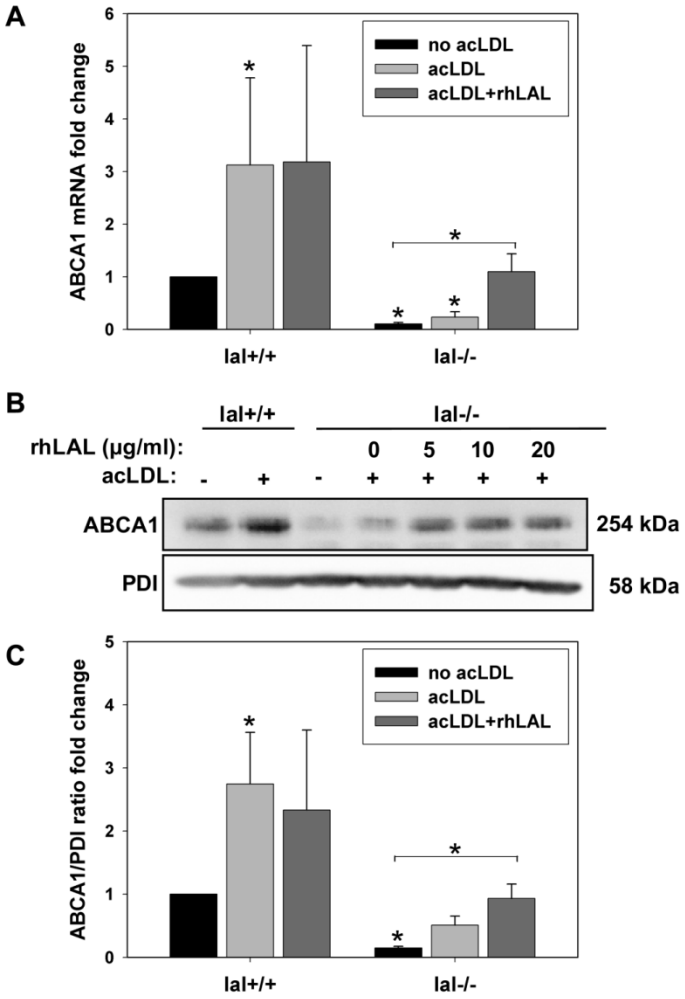

Figure 2.2 ABCA1 mRNA and protein are reduced in lal$^{-/-}$ mouse peritoneal macrophages and partially rescued by rhLAL.
Wild-type (lal$^{+/+}$) and LAL knockout (lal$^{-/-}$) mouse immortalized peritoneal macrophage cell lines were grown to confluence and supplemented without (-) or with (+) 50 µg/ml acetylated LDL (acLDL) for 24 hours. Some dishes of lal$^{-/-}$ cells were also treated with 5, 10 or 20 µg/ml of rhLAL 1 hour prior to and during acLDL loading. **A**. ABCA1 mRNA expression in the absence or presence of acLDL and 20 µg/ml rhLAL was measured by quantitative real time PCR, corrected for the housekeeping gene m-cyclophilin, and normalized relative to the lal$^{+/+}$ control. **B**. ABCA1 protein levels were resolved by SDS-PAGE, detected by Western blotting using polyclonal antibodies against ABCA1 or protein disulfide isomerase (PDI) loading control, and normalized relative to the lal$^{+/+}$ control. Error bars are shown as standard error of the mean (SEM) from (**A**) 6 or (**C**) 8 experiments using ± 20 µg/ml rhLAL (*$p<0.05$, Kruskal-Wallis test with Dunn's comparisons, significantly different from lal$^{+/+}$ with no acLDL, unless otherwise indicated).

The role of LAL in promoting removal of excess cholesterol from macrophage foam cells was then determined following cholesterol loading with acLDL and incubation with apoA-I to determine ABCA1-dependent cholesterol efflux. Cells of both genotypes were loaded with ^{3}H-cholesteryl oleate-labeled acLDL for 24 hours and ^{3}H-UC counts in the medium and ^{3}H-CE and ^{3}H-UC counts in cells were quantified following a 24 hour incubation with or without 10 μg/ml apoA-I (**Figure 2.3**).

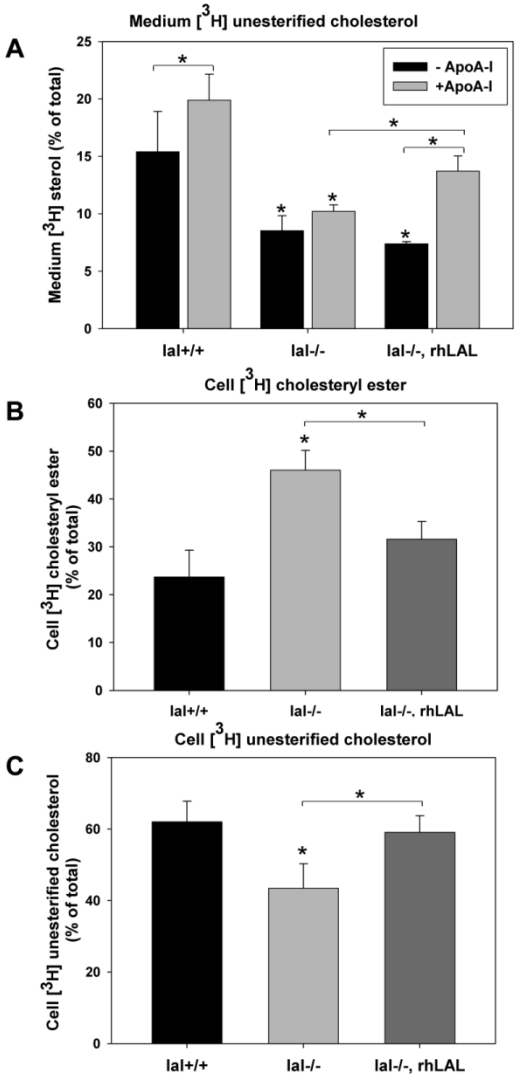

Figure 2.3 Rescue of impaired apoA-I-dependent cholesterol efflux in lal$^{-/-}$ macrophages by treatment with rhLAL.

Immortalized mouse peritoneal macrophages were grown to confluence and loaded with 50 µg/ml ^{3}H-CE-labeled acetylated LDL for 24 hours and then washed and incubated in the presence (+ ApoA-I) or absence (- ApoA-I) of 10µg/ml purified apolipoprotein A-I for 24 hours. Where indicated 20 µg/ml rhLAL was added 1 hour prior to and during acLDL loading. **A**. Medium was removed and ^{3}H-cholesterol was quantified by LSC. **B**, **C**. From cells that were not incubated with apoA-I, cellular lipids were extracted, cellular ^{3}H-cholesteryl esters and ^{3}H-unesterified cholesterol were separated by thin layer chromatography and counted by LSC. Uptake of ^{3}H-CE-acLDL was 2 times higher in lal$^{-/-}$ than lal$^{+/+}$ macrophages (73462±8662 versus 36447±4823 cpm/mg cell protein, respectively; avg±SEM, 3 experiments with n=3 replicates each). Measurements are expressed as the percent of total ^{3}H counts (medium + cell). Error bars are shown as SEM from 7 experiments (*$p<0.05$, One-way ANOVA with Bonferroni comparisons, significantly different from lal$^{+/+}$, unless otherwise indicated).

Elevated levels of ^{3}H-CE and low ^{3}H-UC in lal$^{-/-}$ macrophages prior to addition of apoAI were recapitulated in lal$^{+/+}$ macrophages treated with the lysosomal inhibitor chloroquine, confirming the dependence of this observation in lal$^{-/-}$ macrophages on deficiency of LAL activity (**Figure 2.4**).

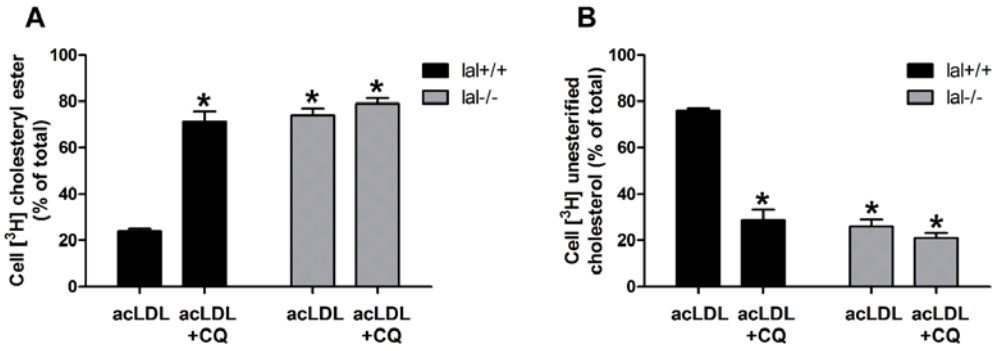

Figure 2.4 Inhibition of lal$^{+/+}$ macrophage lysosomal function with chloroquine recapitulates cholesterol distribution of lal$^{-/-}$ macrophages.
Lal$^{+/+}$ and lal$^{-/-}$ macrophages were grown to confluence in RPMI and 10% FBS. Cells were then treated for 1 hour with or without 100 µM chloroquine followed by incubation with 50 µg/ml [^{3}H]-CE-labeled acLDL with 2 mg/ml fatty acid-free albumin for 24 hr also with or without chloroquine. After a 6 hr equilibration period in medium alone with or without chloroquine cell lipids were extracted with hexane/isopropanol and (**A**) [^{3}H]-CE and (**B**) [^{3}H]-FC were then separated by thin-layer chromatography and the corresponding radioactivity measured. Data are n=6 replicates from 2 experiments (avg±SEM**,** *$p<0.05$, Kruskal-Wallis test with Dunn's comparisons, significantly different compared to lal$^{+/+}$ with acLDL).

Lal$^{+/+}$ macrophages exhibited a high level of efflux to the medium without addition of apoA-I (~15%) (**Figure 2.3 A**), likely due to macrophage-secreted apoE (**Figure 2.5**) promoting cholesterol efflux, as previously reported (251, 252), and which is ABCA1-dependent (253).

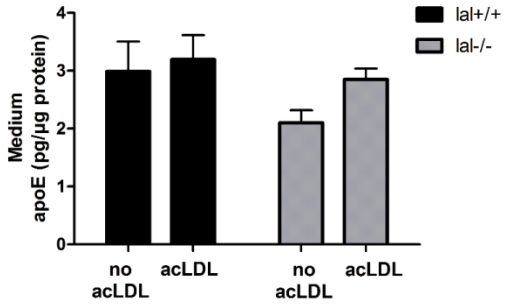

Figure 2.5 ApoE is secreted into medium by lal$^{+/+}$ and lal$^{-/-}$ macrophages.
Lal$^{+/+}$ and lal$^{-/-}$ macrophages were grown to confluence and loaded with 50 µg/ml acLDL for 24 hrs followed by incubation medium alone for 24 hrs. Medium was then collected, centrifuged at 2000 rpm for 10 min and frozen at -80 ^{o}C until analysis. Total apoE secreted into medium was measured using an ELISA kit (AB215086, Abcam) and normalized to cell proteins. Data are from 3 experiments (avg±SEM, One-way ANOVA with Bonferroni comparisons, no statistical difference between treatment groups).

Addition of apoA-I to medium significantly further increased efflux in lal$^{+/+}$ macrophages (**Figure 2.3**). Efflux to medium alone was reduced to almost half of wild-type levels in lal$^{-/-}$ macrophages (**Figure 2.3 A**). This is consistent with both the reduced cellular pool of ^{3}H-UC available for efflux (**Figure 2.3 C**) and reduced ABCA1 (**Figure 2.2**), both reducing the efflux potential of macrophage-secreted apoE (**Figure 2.5**). For the same reasons, addition of apoA-I did not significantly increase efflux from lal$^{-/-}$ macrophages (**Figure 2.3 A**). Treatment of lal$^{-/-}$ cells with 10 µg/ml rhLAL significantly increased cholesterol efflux to apoA-I (**Figure 2.3 A**), consistent with the upregulation of ABCA1 in these cells (**Figure 2.2**) and reduced availability of UC for efflux. As expected, lal$^{-/-}$ macrophages showed increased cellular ^{3}H-CE and reduced ^{3}H-UC when compared to lal$^{+/+}$ macrophages (**Figure 2.3 B&C**). CE hydrolysis in lal$^{-/-}$ macrophages was corrected with a consequent increase in ^{3}H-UC following addition of rhLAL (**Figure 2.3 B&C**). This result is consistent with the ability of exogenous LAL to be taken up,

delivered to lysosomes and mediate neutral lipid hydrolysis in both cultured cells (25, 233) and in vivo (156).

2.4.2 Dysregulation of post-lysosomal cholesterol metabolism in lal$^{-/-}$ macrophages and correction by exogenous LAL.

Reduced release of lipoprotein-derived cholesterol from lysosomes in LAL-deficient human fibroblasts has previously been shown to impair downstream regulatory events including suppression of cholesterol synthesis (68) and upregulation of ABCA1 expression (25). To further investigate the importance of LAL in regulating cholesterol homeostasis in macrophages we measured production of 27-hydroxycholesterol, a key endogenous LXR agonist oxysterol upregulating ABCA1 expression in the artery wall (254), and new cholesterol synthesis from the cholesterol precursor mevalonate, before and after addition of acLDL. Formation of 27-hydroxycholesterol was similar in both lal$^{+/+}$ and lal$^{-/-}$ macrophages in the basal state (0.37±0.06 and 0.54±0.08 ng/mg cell protein respectively, mean±SEM of 7 experiments, p=0.11). 27-hydroxycholesterol synthesis rose significantly in lal$^{+/+}$ but was unaffected in lal$^{-/-}$ macrophages following incubation with acLDL (**Figure 2.6 A**).

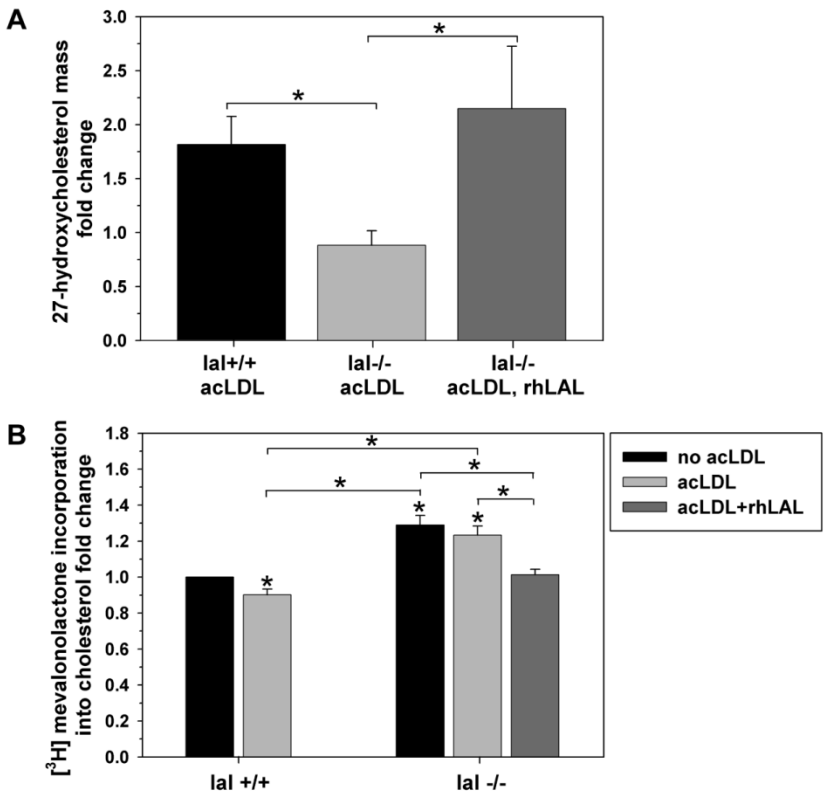

Figure 2.6 Impaired regulation of oxysterol production and cholesterol synthesis in lal$^{-/-}$ macrophages and correction with rhLAL.

A. Immortalized mouse peritoneal macrophages were grown to confluence and treated ± 50 µg/mL acLDL for 24 hrs. In addition, lal$^{-/-}$ macrophages were also pretreated with 10 µg/mL rhLAL 1 hour prior to and during acLDL loading. Cell monolayers were then washed and equilibrated for an additional 24 hrs in medium alone. Following lipid extraction, the mass of 27-hydroxycholesterol was determined by HPLC tandem mass spectrometry and normalized to cell proteins. Results are indicated as fold change relative to non–lipid loaded controls. **B**. Immortalized mouse peritoneal macrophages were grown to confluence and loaded with 0.5 µCi/mL ^{3}H-Mevalonolactone ± 50 µg/mL acLDL. In addition, LAL$^{-/-}$ macrophages were pretreated with 10 µg/mL rhLAL 1 hour prior to and during acLDL loading. After 24 hours cell monolayers were washed and lipids extracted by thin layer chromatography. New cholesterol synthesized was determined by LSC and normalized to cell proteins. Results are indicated as fold change relative to the lal$^{+/+}$ control. Error bars are shown as SEM from (**A**) 6 experiments (n=3 replicates each) or (**B**) 3 experiments (n=3 replicates each) [*$p<0.05$, Kruskal-Wallis test with Dunn's comparisons (A) or one-way ANOVA with Bonferroni comparisons (B), significantly different from the lal$^{+/+}$ control, unless otherwise indicated].

Addition of rhLAL resulted in a similar fold increase in 27-hydroxycholesterol synthesis in $lal^{-/-}$ as seen in $lal^{+/+}$ macrophages treated with acLDL. Incubation with acLDL for 24 hr resulted in a modest but significant reduction of new cholesterol synthesis from mevalonate in $lal^{+/+}$ macrophages (**Figure 2.6 B**). $Lal^{-/-}$ macrophages showed significantly higher new cholesterol synthesis in the basal condition and after loading with acLDL compared to $lal^{+/+}$ macrophages. Addition of rhLAL to $lal^{-/-}$ macrophages reduced their synthesis of new cholesterol down to a level similar to $lal^{+/+}$ cells (**Figure 2.6 B**). These two results confirm the dysregulation of cholesterol homeostasis in $lal^{-/-}$ macrophages, and provide a likely reason for impaired upregulation of ABCA1 following addition of acLDL, failure to increase formation of the key LXR agonist 27-hydroxycholesterol in the presence of LAL deficiency. Supplementation of exogenous rhLAL corrects these pathways as reflected in the increased ABCA1 expression, correction of cholesterol efflux to apoA-I by $lal^{-/-}$ macrophages, and suppression of de novo cholesterol synthesis.

Previously it has been shown that release of lysosomal lipoprotein-derived cholesterol for re-esterification in the endoplasmic reticulum via ACAT is impaired in human CESD fibroblasts (68). To further investigate the role of LAL in cholesterol metabolism downstream of the lysosome, we measured cholesteryl ester formation via ACAT with and without acLDL loading as measured by incorporation of [^{14}C]oleate to form cholesteryl [^{14}C]oleate in $lal^{+/+}$ and $lal^{-/-}$ macrophages (**Figure 2.7**).

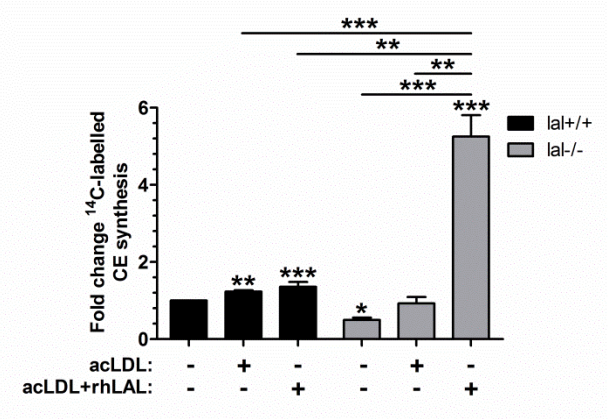

Figure 2.7 Impaired cholesterol esterification in lal-/- macrophages and correction with rhLAL.
Lal$^{+/+}$ and lal$^{-/-}$ macrophages were grown to confluence in RPMI and 10% FBS followed by treatment with or without 50 µg/ml acetylated LDL (acLDL) for 24 hours in RPMI containing 2 mg/mL FAFA. Lal+/+ and lal-/- cells treated with 10 ***µ***g/mL rhLAL was 1 hour pior to and during acLDL loading. Cells were then incubated with [^{14}C]oleate for 1 hr followed by lipid extraction and TLC separation of newly formed cholesteryl [^{14}C]oleate. Radioactivity was determined by LSC and normalized to cell proteins. Data are reported as the fold change relative to the lal$^{+/+}$ non-lipid loaded control. Results are from 3 experiments with n=4 replicates each (avg±SEM**,** ***p<0.001, Kruskal-Wallis test with Dunn's comparisons, significantly different from the lal$^{+/+}$ control, unless otherwise indicated).

Consistent with our finding of impairment of lysosomal cholesterol release to the endoplasmic reticulum for downregulation of new cholesterol synthesis (**Figure 2.6 B**), basal levels of cholesteryl ester formation were significantly lower in lal$^{-/-}$ macrophages compared to lal$^{+/+}$ macrophages. Treatment of lal$^{+/+}$ macrophages with acLDL resulted in significant increase in cholesteryl ester formation with no further increase from addition of rhLAL (**Figure 2.7**). Consistent with our results indicating presence of a non-lysosomal hydrolysis pathway (**Figure 2.3 C & Figure 2.4**) we found a trend towards increased new cholesteryl ester formation after exposure of lal$^{-/-}$ macrophages to acLDL, which was not statistically significant compared to the lal$^{-/-}$ control. Addition of both acLDL and rhLAL in lal$^{-/-}$ macrophages resulted in a significant increase in cholesteryl ester formation by ~5.7-fold relative to acLDL treatment alone in lal$^{-/-}$

macrophages (**Figure 2.7**). Release of free cholesterol for re-esterification via ACAT in $lal^{-/-}$ macrophages with rhLAL treatment was consistent with lipoprotein-derived cholesteryl ester sequestration in $lal^{-/-}$ macrophages. Treatment of $lal^{-/-}$ macrophages with acLDL and rhLAL also resulted in a ~4.3-fold increase in cholesterol re-esterification relative to acLDL loaded $lal^{+/+}$ macrophages. An increase in cholesterol re-esterification significantly above levels observed in acLDL loaded $lal^{+/+}$ macrophages following rhLAL treatment in acLDL loaded $lal^{-/-}$ macrophages was consistent with the observed ~2-fold higher uptake of acLDL in $lal^{-/-}$ macrophages (**refer to Figure 2.3 legend**) and perhaps lysosomal sequestration of endogenous cholesteryl esters derived from cytosolic compartments via lipophagy (87). These results further demonstrate dysregulation of cholesterol homeostasis in $lal^{-/-}$ macrophages with restoration of lysosomal cholesterol release for cholesterol re-esterification following rhLAL treatment, consistent with a previous report in CESD fibroblasts (233).

2.5 Discussion

Lysosomal acid lipase is the sole lysosomal enzyme mediating hydrolysis of cholesteryl esters derived from endocytosed lipoproteins and also stored cholesteryl esters delivered to lysosomes by lipophagy. In the current studies we provide evidence for a critical role of LAL in driving expression of ABCA1 in macrophages, regulation of cellular cholesterol homeostasis, and cholesterol efflux. In addition, we show that reduced cholesterol flux from lysosomes due to LAL deficiency results in impaired oxysterol generation and failure of lipoprotein-derived cholesterol to reach the endoplasmic reticulum for both suppression of de novo cholesterol synthesis and re-esterification via ACAT in macrophages following cholesterol loading with acLDL. Correction of these defects was achieved following treatment with supplemental LAL. These results extend our previous findings of the impaired ABCA1 expression and cholesterol

efflux machinery in fibroblasts of patients with LAL deficiency (25), and indicate a major role for LAL as a regulator of cellular cholesterol homeostasis in macrophages.

Using immortalized peritoneal macrophages, we found reduced basal and lipoprotein-stimulated ABCA1 expression and reduced apoAI-dependent cholesterol efflux in $lal^{-/-}$ compared to $lal^{+/+}$ macrophages, with partial correction of ABCA1 expression and cholesterol efflux from these cells by addition of rhLAL. Supplementation with rhLAL resulted in normalization of elevated radiolabeled cholesteryl esters and an increase in free cholesterol in $lal^{-/-}$ macrophages. This correlated directly with correction of production of 27-hydroxycholesterol, produced in mitochondria by sterol-27-hydroxylase and a necessary driver of ABCA1 expression in macrophages via activation of the nuclear receptor liver X receptor on the promoter region of *ABCA1* (255), in $lal^{-/-}$ macrophages. These results provide evidence that LAL is critical in regulating both the expression of ABCA1 by generating lysosomally-derived cholesterol for 27-hydroxycholesterol production, and by providing a substrate for ABCA1-dependent cholesterol efflux from macrophages. We also found an inability of acLDL loading to suppress new cholesterol synthesis in $lal^{-/-}$ macrophages, and correction of this defect following addition of rhLAL. These results are consistent with a similar inability of LDL loading to suppress new cholesterol synthesis in LAL-deficient human fibroblasts (68). Additionally, treatment with rhLAL in $lal^{-/-}$ macrophages was able to restore cholesterol re-esterification via ACAT, consistent with a previous finding in human fibroblasts (233) and further demonstrating the critical role of lysosomally-derived cholesterol in regulating downstream cholesterol metabolism in cells.

We also noted a significant level of residual hydrolysis of acLDL in $lal^{-/-}$ macrophages. This is apparently non-lysosomal, as incubation of $lal^{-/-}$ macrophages with chloroquine did not

further reduce CE hydrolysis in the cells (**Figure 2.4**). Despite this finding, this level of hydrolysis did not appreciably affect ABCA1 regulation, further supporting the conclusion that release of lysosomally-derived UC is a key regulator of regulatory oxysterol production and ABCA1 expression, but not cholesterol derived from non-lysosomal CE hydrolysis.

A very recent publication has also found that knockdown of *LIPA* in macrophages derived from human pluripotent stem cells abolished apoAI-mediated efflux of cholesterol derived from ^{3}H-CE-acLDL, but did not find a relationship between *LIPA* and expression of ABCA1 in these cells (234). The reasons for this difference from those in the current studies are not clear. Our previous results using human fibroblasts (25) and results presented here with immortalized mouse peritoneal macrophages are consistent in showing a clear relationship between LAL activity and ABCA1 expression, and are also consistent with our previous findings of the critical role of lysosomally-derived cholesterol in regulating ABCA1 in Niemann Pick Disease Type C (26, 244).

Our *in vitro* results using wild type and lal$^{-/-}$ macrophages clearly indicate LAL as key regulator ABCA1 expression, oxysterol formation, and new cholesterol synthesis (summarized in **Figure 2.8**).

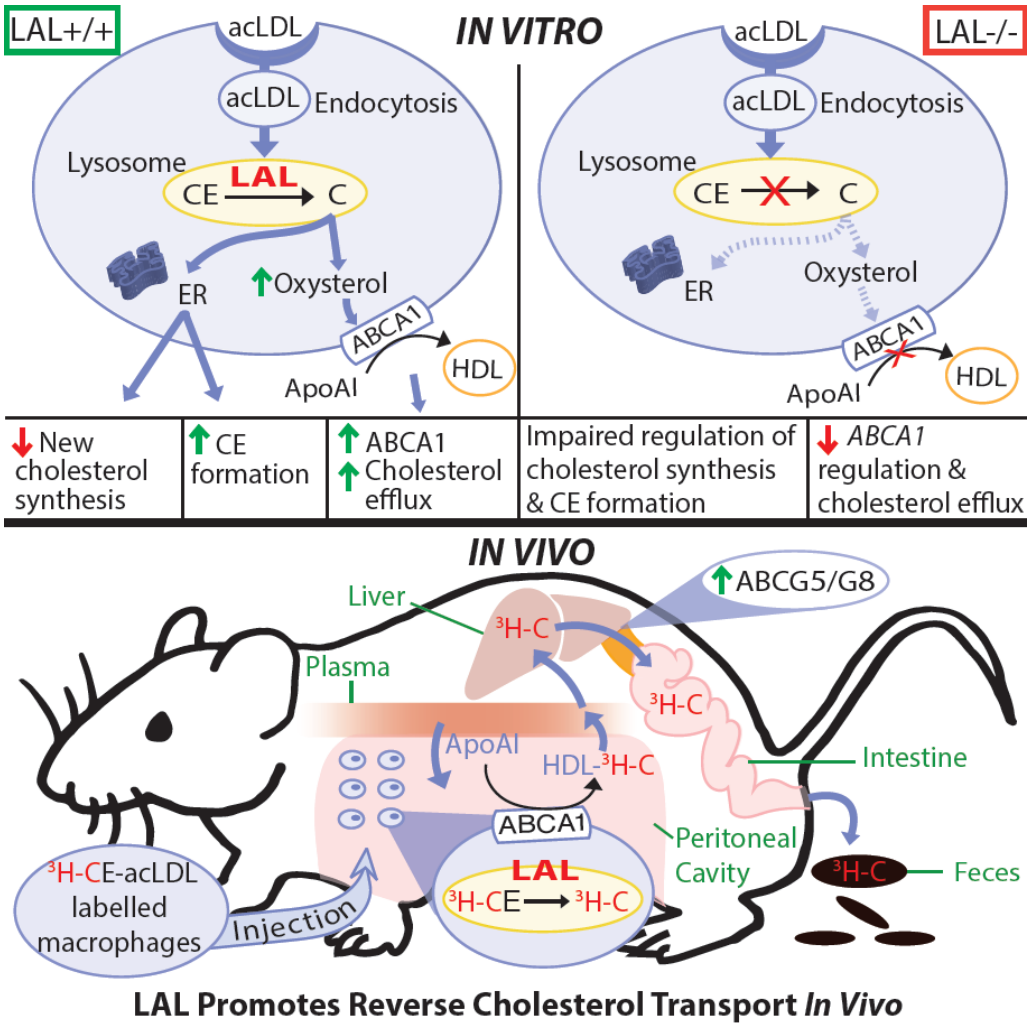

Figure 2.8 LAL promotes reverse cholesterol transport
Graphic created by Josephine Francis.

In addition to our *in vitro* results regarding the critical role of LAL in macrophage cholesterol homeostasis and efflux, we have also investigated the importance of LAL for whole-body reverse cholesterol transport (RCT) (256). *In vivo* RCT experiments using LAL-deficient and wild type mice were conducted by Kristin Bowden (indicated in **Figure 2.8**). $Lal^{+/+}$ and $lal^{-/-}$ macrophages were loaded with [^{3}H]-cholesteryl oleate-labeled acLDL and then injected intraperitoneally into LAL-deficient or wild type mice. LAL-deficient mice injected

intraperitoneally with [^{3}H]-CE labelled acLDL lal$^{-/-}$ macrophages exhibited only 1.55±0.35% total injected [^{3}H]-cholesterol counts appearing in the feces over 48 hrs, compared with 5.38±0.92% in lal$^{+/+}$ mice injected with labeled lal$^{+/+}$ macrophages ($p<0.001$). In order to mimic the therapeutic condition of peripheral delivery of supplemental LAL *in vivo*, lal$^{-/-}$ macrophages were injected intraperitoneally into lal$^{+/+}$ mice, resulting in a significant increase in RCT (2.60±0.46% of ^{3}H-cholesterol counts in feces over 48 hours; $p<0.001$ when compared with injection into lal$^{-/-}$ mice). Consistent with the role of lysosomal cholesterol release for regulation of LXR target genes, lal$^{-/-}$ mice displayed reduced hepatic levels of ABCG5 and ABCG8 relative to lal$^{+/+}$ mice (256). The hepatocyte LXR dependent genes ABCG5 and ABCG8 (257) are necessary for transport of hepatic cholesterol into bile (258). Reduced hepatic levels of ABCG5 and ABCG8 are consisent with subsequent reduced appearance of ^{3}H-cholesterol in the feces of lal$^{-/-}$ mice (256). Our results indicate that LAL is critically important for both regulation of macrophage cholesterol metabolism and efflux, and also whole-body RCT for excretion of cholesterol via the liver.

2.6 Conclusion

In conclusion, these results implicate LAL as a key regulator of cellular cholesterol metabolism including expression of ABCA1 in mouse peritoneal macrophages. Our results clearly demonstrate a beneficial role of LAL supplementation in a deficient state for restoration of cholesterol metabolism and removal of excess cholesterol to apoA-I for subsequent systemic transport back to the liver for excretion via the liver. This suggests that treatment with rhLAL in individuals genetically deficient in LAL may increase reverse cholesterol transport and potentially reduce the elevated risk of premature atherosclerosis. Additionally, in individuals not genetically deficient in LAL it is unknown whether or not a relative deficiency in LAL exists

between different cell types present in atherosclerotic lesions, specifically macrophages and smooth muscles cells, and what cholesterol metabolism difference exist between these cells. The studies presented in Chapter 3 investigate this in detail.

Chapter 3: Arterial SMCs express low levels of LAL relative to macrophages leading to defects in cholesterol metabolism pathways

3.1 Summary

Previous studies by our laboratory have indicated that in addition to macrophages, smooth muscle cells (SMCs) contribute significantly to the foam cell population during the pathogenesis of atherosclerosis. Mechanisms by which macrophages lysosomally process and store excess cholesteryl esters (CEs) derived from atherogenic lipoproteins like low density lipoprotein (LDL) have been extensively characterized, however relatively little is known about SMCs. Release of lipoprotein-derived free cholesterol (FC) from lysosomes upregulates expression of key proteins involved with cellular cholesterol removal such as the ATP-binding cassette transporter A1 (ABCA1), down regulates synthesis of new cholesterol, and increases the acyl-CoA cholesterol acyltransferase (ACAT) substrate pool for cytoplasmic lipid droplet formation. Comparison of these processes indicated that SMCs have reduced lysosomal processing of lipoprotein derived CEs relative to macrophages. Here we report that lysosomal hydrolysis of lipoprotein-derived CEs in SMCs is markedly reduced relative to macrophages as a result of low expression of lysosomal acid lipase (LAL), the sole acidic CE hydrolase. We find the activity of LAL to be 23.4-times lower in aggregated LDL (agLDL)-loaded SMCs relative to macrophages. Treatment of SMCs with LAL-containing medium was able to increase lysosomal CE hydrolysis, reduce new cholesterol synthesis, and enhance efflux to apolipoprotein A1 (apoA1). Interestingly LAL treatment did not have major effects on expression of ABCA1, likely resulting from a combination of low sterol 27-hydroxylase (CYP27A1) and low liver X receptor

(LXR) levels in SMCs compared to macrophages. Despite a lack of major ABCA1 response, increasing LAL in arterial SMCs allowed CEs in lysosomes to be hydrolyzed to FC and become available for efflux. Collectively, our findings now identify low expression of LAL by arterial SMCs as a new mechanism of intracellular lipid retention in atherosclerosis and a potential target of lesion localized therapeutics.

3.2 Introduction

Atherosclerosis is the major cause of heart attacks and strokes, together the leading cause of death worldwide, and the foremost contributor to other circulatory disorders including peripheral vascular disease and aortic aneurysms (1). Fundamentally, plaque formation is driven by the accumulation of cholesteryl esters (CEs) derived from low density lipoprotein (LDL) and other apolipoprotein B (apoB)-containing lipoproteins within the intima of the arterial wall (35, 259). Formation of the human intima begins early in life and is composed mostly of smooth muscle cells (SMCs) and their secreted matrix proteoglycans (169, 170). Over decades the intima thickens and as a result of charge-charge interactions with these matrix proteoglycans, LDL and apoB-containing lipoproteins are retained in the subendothelial space leading to foam cell formation and appearance of a fatty streak. Previous reports using human tissues have suggested that a significant amount of the foam cells found in early atherosclerosis are of SMC origin (17, 18, 168) and are located in the deep intima (18) away from sites of initial macrophage arterial infiltration (175). Building on these initial qualitative observations, our laboratory recently quantified the amount of SMC foam cells found in intermediate human coronary artery atherosclerosis and found that on average ≥50% of the foam cells in these lesions are of SMC and not macrophage origin (24). As the majority of reports regarding cholesterol metabolism, foam cell formation, and lesion regression in atherosclerosis are generally in relation to

macrophages, our findings indicate that further investigation of SMCs is needed to fully understand cholesterol deposition and lesion formation at the cellular level. These studies will have critical importance in furthering our understanding of the fundamental pathogenesis of atherosclerosis, and suggest novel strategies to combat this leading cause of death and mortality worldwide.

Both macrophages and SMCs within the artery wall can become foam cells through excess uptake of modified forms of LDL (aggregated and/or oxidized forms) by phagocytosis and scavenger receptors (227, 260). The CEs within the core of endocytosed lipoproteins are hydrolyzed to free cholesterol (FC) in lysosomes through the actions of lysosomal acid lipase (LAL) (227, 233). Egress of cholesterol from lysosomes is then facilitated by the interactions of the soluble protein Niemann Pick type C2 (NPC2) with the lysosomal membrane protein Niemann Pick type C1 (NPC1) (243, 251). Excess lysosomally-released FC that reaches the endoplasmic reticulum (ER) can be converted back to CEs via acyl-CoA cholesterol acyltransferase (ACAT) for storage in cytosolic lipid droplets leading to a “foamy” appearance (261). The lysosomally-derived cholesterol pool also plays a key role in the ER by inhibiting new cholesterol synthesis through interaction with the sterol regulatory element-binding protein (SREBP) cleavage-activating protein (SCAP) (65, 262). Additionally, the flux of lysosomal cholesterol effects the expression of proteins involved in cholesterol removal via conversion of FC to oxysterols that subsequently bind to the nuclear liver X receptor (LXRs) promoting gene transcription (263, 264). One of these genes is the plasma membrane protein ATP-binding cassette transporter A1 (ABCA1) that facilitates cholesterol efflux to apolipoprotein AI (apoAI), the initial step in formation of high density lipoprotein (HDL) particles for reverse cholesterol transport (67). The importance of lysosomally-derived cholesterol in the regulation of ABCA1

expression has been demonstrated previously by our laboratory in the lysosomal cholesterol disorders Cholesteryl Ester Storage Disease (CESD) (25) and Niemann Pick type C (27, 265). The genetic mutations causing deficiency in LAL and NPC1 or NPC2 result in profound lysosomal accumulations of CE and FC respectively (266, 267). Lysosomal processing of lipids is, therefore, a key regulatory step in cholesterol homeostasis and may play an important role in the progression and regression of atherosclerosis.

We have found in the intima of human advanced atherosclerotic coronary arteries that SMCs express lower levels of ABCA1 compared to macrophages (24). This observation combined with our knowledge of the importance of lysosomal release of cholesterol for ABCA1 regulation suggested that SMCs, relative to macrophages, may exhibit marked differences in cellular cholesterol metabolism beginning with lysosomal processing of lipoprotein-derived CE. In light of the significant SMC contribution to the foam cell population in atherosclerosis and the fundamentally different physiological roles SMCs and macrophages have in the arterial wall, we now investigate the following questions: (i) is reduced ABCA1 expression in SMCs relative to macrophages associated with differences in cellular cholesterol metabolism; (ii) do SMCs have an inherent phenotype resulting in lysosomal lipid accumulation; and (iii) how might cholesterol metabolism and removal be positively enhanced in SMCs?

3.3 Materials and methods

3.3.1 Materials

Chemicals and reagents used were as follows: cholesterol, cholesteryl oleate, 4-methylumbelliferyl oleate (4-MUO), 4-methylumbelliferone (4-MU), L-α-phosphatidylcholine from egg yolk, and sodium taurodeoxycholate were from Sigma-Aldrich (St. Louis, MO, USA). Sodium acetate and Triton X-100 were from BDH VWR (Radnor, Pennsylvania, USA).

Cholesterol-d7, 27-hydroxycholesterol, and 27-hydroxycholesterol-d6 were obtained from Avanti Polar Lipids, Inc. (Alabaster, AL, USA). [1-^{14}C]-oleate, RS-[5-^{3}H]-mevalonolactone, and cholesteryl oleate [cholesteryl-1,2-^{3}H(N)] were from PerkinElmer (Waltham, Massachusetts, USA). ApoA-I was from Academy Bio-Medical Company (Houston, TX, USA). Methanol, isopropanol, hexanes, and chloroform were all of HPLC grade and purchased from Fisher Scientific (Fair Lawn, NJ, USA). Anhydrous ethyl alcohol was obtained from GreenField Specialty Alcohols Inc. (Brampton, ON, Canada). Butylated hydroxytoluene and Bafilomycin A_1 were from Sigma (St. Louis, Missouri, USA). Potassium hydroxide was purchased from EM Science (Darmstadt, Germany). Normal goat serum was from Life Technologies (Carlsbad, California, USA). The slide mounting media used for microscopy were ProLong Diamond Antifade Mountant from Molecular Probes, Inc.
(Eugene, Oregon, USA) or Fluoromount Aqueous Mounting Medium from Sigma-Aldrich. Complete Mini Protease Inhibitor tablets were from Roche Applied Science (Mannheim, Germany). Nitrocellulose membranes were from Pall Life Sciences (Port Washington, New York, USA). SDS-PAGE supplies and pre-stained protein molecular weight standards were from Bio-Rad (Hercules, California, USA). Super Signal West Femto chemiluminescence substrate was from ThermoFisher Scientific (Waltham, Massachusetts, USA). SYBR Safe DNA gel stain and 100 bp ladder were from Invitrogen (Carlsbad, California, USA). Syber green was from Qiagen (Toronto, Ontario, Canada). Whatman pre-SIL G plastic-backed flexible plates used for thin layer chromatography analysis were from ThermoFisher Scientific. 30 kDa centrifugal concentrators were from Pall Corporation (Port Washington, New York, USA).

Antibodies and fluorescent dyes used were as follows: rabbit polyclonal anti-LAMP1 primary antibody was from Abcam (Cambridge, Massachusetts, USA), rabbit polyclonal anti-

ABCA1 primary antibody and mouse monoclonal anti-β-actin primary antibody were from Novus Biologics (Littleton, Colorado, USA), rabbit IgG polyclonal anti-LAL primary antibody was from OriGene Technologies, Inc. (Rockville, Maryland, USA) or MyBioSource (San Diego, California, USA), and mouse monoclonal IgG anti-CD45 was from R&D Systems (Minneapolis, Minnesota, USA). HiLytePlus 555 goat anti-mouse IgG secondary antibody was from Anaspec (Fremont, California, USA). Alexa Fluor 594-conjugated goat anti-mouse IgG secondary antibody was from Invitrogen. Alexa Fluor 633-conjugated goat anti-rabbit IgG secondary antibody was from Molecular Probes, Inc. The fluorescent dyes BODIPY 493/503, Hoechst 33342, and Lysotracker Red DND-99 were from Molecular Probes, Inc. Filipin was from Sigma-Aldrich. DQ Red BSA was from Life Technologies (Carlsbad, California, USA).

Cell culture materials used were as follows: DMEM and RPMI 1640 were from Hyclone (Logan, Utah, USA); fetal bovine serum (FBS) and penicillin/streptomycin antibiotic were from Gibco; fatty acid free bovine serum albumin (FAFA) was from Sigma Aldrich; TC-coated cell culture plates were from Corning. Lipoprotein deficient serum (LPDS) was prepared by removing lipoproteins by density ultracentrifugation followed by extensive dialysis in a 150 mM NaCl, 50 mM Tris-HCl and 0.3M EDTA buffer at pH 7.4.

3.3.2 Isolation, radiolabeling, and modification of LDL

Pooled human plasma from healthy donors was used to isolate LDL by gradient ultracentrifugation (235). Radiolabeling of LDL with ^{3}H-cholesteryl oleate was performed as previously described (236). Aggregates of LDL were prepared by vortexing in PBS for 60 seconds as previously described (268).

3.3.3 Cell culture of human SMCs and mouse SMCs

Human aortic SMCs isolated from the abdominal aorta of an 11-month-old child (CRL-1999) were obtained from American Type Culture Collection (Manassas, VA). Mouse aortic SMCs were isolated from 4-week-old Balb/c mice. Both human and mouse SMCs were grown in DMEM supplemented with 10 % FBS and used for experiments at a confluency of ~60 % between the 8^{th} and 14^{th} passage after receiving the cell line.

3.3.4 Isolation and differentiation of human monocytes

Human peripheral blood mononuclear cells (PBMCs) were isolated from healthy donors and differentiated into macrophages as previously described (269). Collection was in accordance with the ethical approval guidelines of the University of British Columbia. Briefly, after PBMC isolation in PBS by density gradient centrifugation using Lymphoprep (StemCell Technologies, Vancouver, Canada) cells were re-suspended in serum-free RPMI 1640, plated at, 1-2x10^6 cells/mL and rested for 45 minutes before changing the medium to RPMI 1640 containing 10% FBS (day 1). After 24 hours the medium was refreshed and supplemented with recombinant human macrophage-colony stimulating factor (M-CSF) (StemCell Technologies, Vancouver, BC) at a final concentration of 10 ng/mL. On day 6 the cells were washed and the medium was again refreshed with medium containing 10 ng/mL M-CSF. After 24 hours cells were again washed and used for experiments. HMMs were found to express the macrophage specific marker CD45 and not SM α-actin, whereas SMCs were found to express SM α-actin and not CD45 as determined by flow cytometry and Western blot analysis.

3.3.5 Lipid loading of macrophages and SMCs

Experiments using HMMs and SMCs or mouse RAW 264.7 monocytes/macrophages (American Type Culture Collection, TIB-71) and mouse aortic SMCs (mSMC) were conducted

in parallel. Cells were first washed with PBS containing 1 mg/mL FAFA (fatty acid free albumin) followed by PBS alone and then treated with RPMI (macrophages) or DMEM (SMCs) medium containing 10% LPDS. After 24 hours cells were again washed with PBS containing 1 mg/mL FAFA followed by PBS alone and then treated with medium containing 2 mg/mL FAFA ± 100 µg/mL LDL or agLDL for 24 hours. Cells were then washed with PBS containing 1 mg/mL FAFA followed by PBS alone and either collected immediately or equilibrated for a further 24 hours in medium containing 1 mg/mL FAFA. All cell culture experiments were maintained in a humidified incubator at 37 ^{o}C with 5% CO_2 and all mediums used were supplemented with 1% penicillin/streptomycin.

3.3.6 LC/MS/MS analysis of total cholesterol, free cholesterol, and cholesteryl esters

HMMs and SMCs were cultured in 12-well plates, lipid loaded as described in **Section 3.3.5**, and then placed on ice and washed extensively with PBS containing 1 mg/mL FAFA followed by PBS alone. Plate wells were then treated with 1 mL of hexanes:isopropanol (3:2) at room temperature for 20 minutes, similar to previously described (247). The solvent extracts were transferred to 75x100 mm glass test tubes and the cell monolayers were quickly re-extracted with an additional 1 mL of solvent. The extracts were combined and evaporated under a positive stream of air using a heating block. Ethanol (2 mL) and 4 µg/mL cholesterol-d7 (100 µL) were added to the residues and the samples were then quickly vortexed followed by 5 minutes of sonication in a water bath sonicator at room temperature. For total cholesterol analysis 1 mL of the reconstituted samples were then transferred to 75x100 mm screw capped test tubes. The remaining sample in the glass test tubes was evaporated under a positive stream of air using a heat block for free cholesterol analysis. Hydrolysis of cholesteryl esters for total cholesterol analysis was achieved by addition of 1 mL of 0.625 N ethanoic potassium hydroxide

(KOH) containing trace amounts of deionized water to the screw capped test tubes followed by vortexing and heating in a water bath at 80 ^{o}C for 30 minutes. The solvent was then evaporated under a positive stream of air in a heating block. Extraction by the method of Folch, *et al*.(240) was performed by the addition of 1 mL of deionized water and 4 mL of chloroform:methanol (2:1) to the screw capped test tubes. After vortexing and equilibration at room temperature, the aqueous upper layer was suctioned off. The organic layer was then washed by adding 1 mL of deionized water. After removing the aqueous layer, the organic solvent was evaporated under a positive stream of air using a heating block. The residues of the test tubes for both free cholesterol and total cholesterol analysis were then reconstituted with 200 µL of methanol. After vortexing and 5 minutes of sonication in a water bath sonicator at room temperature the samples were transferred to a 96-well plate and 30 µL was analyzed by LC/MS/MS.

Masslynx 4.1 software was used to control a sample manager (Waters model 2777C), HPLC (Waters model 1525µ binary pump), and triple quadrupole mass-spectrometer (Waters Quattro Micro^{TM}). Chromatography was performed using a Phenomenex Luna 5µ C8 110Å 50x2.0 mm column with a 0.5 micron pre-column depth filter. Elution solvents were de-ionized water + 0.1% formic acid (A) and methanol + 0.1% formic acid (B) at a flow rate of 0.4 mL/min (solvent gradient: 0 min, 50% B; 1 min, 50% B; 1.5 min, 95% B; 7 min, 95% B; 7.1 min, 50% B; 12 min, 50% B). Cholesterol eluted at approximately 4.7 minutes. Pre and post-sample injection needle-washes and valve-washes was performed using de-ionized water:methanol (1:1) and methanol:isopropanol (80:20).

Cholesterol and the internal standard cholesterol-d7 were detected by multiple-reaction monitoring (MRM) using mass spectrometry (MRM m/z: cholesterol 369.2>161.0, cholesterol-d7 376.2>161.0). The mass spectrometer was operated in positive atmospheric chemical

ionization (APCI+) mode with instrument parameters as follows: Nitrogen was used as the desolvation gas at a flow rate of 200 L/h and temperature of 450 ^{o}C. The ion source temperature was 130 ^{o}C with the corona needle set to 5 μA and the cone voltage set to 30 V. The cone gas (nitrogen) was set to 30 L/hr. The extractor and RF lens voltages were set to 2.2 and 0.2 V respectively. Q1 parameters were: LM 1 resolution 14.0; HM 1 resolution 14.0; ion energy 0.1. Argon was used as the collision cell gas at a pressure of 4.3 e^{-3} mbar and the collision cell energy was set to 25 eV. The collision cell entrance and exit potentials (V) were set to 0 and 1 respectively. Q3 parameters were: LM 1 resolution 13.0; HM 1 resolution 13.0; ion energy 2.0. The detector multiplier was set to 650 V.

Quantlynx 4.1 software was used to analyze MRM data. The amount of cholesterol was determined using the peak area ratio of cholesterol to cholesterol-d7 and calibration curves ($R^2 >$ 0.99, 1/x regression weighting, range: 0.259 to 77.6 nmols) generated from spiked standards that were extracted as described above. Cholesteryl ester content was calculated by subtracting the free cholesterol from the total cholesterol amount found in each sample. The amount of free cholesterol, total cholesterol, and total cholesteryl esters was normalized to mg of cell proteins as determined by the method of Lowry (245). To validate our LC/MS/MS method we analyzed the total cholesterol in 5 human heparin plasma samples and compared against results determined by routine enzymatic method in the St. Paul's Hospital Pathology Laboratory (Siemens Advia 1800 analyzer using the cholesterol_2 method). The percent difference, indicated as median (range), in total cholesterol determined by LC/MS/MS and enzymatic method was only 2.6% (0.5, 10.9).

3.3.7 LC/MS/MS analysis of 27-hydroxycholesterol production

HMMs and SMCs were cultured in 60 mm dishes and lipid loaded with equilibration as described in **Section 3.3.5**. Dishes were then placed on ice and the media (2 mL) was transferred

to 13x100mm glass screw capped tubes. Cells were then washed with PBS once and collected by scraping in 500 µL of PBS. The cell extracts were homogenized with metal beads using a TissueLyser LT (Qiagen) and 400 µL of the cell lysate was then added to the medium. The internal standard 27-hydroxycholesterol-d6 (50 µL of a 50 ng/mL solution in methanol) was added followed by the addition of 2 mL of hexanes containing 20 µg/mL butylated hydroxytoluene. Samples were vortexed, set at room temperature for 10 minutes, followed by centrifugation at 500 rpm for 1 minute. The aqueous layer was re-extracted and the organic layers were combined in clean 13x100 mm glass test tubes. The solvent was removed under a positive pressure of nitrogen without heating. Residues were reconstituted with 100 µL of methanol. After vortexing and brief sonication in a water bath sonicator at room temperature the samples were transferred to a 96-well plate and 40 µL was analyzed by LC/MS/MS. ABSCIEX Analyst software version 1.6 was used to control a Shimadzu Prominence HPLC system and an ABSCIEX 5500 triple quadrupole mass spectrometer. Chromatography was performed using a Phenomenex Luna 3µ C18 100Å 50x2.0 mm column with a 0.5 micron pre-column depth filter (oven heated to 50 ^{o}C). Elution solvents were de-ionized water + 0.1% formic acid (A) and methanol + 0.1% formic acid (B) at a flow rate of 0.4 mL/min (solvent gradient: 0 min, 50% B; 2 min, 50% B; 9 min, 98% B; 14 min, 98% B; 14.2 min, 50% B; 18 min, 50% B). 27-hydroxycholesterol eluted at approximately 9.65 minutes.

27-hydroxycholesterol and the internal standard 27-hydroxycholesterol-d6 were detected by multiple-reaction monitoring (MRM) using mass spectrometry (MRM m/z: 27-hydroxcholesterol 385.2>109.0, 27-hydroxycholesterol 391.4>161.1). The mass spectrometer was operated in APCI+ mode with instrument parameters as follows: CE (27-hydroxcholesterol) 37 V, CE (27-hydroxycholesterol-d6) 30 V, nitrogen CAD gas at high setting, GS1 50, GS2 0,

nitrogen CUR gas 35, nebulizer current 4, TEM 550 ºC, DP 100 V, EP 10 V, CXP 15 V, vacuum gauge 3.1 x $10e^{-5}$ Torr, unit resolution for Q1 and Q3, and detector CEM 2200.

ABSCIEX Analyst 1.6 software was used to analyze MRM data. The amount of 27-hydroxycholesterol was determined using the peak area ratio of 27-hydroxycholesterol to 27-hydroxycholesterol-d6 and calibration curves ($R^2 > 0.99$, $1/x^2$ regression weighting, range: 0.05 to 50.0 ng) generated from spiked standards that were extracted as described above. The amount of 27-hydroxycholesterol was normalized to mg of cell proteins as determined using reagents from Bio-Rad.

3.3.8 Mevalonolactone incorporation assay

Regulation of cholesterol synthesis with lipid challenge was investigated in HMMs and SMCs by incorporation of RS-[5-^{3}H]-mevalonolactone, a precursor of cholesterol. Cells were grown and lipid loaded in 12 well plates as described above for 24 hrs in the presence of 0.5 µCi/mL of [^{14}C]mevalonolactone and then washed extensively with cold PBS, followed by PBS containing 1 mg/mL FAFA. Free cholesterol and cholesteryl esters were separated by thin-layer chromatography as previously described (246) and radioactivity was determined by liquid scintillation counting. Mevalonolactone incorporation was reported as the amount of new total cholesterol formed per mg of cell proteins determined by the method of Lowry.(245)

3.3.9 ACAT activity

Cytosolic CE lipid droplet formation in HMMs and SMCs was investigated by analysis of acyl-CoA:cholesterol acyltransferase (ACAT) activity. HMMs and SMCs were grown and lipid loaded in 24 well plates as described above for 24 hrs followed by extensive washing with PBS containing 1 mg/mL FAFA and then incubated for 1 hr at 37 °C with medium containing 9 µM [^{14}C]oleate bound to 3 µM FAFA (246). Cells were then placed on ice, washed with cold

PBS containing 1 mg/mL FAFA followed by cold PBS alone and extracted using hexanes:isopropanol (3:2) (247). Separation of lipid species by thin-layer chromatography was done as previously described (246) and cholesteryl [^{14}C]oleate radioactivity was determined by liquid scintillation counting. ACAT activity was reported as the amount of cholesteryl ester formed per mg of cell proteins as determined by the method of Lowry (245).

3.3.10 Reverse transcription-PCR analysis of ABCA1, ABCG1, and LIPA mRNA

Total RNA was extracted from HMMs and SMCs using Ribozol or Trizol (Amresco). Synthesis of cDNA was conducted by reverse transcription as previously reported.(27) Amplification of *ABCA1*, *LIPA,* and m-cyclophilin mRNA was performed also as previously reported by Choi *et al.*(27) using the following annealing temperatures, cycle numbers, and primers: *ABCA1*, annealing temperature 58.5 ^{o}C, 33 cycles, forward (5'→3') AGT ACC CCA GCC TGG AAC TT, and reverse (5'→3') TGG GTT TCC TTC CAT ACA GCG; *LIPA*, annealing temperature 56.2 ^{o}C, 34 cycles, forward (5'→3') GCT GGC AGA TTC TAG TAA CTG GG, and reverse (5'→3') GCC TTG AGA ATG ACC CAC; *ABCG1*, annealing temperature 60.9 ^{o}C, 32 cycles, forward (5'→3') AAG GCC TAC TAC CTG GCA AAG A, and reverse (5'→3') GCA GTA GGC CAC AGG GAA CA; m-cyclophilin, annealing temperature 58.5 ^{o}C, 33 cycles, forward (5'→3') TCC AAA GAC AGC AGA AAA TTT CG and reverse (5'→3') TCT TCT TGC TGG TCT TGC CAT TCC; mouse *LIPA*, annealing temperature 58.5 ^{o}C, 40 cycles, forward (5'→3') GGC TGA GCA TTC ACG TTT GC, and reverse (5'→3') TTG CAC AGA AGT TCC CGC. PCR products were electrophoresed on a 1.1% agarose gel and detected by SYBR Safe DNA gel stain fluorescence using a GeneFlash (Syngene) detection unit. Mouse *LIPA* mRNA levels were analyzed by using Applied Biosystems® ViiA^{TM} 7 real-time qPCR with SYBR Green detection (Qiagen).

3.3.11 High throughput RNA analysis

HMMs and primary human aortic SMCs isolated from the intima and media of the arterial wall were treated with and without agLDL for 24 hrs as indicated in **Section 3.3.5** and RNA extracted with Ribazole or Triazol (RNA from primary SMCs obtained by collaboration with laboratory of Jean-Baptiste Michel located at the French Institute of Health and Medical Research, Paris Inserm). For high throughput analysis total RNA was hybridized and quantified with the nCounter Analysis System (NanoString Technologies) as per the manufactures protocol. An nCounter Custom CodeSet was created using MTE primers obtained from Integrated DNA Technologies (**Table 3.1**). Data was analyzed using NanoString nSolver 4.0 with normalization to ACTB, B2M, GAPDH, and TUBB. Gene expression profiling of HMMs and aortic SMCs (obtained from ATCC) was also conducted using the Clariom S Assay, Human (ThermoFisher Scientific) on the Affymetrix microarray platform (ThermoFisher Scientific) at McGill University and Génome Québec Innovation Centre. Human cells were lipid loaded as indicated in **Section 3.3.5** for 72 hrs and RNA was extracted with Ribazole, Triazol, or using the RNeasy Kit (Qiagen). Data was analyzed using Transcriptome Analysis Console software with manufacture specified internal normalization.

Gene Name	Accession	FWD Seq	REV Seq	NSID (NanoString internal identifier)
ABCA1	NM_005502.2	TTCGGCTGAGCTACCCAC	GAACAGGCGAGCCACAAT	NM_005502.2:471
ABCG1	NM_207174.1	GGGTCGCTCCATCATTTG	CACCAGCCGACTGTTCTG	NM_207174.1:943
CYP27A1	NM_000784.3	CAGAGAGTGCTTCGGGGA	ACTTGGGGAGGAAGGTGG	NM_000784.3:1083
DHCR24	NM_014762.2	CGTGGAAGGGCTGCTCTA	GCTCCCAGAAGATGCTGC	NM_014762.2:975
HMGCR	NM_000859.2	GAAGCTTTGCCCTTTTTCC	GCAGCCAAAGCAGCACAT	NM_000859.2:555
LDLR	NM_000527.2	TGGATCGTTTGACGGGAC	GGGACGCATTTACGTGCT	NM_000527.2:4625
LIPA	NM_001127605.1	TGGGGATTCCCTAGTGAGG	GTTGCCCATCCACACGTC	NM_001127605.1:406
NPC1	NM_000271.3	TGACCTACCACACCGTGC	CACCAGAAATATCGCGCC	NM_000271.3:3300
NPC2	NM_006432.3	CCGGTGCAGTTCAAGGAC	CAGGCTCAGGAATGGGAA	NM_006432.3:193
LXRα	NM_005693.2	TGCGTCTGCAGGACAAAA	TTTAATGCCACGGGAGGA	NM_005693.2:1575
STARD3	NM_006804.3	AGAAGCGAAGGGCCATCT	CGGCATAGCCTAGGAGCA	NM_006804.3:350

Table 3.1 NanoString Custom Codeset for RNA analysis.

3.3.12 Western blot analysis of ABCA1 and LAL protein

HMMs and SMCs were placed on ice, washed with cold PBS, collected in lysis buffer (0.4% maltoside, 20 mM Tris, 5 mM EDTA, and 5 mM EGTA, and 1x Complete Mini Protease Inhibitor (Roche Applied Science). Samples were then homogenized with metal beads at 50 oscillations per second for 20 seconds using a TissueLyser LT (Qiagen). Cell proteins were determined using reagents from Bio-Rad and 12 µg of protein was used for SDS-PAGE. Samples for LAL analysis were first boiled for 5 minutes and then proteins were separated by 15% SDS-PAGE. Samples for ABCA1 analysis were allowed to stand at room temperature for 1 hour and then proteins were separated by 7.5% (top half) and 12% (bottom half) SDS-PAGE. Proteins were transferred to nitrocellulose overnight (4 ^{o}C) at 35 V. Immunoblotting was performed using a rabbit polyclonal anti-ABCA1 antibody (1:500), a rabbit IgG polyclonal anti- LAL antibody (1:1000), a mouse monoclonal anti-β-actin antibody (1:2000), a goat anti-rabbit IgG horseradish peroxidase-conjugated secondary antibody (1:10,000, Sigma), and a rabbit anti-mouse IgG (whole molecule) peroxidase-conjugated secondary antibody (1:10,000, Sigma).

Chemiluminescence was detected using SuperSignal West Femto (ThermoFisher Scientific) and a GBox Chemi gel imager (Syngene). Densitometry was conducted using ImageJ software.

3.3.13 Lysosensor Yellow/Blue DND-160 Assay

HMMs and SMCs were cultured in black-bottomed 96-well bottomed plates, treated with 10% LPDS in medium for 24 hrs, and then lipid loaded with and without 100 μg/mL agLDL for 24 hrs as described in **Section 3.3.5**. Cells were then washed with PBS and treated with and without 100 nM Bafilomycin A1 for 1.5 hours in medium containing 2 mg/mL FAFA. After washing with PBS, lysosomal compartments were labeled with 100 μL of 100 μM Lyososensor Yellow/Blue DND-60 (ThermoFisher Scientific, Waltham, Massachusetts, USA) in medium containing 2 mg/mL FAFA for 15 min. Cells were then washed twice with PBS, 100 μL of PBS was added to each well and the fluorescence was read using a Tecan Safire II plate reader at 37 ^{o}C. The dual fluorescence emission of Lysosensor Yellow/Blue (pKa 4.2) allows for analysis of changes in lysosomal pH by ratio analysis. At low pH, Lysosensor fluorescence at an excitation of 384 nm and emission of 540 nm increases, whereas at higher pH fluorescence at an excitation of 329 nm and emission of 440 nm increases. Therefore, the acidic/basic ratio of [(384/540)/(329/440)] can then be used to assess for significant changes in lysosomal pH relative to a control as previously reported (54).

3.3.14 DQ-bovine serum albumin assay

HMMs and SMCs were cultured in 12-well plates and lipid loaded with and without 100 μg/mL agLDL or HMM CM for 24 hrs as described in **Section 3.3.5**. Cells were then washed with PBS and treated with 0.5 mL of 5 μg/mL DQ Red BSA (Life Technologies, Carlsbad, California, USA) in medium containing 2 mg/mL FAFA for 2 hrs. DQ Red BSA is a fluorescent derivative of BSA containing high labeling with BODIPY dye. High protein labeling

concentrations of BODIPY are self-quenching, but upon proteolytic hydrolysis to single-dye labeled peptides become strongly fluorescent. After washing with PBS, the cells were equilibrated with and without 100 nM Bafilomycin A1 in medium containing 2 mg/mL FAFA for 2 hrs. HMMs and SMCs were washed with PBS and 200 µL of 50 mM Tris-HCl (pH 8.8) containing 1 % w/v Triton X-100 was added (270). After scraping, 150 µL of the lysate was added to a black flat-bottomed 96-well plate and read using a Tecan Safire II plate reader (excitation 590 nm, emission 620 nm). Fluorescence was normalized to µg of protein as determined using reagent from Bio-Rad.

3.3.15 Lysosomal acid lipase enzyme activity assay

LAL enzyme activity from HMM and SMC or mouse monocyte/macrophage RAW 264.7 and mouse SMC cell lysates and medium was quantified by modification of previously reported methods (40, 249). Cells were cultured and lipid loaded for 24 hrs as described in **Section 3.3.5**. Subsequently the medium was removed and centrifuged at 1100 rpm to remove any dead cells and debris. Cell monolayers were then washed with cold PBS, scraped in 500 µL of PBS, and transferred to 2 mL micro tubes. Cell lysates were homogenized with metal beads at 50 oscillations per second for 20 seconds using a TissueLyser LT (Qiagen). All samples were stored at -80 ^{o}C until analysis. The enzyme substrate was prepared by dissolving 5.5 mg (12.5 µmol) of 4-methylumbelliferyl oleate (4-MUO) in 100 µL of hexanes and combining with 310 µL of a 100 mg/mL L-α-phosphatidylcholine in chloroform solution. After evaporation of the organic solvents with a stream of nitrogen, the lipids were reconstituted with 5 mL of 2.4 mM sodium taurodeoxycholate and sonicated in an ice bath for 3 minutes. 50 µL of the resulting 2.5 mM 4-MUO liposomal substrate was combined with 400 µL of a 0.2 M sodium acetate pH 4.0 buffer. 10-40 µL of medium or cell lysate (approximately between 2 and 10 µg cell proteins as

quantified using reagents from Bio-Rad) was then added, briefly vortexed, and 200 µL of the complete reaction medium was then added to a 96-well black-bottomed plate. The plate was incubated at 37 ºC in a Tecan Safire II plate reader (Mannedorf, Switzerland) and the fluorescence generated by cleavage of 4-MUO to 4-methylumbelliferone (4-MU) was measured at an excitation wavelength of 335 nm and emission wavelength of 455 nm every 5 minutes over the course of 1 hour. Fluorescence was quantified using a standard curved generated from 4-MU in complete reaction medium (calibration range 0.482-20.3 nmol 4-MU). One unit of LAL activity was reported as nmol 4-MU/mg protein/min.

3.3.16 LAMP1 and BODIPY fluorescent cellular staining

HMMs and SMCs or mouse monocyte/macrophage RAW 264.7 and mouse SMC cells were grown on glass cover slips in 24-well plates and were lipid loaded followed by a 24 hour equilibration without lipids as described above. Cells were then washed, fixed with 3% v/v paraformaldehyde (PFA) in PBS for 20 minutes, and blocked with 3% v/v goat serum containing 0.1% w/v saponin in PBS for 30 minutes. After 2 quick washes and a 5 minute wash with 0.1% goat serum containing 0.1% saponin in PBS (now on referred to as saponin buffer), rabbit polyclonal anti-LAMP1 antibody (1:200 in saponin buffer) was applied for 1 hour at room temperature. Following washes with saponin buffer (2x quickly followed by 3x5 minute), AlexaFluor 633-conjugated goat anti-rabbit IgG secondary antibody (1:200 in saponin buffer) was applied for 1 hour at room temperature covered from light. Cells were then washed with saponin buffer (2x quickly followed by 3x5 minutes) and washed with PBS (2x quickly). Subsequently, cells were stained with Bodipy 493/503 (10 µg/mL) for 30 minutes in the dark for visualization of neutral lipids. After washing with PBS (2x quickly followed by 2x5 minutes),

cover slips were dried for 45 minutes in the dark and mounted using ProLong Diamond Antifade Mountant. Slides were imaged using confocal microscopy as indicated below.

3.3.17 Lysotracker red and BODIPY fluorescent cellular staining

HMMs and SMCs were grown on glass cover slips in 24-well plates and were lipid loaded followed by a 24 hour equilibration without lipids as described above. Medium containing 500nM of LysoTracker Red DND-99 was added for 10 minutes for labeling of acidic organelles. BODIPY 493/503 was then spiked into the medium at a final concentration of 5μg/mL and the cells were incubated a further 15 minutes. During fluorescent staining cells were kept at 37^{o}C and 5% CO_2. After removing the medium and washing with PBS, cells were fixed with 3% PFA in PBS for 5 minutes at room temperature. After washing with PBS, cover slips were briefly dried for 5 minutes, the remaining liquid droplets dabbed away with a Kim wipe, and mounted using Fluoromount Aqueous Mounting Medium. Slides were imaged using confocal microscopy as indicated below.

3.3.18 Lysotracker red and filipin fluorescent cellular staining

HMMs and SMCs were grown on glass cover slips in 24-well plates and were lipid loaded followed by a 24 hour equilibration without lipids as described above. Medium containing 500nM of LysoTracker Red DND-99 was added for 15 minutes at 37^{o}C and 5% CO_2 for labeling of acidic organelles. After removing the medium and washing with PBS, cells were fixed with 3% PFA in PBS for 5 minutes at room temperature. After washing with PBS, cellular free cholesterol was stained with filipin (50 μg/mL in PBS) for 20 minutes. Cover slips were briefly dried for 5 minutes, the remaining liquid droplets dabbed away with a Kim wipe, and mounted using Fluoromount Aqueous Mounting Medium. Slides were imaged using fluorescent microscopy as indicated below.

3.3.19 LAMP1 and filipin fluorescent cellular staining

HMMs and SMCs were grown on glass cover slips in 24-well plates and were lipid loaded followed by a 24 hour equilibration without lipids as described above. Cells were then washed, fixed with 3% paraformaldehyde (PFA) in PBS for 20 minutes, and blocked with 3% goat serum containing 0.1% saponin in PBS for 30 minutes. After 2 quick washes and a 5 minute wash with 0.1% goat serum containing 0.1% saponin in PBS (now on referred to as saponin buffer), rabbit polyclonal anti-LAMP1 antibody (1:200 in saponin buffer) was applied for 1 hour at room temperature. Following washes with saponin buffer (2x quickly followed by 3x5 minute), AlexaFluor 633-conjugated goat anti-rabbit IgG secondary antibody (1:200 in saponin buffer) was applied for 1 hour at room temperature covered from light. Cells were then washed with saponin buffer (2x quickly followed by 3x5 minutes), washed with PBS (2x quickly), and treated with 0.15% w/v glycine in PBS for 10 minutes at room temperature. Cellular free cholesterol was then stained with filipin (50μg/mL in PBS) for 30 minutes in the dark. After washing with PBS (2x quickly followed by 2x5 minutes), cover slips were dried for 45 minutes in the dark and mounted using ProLong Diamond Antifade Mountant. Slides were imaged using fluorescent microscopy as indicated below.

3.3.20 LAL and CD45 fluorescent staining of human coronary artery sections

Optimal cutting temperature (OCT)-embedded human coronary artery sections were obtained from the Cardiovascular Registry at St. Paul's Hospital, University of British Columbia. Specimens were from patients with the primary diagnosis of coronary heart disease (approval for use of human tissues was by UBC-PHC Research Ethics Board #H09-00442). For immunofluorescent staining, sections were briefly warmed to room temperature, fixed with 3% PFA for 10 minutes, and washed with PBS. After blocking with 5% goat serum for 20 minutes

slides were washed with PBS and treated with rabbit polyclonal anti-LAL antibody and mouse monoclonal anti-CD45 (1:50 dilution with 1% goat serum for all antibody treatments, incubated overnight at 4 ^{o}C). Slides were then washed (2x quickly followed by a 2x5 minute washes) and the secondary antibodies Alexa Fluor 594-conjugated goat anti-mouse IgG or HylitePlus 555 goat anti-mouse IgG and Alexafluor 633 goat anti-rabbit IgG (1:200 dilutions) were applied for 1 hour at room temperature covered from light. After extensive washes with PBS, BODIPY 493/503 (10 μg/mL) was added for 30 minutes in the dark for visualization of neutral lipids. Nuclei were then stained with Hoechst 33342 (1:5000 dilution) by incubation at room temperature for 10 minutes. Slides were then washed with PBS, dried for 45 minutes in the dark, and mounted using ProLong Diamond Antifade Mountant. Images were collected using confocal microscopy as indicated below.

3.3.21 Microscopy

Confocal images were acquired with a Leica TCS SP8 (Child & Family Research Institute, Vancouver, BC, Canada) using a 63x/1.4 oil immersion objective or a Zeiss LSM 880 (The Centre for Heart Lung Innovation – St.Paul's Hospital, Vancouver, British Columbia, Canada) using a 63x/1.4 oil immersion objective or a 20x/0.8 air objective. The laser lines were: 488 nm for analysis of BODIPY; 543, 561 or 594 nm for analysis of lysotracker red or CD45; and 633 nm for analysis of LAMP1 or LAL. For images acquired with filipin costain, a Leica DMI6000 inverted microscope equipped with a Leica DFC365 FX digital camera was used. Filter cube 1 (analysis of filipin), excitation filter (340-380 nm), dichromatic mirror (400 nm), emission filter (LP 425 nm); filter cube 2 (analysis of LAMP1 or lysotracker red) excitation filter (515-560 nm), dichromatic mirror (580 nm), and emission filter (LP 590 nm). Adjustment of image brightness or color balance was done in Velocity (Leica) or ZEN (Zeiss) software.

Quantitative colocalization or fluorescence intensity analysis on unedited images was conducted in Velocity or Zen software.

3.3.22 Statistical analysis

Results were analyzed using GraphPad Prism version 5.0 for statistical significance between treatment groups. The normality of data for figures was determined by performing a D'Agostino & Pearson omnibus normality test (alpha=0.05) and by visual inspection of normality using Q-Q plots. Normally distributed data was analyzed using parametric tests, either a one-way ANOVA with Bonferroni post-hoc comparisons or a Students T-test, as indicated in the figure legends. Data not normally distributed was analyzed using non-parametric tests, either a Kruskal-Wallis test with Dunn's comparisons or a Mann Whitney test, also as indicated in the figure legends. A p-value <0.05 was considered significant.

3.4 Results

3.4.1 Defective SMC ABCA1 expression is associated with impaired cellular cholesterol metabolism

Previous reports have indicated that a major portion of modified LDL found in human atherosclerotic arteries is aggregated (107, 119). We therefore utilized aggregated LDL (agLDL), to overload both macrophages and SMCs *in vitro* with lipoprotein-derived cholesterol. AgLDL is taken up by macrophages and SMCs via several endocytic internalization mechanisms. In macrophages these include phagocytosis and pinocytosis (117), sequestration in cell surface-connected compartments (a process called patocytosis) (117, 221) and also via low density lipoprotein receptor-related protein 1 (LRP1) (271). In SMCs, uptake of agLDL has been described to occur through LRP1 (224, 272) and also by phagocytosis (119). We analyzed increases in the CE mass after 24 hrs of agLDL treatment by LC/MS/MS in both human

monocyte-derived macrophages (HMMs) and human aortic SMCs. CE mass was determined by subtraction of free cholesterol from the total cholesterol measured (**Figure 3.1 A-C**).

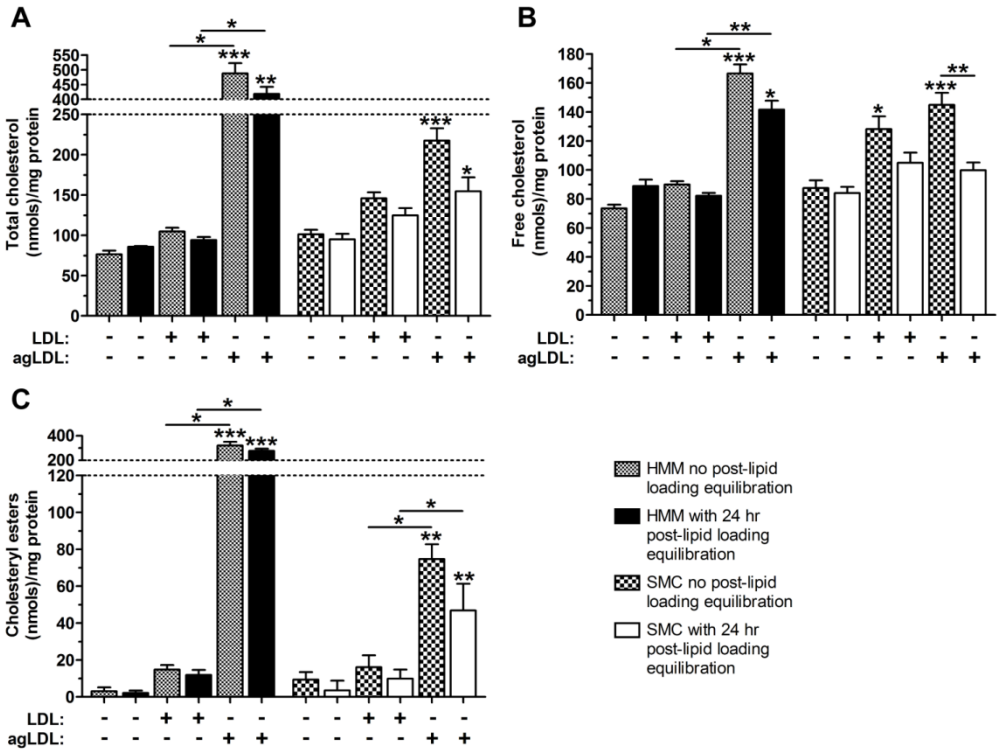

Figure 3.1 Excess lipid accumulation in HMMs and SMCs with agLDL treatment. HMMs and SMCs were cultured as described in the Methods section and subsequently treatment for 24 hrs with medium containing 10% LPDS. Cells were then extensively washed with PBS and fresh medium containing 2 mg/mL FAFA ± 100 µg/mL LDL or agLDL was applied. After 24 hrs, cells were washed and either collected or equilibrated in medium containing 1 mg/mL FAFA for a further 24 hrs. Lipids were then extracted and analyzed by LC/MS/MS for (**A**) TC and (**B**) FC content as described in the Supplemental Methods section. Experimental replicates were normalized to cell protein (mg) and (**C**) CE content was then calculated by subtracting the FC from the TC. Results are mean±SEM for HMMs (3 experiments using different donors with n=3 replicates) and SMCs (3 experiments each with n=3 replicates). Statistical analysis was done using Kruskal-Wallis test with Dunn's comparisons (*p<0.05, **p<0.01, ***p<0.001, statistically different compared to corresponding non-lipid loaded control in each cell type at the same collection time point unless otherwise indicated).

In addition to comparing increases in agLDL-derived CE mass with non-lipid loaded controls, we included a comparison with the highly regulated process of LDL uptake (34) in order to evaluate excess lipid uptake. Exposure of HMMs to agLDL significantly increased CE mass by 106-fold compared to non-lipid loaded controls and by 21-fold relative to LDL treatment. In SMCs, exposure to agLDL significantly increased CE mass by 8-fold compared to non-lipid loaded controls and by 5-fold relative to LDL treatment. No significant differences in the CE mass with or without a 24 hr post-lipid loading equilibration in either cell types were observed. Consistent with the inherent phagocytic role of macrophages (111, 273), our results indicated significantly higher accumulation of agLDL-derived CE in HMMs relative to SMCs ($p<0.05$), which is also consistent with previous reports that SMCs are difficult to lipid load in culture in comparison to macrophages (80, 201, 228, 229, 274, 275).

We then investigated the effect of excess lipid uptake on the expression of ABCA1 in both HMMs and SMCs (**Figure 3.2 A-C**). In response to 24 hrs of agLDL loading, macrophages significantly increased expression of ABCA1 mRNA by 1.6-fold (**Figure 3.2**) and protein by 2.2-fold (**Figure 3.2 B&C**). We found an absence of ABCA1 response to agLDL exposure in SMCs at both the protein and mRNA level, a result consistent with our previous *in vivo* observation of lower ABCA1 expression in SMCs relative to macrophages in human advanced coronary atheromas (24). This was also similar to our previous *in vitro* finding of reduced ABCA1 response to free cholesterol exposure in rat epithelioid SMCs (23). As ABCA1 expression is highly dependent on lysosomal release of cholesterol (25, 27, 265), these findings suggested the presence of acute difference(s) between macrophages and SMCs in regard to lysosomal processing of lipoprotein-derived CE.

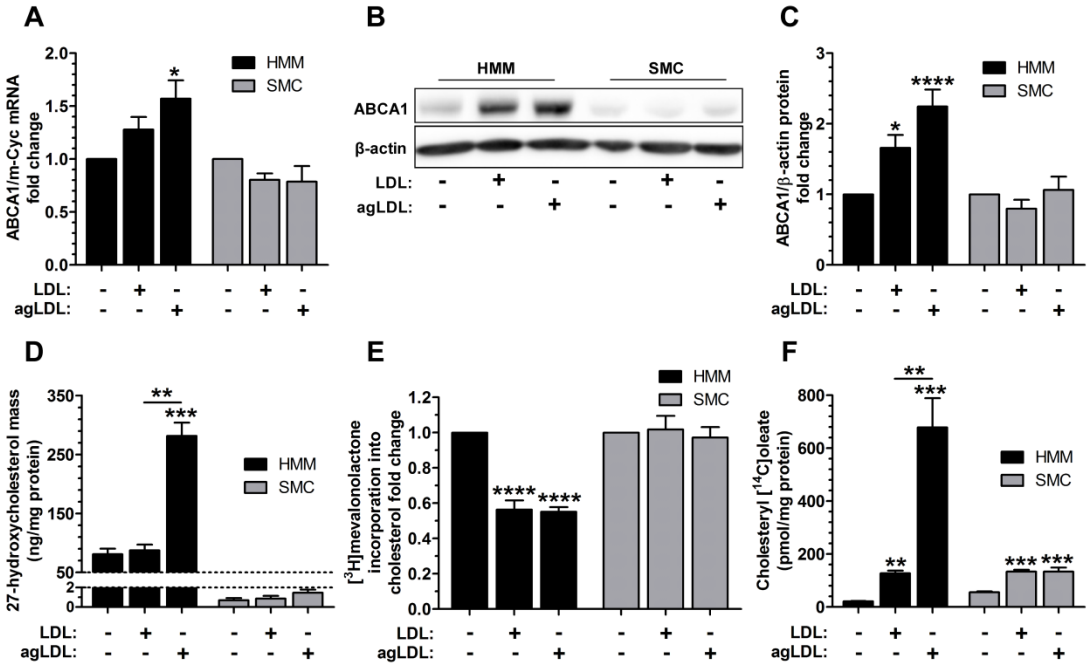

Figure 3.2 SMCs display absence of ABCA1 response and defects in sterol regulatory events downstream of lysosomal processing.

HMMs and SMCs were cultured as described in the Methods section and subsequently treated for 24 hrs with medium containing 10% LPDS. Cells were then extensively washed with PBS and fresh medium containing 2 mg/mL FAFA ± 100 µg/mL LDL or agLDL was applied for 24 hrs. (**A**) RNA extracts were analyzed by PCR using primers for human ABCA1 and m-cyclophilin. Results are fold increase in ABCA1 relative to the non-lipid loaded control in each respective cell type. (**B**) Cell proteins were separated by SDS-PAGE and visualized by Western blot using antibodies for ABCA1 and the loading control β-actin. (**C**) Western blots were analyzed by densitometry and the results expressed as the fold increase in ABCA1 relative to the non-lipid loaded control in each respective cell type. (**D**) Cellular 27-hydroxycholesterol production was performed by lipid loading for 24 hrs as indicated above followed by a further 24 hr incubation in the absence of lipids. The medium and cells were then collected and analyzed for 27-hydroxycholesterol production by LC/MS/MS. (**E**) For evaluation of new cholesterol synthesis, 24 hr lipid loading was performed in the presence of 0.5 µCi/mL of [^{14}C]mevalonolactone. After lipid extraction and TLC separation, the TC radioactivity was determined by liquid scintillation counting. (**F**) Cholesterol re-esterification was evaluated by lipid loading cells for 24 hrs as indicated above, followed by incubation with [^{14}C]oleate for 1 hr. After lipid extraction and TLC separation, cellular cholesterol levels available for esterification were indicated by the radioactivity of cholesteryl [^{14}C]oleate as determined by liquid scintillation counting. Results are mean±SEM (**A**, 6 experiments; **C**, 12 experiments; **D**, 3 experiments with n=3 replicates each; **E**, 4 experiments with n=3 replicates each; **F**, 4 experiments with n=4 replicates each). Statistical analysis was done using (**A**, **C**, **E**) one-way ANOVA with Bonferonni corrections or (**D**, **F**) Kruskal-Wallis test with Dunn's Multiple Comparisons post-hoc test (*p<0.05, **p<0.01, ***p<0.001, ****p<0.0001, statistically different compared to corresponding non-lipid loaded control in each cell type unless otherwise indicated).

We also evaluated the expression of the ATP-binding cassette transporter G1 (ABCG1), another plasma membrane cholesterol transporter LXR target gene (202) involved in lipidation of HDL (68). In response to agLDL loading *ABCG1* mRNA levels increased significantly in HMMs by 2.3-fold but did not increase in SMCs (**Figure 3.3**). Similar to agLDL exposure, regulated lipid uptake with LDL treatment resulted in trends towards higher ABCA1 and ABCG1 expression in HMMs but not SMCs (**Figure 3.2 A-C and Figure 3.3**). This initial data strongly suggested the presence of impaired lysosomal lipoprotein-derived CE metabolism in SMCs relative to macrophages.

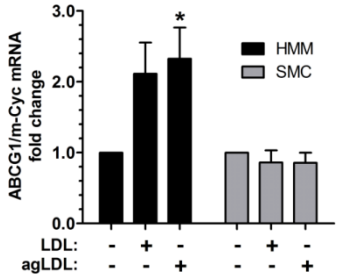

Figure 3.3 SMCs display absence of ABCG1 response to lipid loading.
HMMs and SMCs were treated as described in **Figure 1** with and without 100 µg/mL LDL or agLDL for 24 hrs. RNA extracts were analyzed by PCR using primers for human ABCG1 and m-cyclophilin. Results are fold increase in ABCG1 relative to the non-lipid loaded control in each respective cell type (mean±SEM from 3 experiments). Statistical analysis was done using Kruskal-Wallis test with Dunn's comparisons (*$p<0.05$, statistically different compared to corresponding non-lipid loaded control in each cell type).

An important inducer of ABCA1 and ABCG1 expression is 27-hydroxycholesterol (27-OHC), which has been reported to be the predominant oxysterol found in human atherosclerotic lesions (276-279). Cholesterol released from lysosomes is hydroxylated in the mitochondria by sterol 27-hydroxylase (CYP27A1) to form 27-OHC (263). Sequestration of lipids in lysosomes, as found in CESD, is known to lead to reduced levels of 27-OHC in response to lipid loading (25). We measured by LC/MS/MS the production of 27-OHC after lipid overload as an

indication of lysosomal release of cholesterol (**Figure 3.2 D**). Consistent with normal lysosomal cholesterol release, the mass of 27-OHC significantly increased after agLDL loading by 3.5-fold relative to the non-lipid loaded control in HMMs. In SMCs 27-OHC levels rose by 2.1-fold after agLDL treatment compared to the non-lipid loaded control, but was not found to be significantly different. Exposure to LDL did not significantly increase 27-OHC production in either HMMs or SMCs, consistent with lower lipid accumulation from regulated uptake of LDL. Similar to our results of reduced 27-OHC production in response to acLDL loading in $lal^{-/-}$ mouse peritoneal macrophages relative to wild type (**Figure 2.6 A**), a lack of significantly increased 27-OHC production after agLDL treatment in SMCs initially hinted at an association with decreased lysosomal cholesterol release in SMCs relative to macrophages. Additionally, basal levels of 27-OHC production were 115-fold higher in macrophages than SMCs ($p<0.0001$, Mann-Whitney test), a result consistent with our findings of lower CYP27A1 expression in SMCs compared to macrophages discussed later in this Chapter and also others (280).

Lipoprotein-derived cholesterol released from lysosomes is also trafficked to the ER, where it both downregulates new cholesterol synthesis by inhibition of SREBP mediated gene transcription of enzymes in the cholesterol synthesis cascade and is re-esterified by ACAT for storage in cytoplasmic lipid droplets (65, 281). As expected, new cholesterol synthesis measured by [^{3}H]mevalonolactone incorporation was significantly decreased in HMMs by ~45% with either LDL and agLDL treatment relative to the non-lipid load control (**Figure 3.2 E**). In comparison, there was no significant reduction in new cholesterol synthesis when SMCs were treated with LDL or agLDL, similar to what was found with acLDL treatment of $lal^{-/-}$ macrophages (**Figure 2.6 B**) and also consistent with a previous report of reduced suppression of new cholesterol synthesis in in CESD fibroblasts relative to normal fibroblasts (68). In parallel to

reduced 27-OHC productions, this finding also suggested an association with decreased lysosomal cholesterol release in SMCs relative to macrophages. Consistent with this finding, gene expression of HMG-CoA reductase, the rate limiting enzyme in the cholesterol synthesis pathway, significantly decreased in HMMs after agLDL loading and was less reduced in SMCs (discussed later in this Chapter). Cholesterol re-esterification, determined by incorporation of [^{14}C]oleic acid into newly-formed cholesteryl esters, also referred to here as ACAT activity, was significantly increased in HMMs after agLDL treatment relative to non-lipid loaded (32.2-fold) or LDL loaded (5.3-fold) samples (**Figure 3.2 F**). In SMCs, ACAT activity after agLDL loading was significantly different from the non-lipid loaded control by 2.4-fold, but not different compared to the LDL treatment. Reduced ACAT activity in response to agLDL loading in SMCs compared to macrophages is similar to what was found with acLDL treatment of lal$^{-/-}$ macrophages compared to wild type (**Figure 2.7**) and consistent with a previous report of reduced ACAT activity in response to lipoprotein loading in CESD fibroblasts relative to normal fibroblasts (68). Collectively our initial data showing reduced 27-OHC production, lack of suppression of new cholesterol synthesis, and reduced ACAT activity in response to agLDL loading suggested an association with lysosomal lipid sequestration in SMCs.

3.4.2 SMCs tend to sequester lipoprotein derived CE in lysosomes

We next utilized confocal microscopy to determine whether or not SMCs had higher sequestration of lipoprotein-derived CE in lysosomes relative to macrophages. HMMs and SMCs were lipid loaded with agLDL for 24 hours followed by equilibration without lipids for an additional 24 hours to allow processing of lipids. CEs were identified by the neutral lipid dye BODIPY 493/503 and lysosomal compartments by either lysosomal-associated membrane protein 1 (LAMP1) (**Figure 3.4 A i**) or the pH sensitive small molecule dye Lysotracker (**Figure**

3.4 B i). By visual inspection neutral lipids were primarily localized to cytosolic compartments in HMMs and to lysosomal compartments in SMCs. Quantitative analysis using the Pearson correlation coefficient indicated significantly higher colocalization of BODIPY with LAMP1 (**Figure 3.4 A ii**) or BODIPY with Lysotracker (**Figure 3.4 B ii**) in SMCs compared to HMMs.

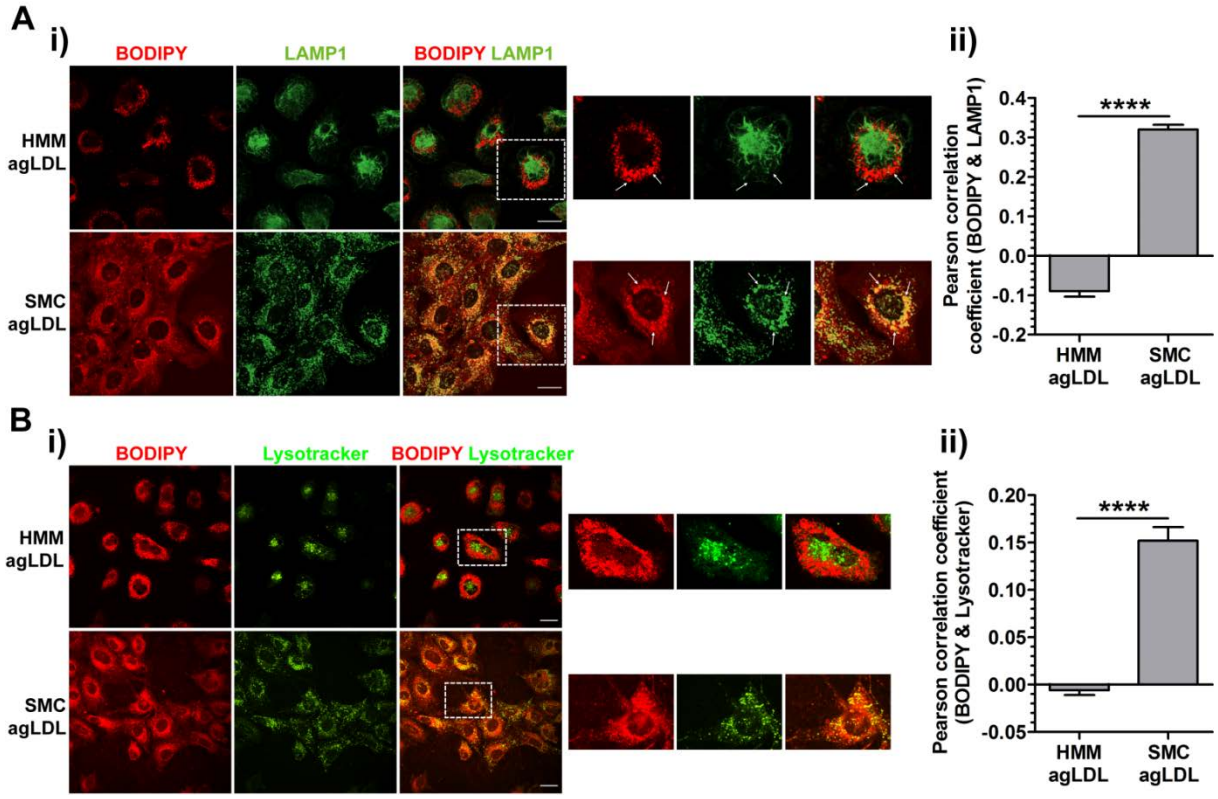

Figure 3.4 Neutral lipid staining patterns are cytosolic in HMMs and lysosomal in SMCs with agLDL loading.
HMMs and SMCs were grown on glass cover slips as described in the Methods section and subsequently treatment for 24 hrs with medium containing 10% LPDS. Cells were then extensively washed with PBS and fresh medium containing 2 mg/mL FAFA and 100 µg/mL agLDL was applied. After 24 hrs, cells were washed and equilibrated in medium containing 1 mg/mL FAFA for a further 24 hrs. As described in the Methods section, cells were then stained with (**A, i**) BODIPY (red) for neutral lipids and LAMP1 (green) antibody for lysosomal compartments or (**B, i**) BODIPY (red) for neutral lipids and lysotracker (green) for lysosomal compartments. Images were obtained by confocal microscopy using a 63x/1.4 oil immersion objective and are representative of (**A**) 6 experiments or (**B**) 4 experiments. Scale bars are 20 µm. Colocalization of BODIPY with either (**A, ii**) LAMP1 or (**B, ii**) Lysotracker was quantified by Pearson correlation (mean±SEM) as determined by analysis of (**A, ii**) n>100 cells from 3 experiments or (**B, ii**) n>55 cells from 2 experiments. Statistical analysis was done using Mann-Whitney test, ****p<0.0001.

Similarly we found significantly higher colocalization of BODIPY with LAMP1 in mouse SMCs compared to mouse RAW 264.7 macrophages loaded with agLDL (**Figure 3.5**).

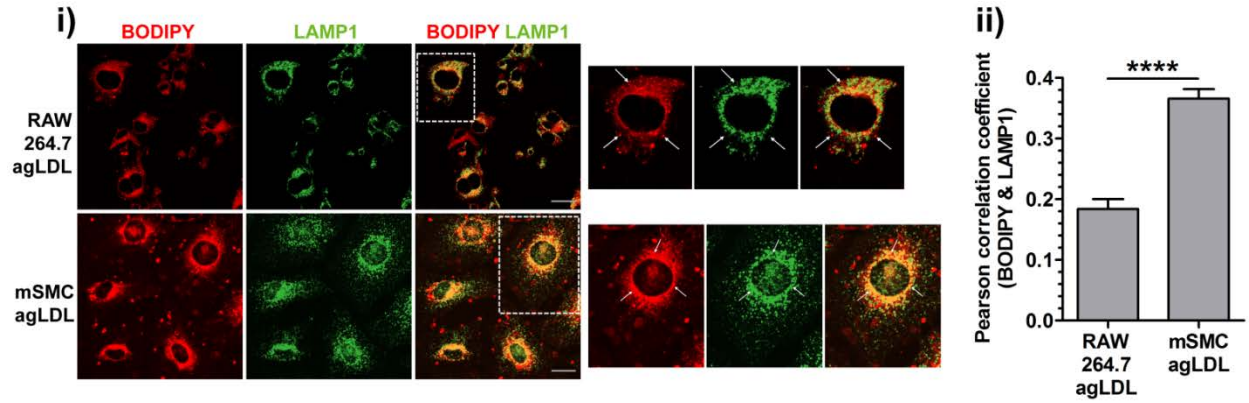

Figure 3.5 Neutral lipid staining patterns are significantly more localized to lysosomes in mouse SMCs compared to mouse macrophages.
Raw 264.67 mouse macrophages and mouse aortic SMCs (mSMC) were grown on glass cover slips as described in the Methods section and subsequently treatment for 24 hrs with medium containing 10% LPDS. Cells were then extensively washed with PBS and fresh medium containing 2 mg/mL FAFA and 100 µg/mL agLDL was applied. After 24 hrs, cells were washed and equilibrated in medium containing 1 mg/mL FAFA for a further 24 hrs. As described in the Methods section, cells were then stained with BODIPY (red) for neutral lipids and LAMP1 (green) antibody for lysosomal compartments. (**i**) Images were obtained by confocal microscopy using a 63x/1.4 oil immersion objective and are representative of 3 experiments. Scale bars are 20 µm. (**ii**) Colocalization of BODIPY with LAMP1 was quantified by Pearson correlation (mean±SEM) as determined by analysis of n>100 cells from 3 experiments. Statistical analysis was done using Students T-test, ****$p<0.0001$.

Additionally supporting our findings, the same cellular CE staining patterns indicated with BODIPY in HMMs and SMCs were found using Nile Red, another commonly used neutral lipid dye (data not shown). These results strongly indicated that CEs derived from excess lipoprotein loading were associated with increased sequestration in lysosomal compartments of SMCs and not HMMs, suggesting major differences in lipid metabolism capacity. Lysosomal CE sequestration in SMCs is therefore the likely reason for our results indicating reduced 27-OHC

production, lack of new cholesterol synthesis suppression, and reduced ACAT activity (**Figure 3.2 D-F**) in response to lipoprotein treatment.

3.4.3 SMCs do not display an affinity for losing lysosomal acidity from excess lipid loading

It has previously been reported that exposure of macrophages to modified forms of LDL, including agLDL, can result in a loss of lysosomal acidity (126, 128), but it is unknown whether or not this is a feature of SMCs. Using the pH sensitive dual fluorescence ratiometric probe Lysosensor Yellow/blue as previously reported (54) we found that after 24 hrs agLDL treatment, HMMs but not SMCs (**Figure 3.6 A**) displayed a significant loss of lysosomal acidity.

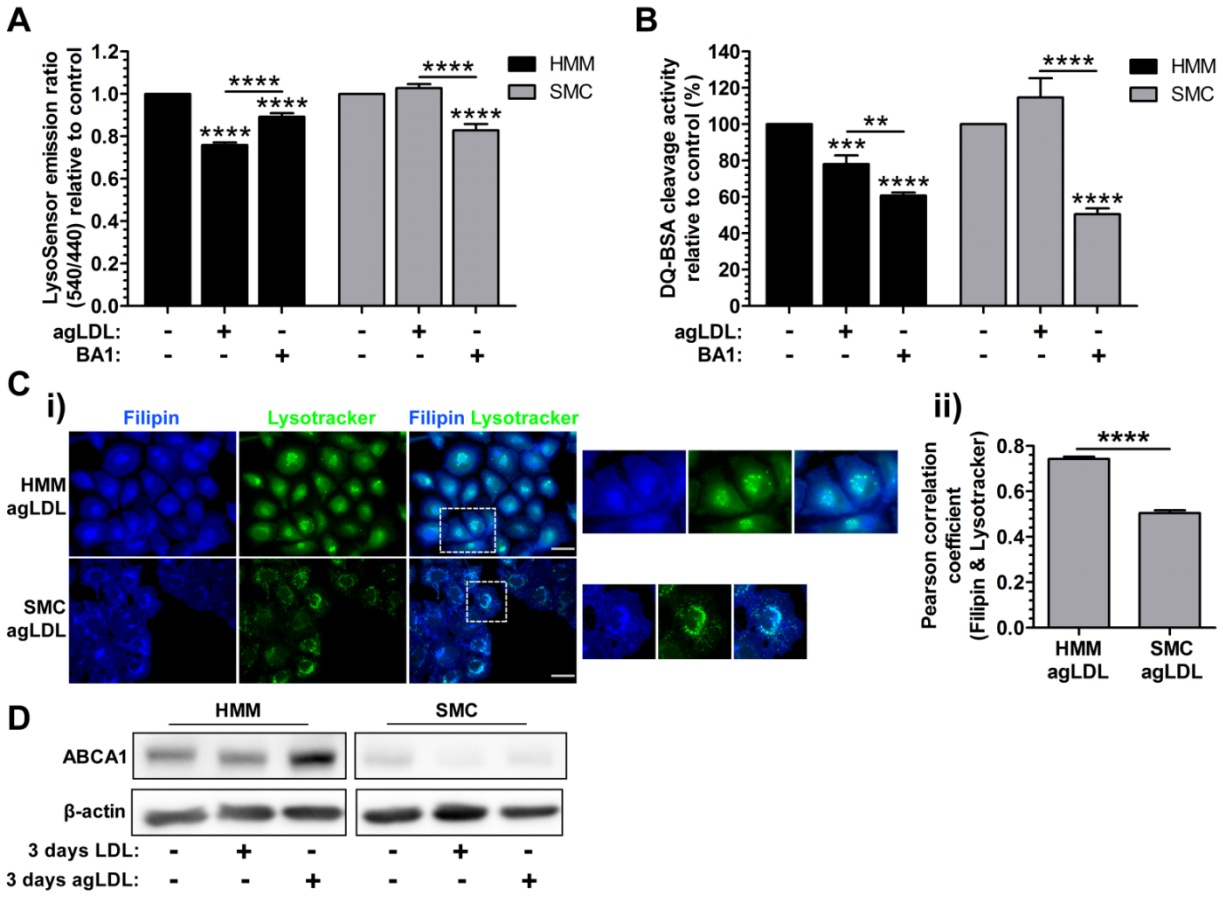

Figure 3.6 SMCs do not display a functional defect in control of lysosomal acidity with excess agLDL loading.

Figure 3.6 SMCs do not display a functional defect in control of lysosomal acidity with excess agLDL loading.
HMMs and SMCs were cultured as described in the Methods section and subsequently treated for 24 hrs with medium containing 10% LPDS. Cells were then extensively washed with PBS and fresh medium containing 2 mg/mL FAFA ± 100 μg/mL LDL or agLDL was applied for 24 hrs. (**A**) Changes in lysosomal acidity were evaluated using the pH sensitive dual fluorescence probe Lysosensor Yellow/Blue DND-160. After lipid loading cells were treated with and without 100 nM Bafilomycin A1 for 1.5 hours in medium containing 2 mg/mL FAFA. Lysosomal compartments were then labeled with 100 μL of 100 μM Lysosensor Yellow/Blue DND-60 in medium containing 2 mg/mL FAFA for 15 min. Fluorescence was then determined using a plate reader, the acidic/basic ratio of [(384/540)/(329/440)] was then be used to assess for significant changes in lysosomal pH relative to untreated controls. (**B**) Changes in lysosomal function were evaluated using DQ Red BSA. After lipid loading cells were treated with 5 μg/mL DQ Red BSA in medium containing 2 mg/mL FAFA for 2 hrs. Cells were then equilibrated for 2 hrs with and without 100 nM Bafilomycin A1 in medium containing 2 mg/mL FAFA and subsequently lysed. Fluorescence of cell extracts at 590/620 nm was measured using a plate reader and normalized to proteins. (**C, i**) Lysosomal levels of free cholesterol were evaluated by fluorescent microscopy. After lipid loading cells were equilibrated for 24 hrs without lipids and then treated with 500nM of LysoTracker for 15 minutes at 37^{o}C to label acid organelles. After fixation with 3% PFA and staining for free cholesterol using 50 μg/mL filipin for 20 minutes slides were imaged by fluorescent microscopy using a 63x/1.4 oil immersion objective. Scale bars are 20 μm. (**C, ii**) Colocalization of filipin with Lysotracker was quantified by Pearson correlation as determined by analysis of n>100 cells. (**D**) HMMs and SMCs were cultured as described above and treated with 100 μg/mL LDL or agLDL for 3 days. Cell proteins were separated by SDS-PAGE and visualized by Western blot using antibodies for ABCA1 and the loading control β-actin. HMMs and SMCs proteins were analyzed on the same gel for each experiment (representative of 5 experiments with similar results). Results are mean±SEM (**A**, 3-4 experiments with n=3 replicates; **B**, 2-3 experiments with n=3-6 replicates; **C**, 2 experiments). Statistical analysis was done using (**A**, **B**) one-way ANOVA with Bonferonni corrections and (**C**) Mann-Whitney test (**p<0.01, ***p<0.001, ****p<0.0001, statistically different compared to corresponding non-lipid loaded control in each cell type unless otherwise indicated).

Bafilomycin A1 (BA1), a potent vacuolar H^{+}-ATPase inhibitor (273) was used as a positive control for loss of lysosomal acidity. Using the DQ Red BSA assay as a measure of lysosomal function (270) we also found significantly reduced proteolytic cleavage activity after agLDL treatment in HMMs but not in SMCs (**Figure 3.6 B**).

Accumulation of free cholesterol in lysosomes of macrophages after modified LDL loading has been previously demonstrated (80, 267), and increases in lysosomal membrane

cholesterol have been reported to inhibit vacuolar H^+-ATPase pumping resulting in lysosomal alkalinization (126). Consistent with our analysis of the effect of agLDL on lysosomal acidity and function using both Lysosensor and DQ Red BSA, we found by confocal microscopy significantly higher colocalization of free cholesterol with lysosomes in macrophages relative to SMCs stained with filipin for free cholesterol and lysotracker for acid organelles (**Figure 3.6 C**). Similarly, we found higher macrophage lysosomal free cholesterol levels after agLDL treatment using filipin and LAMP1 (**Figure 3.7**).

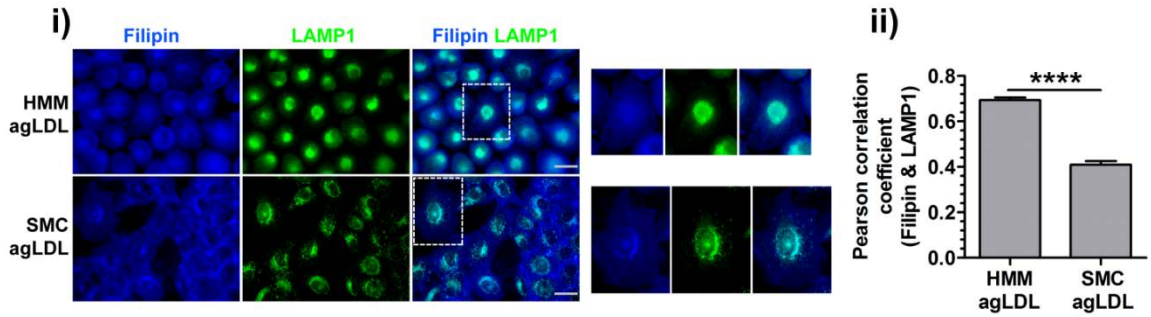

Figure 3.7 Macrophages have elevated lysosomal FC accumulation relative to SMCs. HMMs and SMCs were grown on glass coverslips as described in the Methods section and subsequently treatment for 24 hrs with medium containing 10% LPDS. Cells were then extensively washed with PBS and fresh medium containing 2 mg/mL FAFA and 100 µg/mL agLDL was applied. After 24 hrs, cells were washed and equilibrated in medium containing 1 mg/mL FAFA for a further 24 hrs. As described in the Methods section, cells were then stained with filipin (blue) for free cholesterol and LAMP1 (green) antibody for lysosomal compartments. (**i**) Images were obtained by fluorescent microscopy using a 63x/1.4 oil immersion objective and are representative of 2 experiments. Scale bars are 20 µm. (**ii**) Colocalization of filipin with LAMP1 was quantified by Pearson correlation as determined by analysis of n>100 cells. Scale bars are 20 µm. Results are mean±SEM (2 experiments). Statistical analysis was done using Mann-Whitney test, ****p<0.0001.

Elevated lysosomal levels of free cholesterol in macrophages was also consistent with our observation of significantly higher cellular free cholesterol levels after agLDL loading and equilibration relative to controls in macrophages but not SMCs (**Figure 3.1 B**). Our results indicated that agLDL loading resulted in free cholesterol-induced loss of lysosomal acidity in

macrophages, consistent with previous reports (126, 128), but was not found to be a feature of SMCs.

Further corroborating previous reports following chronic lipid loading of macrophages (80, 126), we did find evidence of CE accumulations occurring in macrophage lysosomes with 3 days of agLDL exposure as determined by confocal microscopy, which also correlated with significant loss of lysosomal acidity evaluated using Lysosensor Yellow/Blue (Data not shown). Although macrophages may accumulate lysosomal CE after chronic lipid overload we found that ABCA1 levels remained higher in macrophages then SMCs after 3 day lipid loading (**Figure 3.6 D**) indicating that enough cholesterol was leaving lysosomal compartments in macrophages to stimulate transcription via LXR. Overall, we did not find evidence of a functional defect in lysosomal pH control associated with CE accumulation in SMCs, although the tendency for loss of lysosomal acidity after excess lipid loading appears to be pertinent to macrophage cholesterol metabolism.

3.4.4 Lysosomal CE accumulation in SMCs is a result of low LAL expression

As we did not find clear indications of inducible lysosomal pH-related dysfunction in SMCs compared the macrophages, we next investigated differences in expression and activity of LAL, the sole lysosomal CE hydrolase (227). We found significantly higher expression of LAL in HMMs relative to SMCs at both the mRNA and the protein level (**Figure 3.8 A-C**).

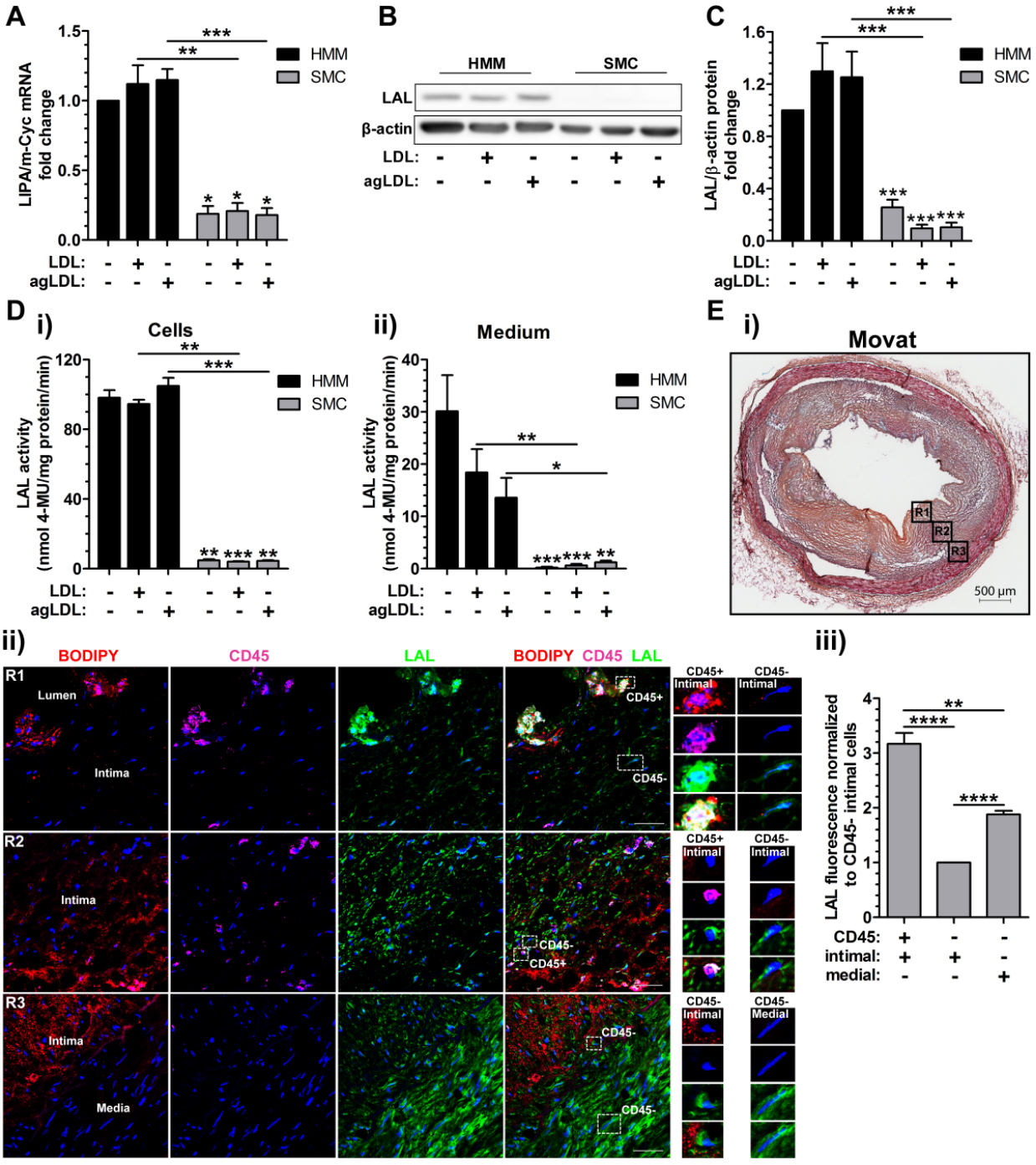

Figure 3.8 LAL expression is reduced in SMCs compared to macrophages.

Figure 3.8 LAL expression is reduced in SMCs compared to macrophages.
HMMs and SMCs were cultured as described in the Methods section and subsequently treatment for 24 hrs with medium containing 10% LPDS. Cells were then extensively washed with PBS and fresh medium containing 2 mg/mL FAFA ± 100 μg/mL LDL or agLDL was applied for 24 hrs. (**A**) RNA extracts were analyzed by PCR using primers for human LAL and m-cyclophilin. Results are fold increase in LIPA relative to the HMM non-lipid loaded control. (**B**) Cell proteins were separated by SDS-PAGE and visualized by Western blot using antibodies for LAL and the loading control β-actin. (**C**) Western blots were analyzed by densitometry and the results expressed as the fold increase in LAL relative to the HMM non-lipid loaded control. (**D**) The activity of LAL in both (**i**) cell lysates and (**ii**) medium was evaluated by kinetic measurement of fluorescence intensity (335 nm excitation and 455 nm emission) upon cleavage of the enzyme substrate 4-MUO at pH 4.0. (**E, i**) Movat stain of human coronary artery OCT section. (**E, ii**) OCT serial section from human coronary shown in (**E, i**) was stained with BODIPY, CD45, and LAL. Images of regions R1 (lumen & intima), R2 (middle & deep intima), and R3 (deep intima & media) shown in (**E, i**) were obtained by confocal microscopy using a 20x/0.8 air objective. (**E, iii)** Comparison of LAL levels between macrophage cells identified by Hoechst and strong fluorescence for CD45 (CD45+) and SMCs identified by Hoechst and lack of CD45 fluorescence (CD45-) found in the intima and media. LAL fluorescence intensity was normalized to CD45- intimal cells in each image collected. Results are mean±SEM (**A**, 8 experiments; **C,** 8 experiments; **D**, 3 experiments with n=3 replicates; **E**, >160 cells for each group were analyzed from images collected from 10 subjects). Statistically significant differences were evaluated using (**A**, **C**, **D**, **E**) Kruskal-Wallis test with Dunn's Multiple Comparisons post-hoc test (*p<0.05, **p<0.01, ***p<0.001, ****p<0.0001, statistically different compared to HMM non-lipid loaded control unless otherwise indicated).

Differences in enzymatic activity of LAL at pH 4.0 were determined by measuring change in fluorescence after cleavage of 4-methylumbelliferyl oleate (4-MUO) (40). We found LAL activity in cell lysates to be 23.4-times higher in agLDL loaded HMMs compared to agLDL loaded SMCs (**Figure 3.8 D i**). The mRNA, protein, and activity of LAL in cells were not appreciably affected by lipid loading with LDL or agLDL. In parallel with our *in vitro* human findings, we also found significantly higher expression and activity of LAL in cultured mouse RAW 264.7 macrophages compared to cultured mouse SMCs (**Figure 3.9**).

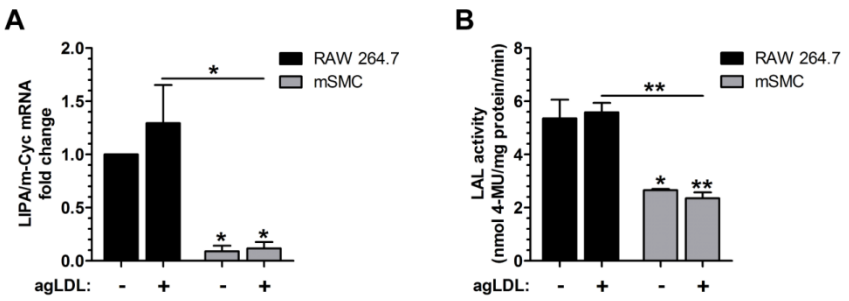

Figure 3.9 LAL expression is reduced in mouse SMCs compared to mouse macrophages. RAW 264.7 macrophages and mouse SMCs (mSMCs) were cultured as described in the Methods section and subsequently treatment for 24 hrs with medium containing 10% LPDS. Cells were then extensively washed with PBS and fresh medium containing 2 mg/mL FAFA ± 100 µg/mL LDL or agLDL was applied for 24 hrs. (**A**) RNA extracts were analyzed by quantitative real-time PCR using primers for mouse LAL and m-cyclophilin. The fold increase in LAL relative to the macrophage non-lipid loaded control is shown. (**B**) The activity of LAL in cell lysates was evaluated by kinetic measurement of fluorescence intensity (335 nm excitation and 455 nm emission) upon cleavage of the enzyme substrate 4-MUO at pH 4.0. Results are mean±SEM (**A**, 4 experiments; **B,** 4 experiments). Statistically significant differences were evaluated using (**A**) Kruskal-Wallis test with Dunn's Multiple Comparisons post-hoc test and (**B**) one-way ANOVA with Bonferonni corrections (*$p<0.05$, **$p<0.01$ statistically different compared to RAW 264.7 non-lipid loaded control unless otherwise indicated).

Additionally, as LAL is also secreted from cells and can be taken up endocytically via the mannose 6-phosphate receptor (39), we evaluated LAL activity levels in medium. HMMs were found to secrete significantly higher levels of LAL into medium relative to SMCs (**Figure 3.8 D ii**).

We also analyzed differences in LAL expression between macrophages and SMCs within human atherosclerotic coronary arteries (**Figure 3.8 E**). OCT sections were incubated with primary antibodies for the macrophage marker CD45 and LAL followed by treatment with fluorescent secondary antibodies for confocal microscopy analysis. Macrophage cells were identified by strong fluorescence for CD45, a leukocyte marker (282) not expressed by SMCs (283-286). Our own analyses by flow cytometry and confocal microscopy indicated CD45 was expressed in cultured HMMs but not human SMCs (data not shown). CD45 negativity was used

for identification of SMCs and not classic SMC markers such as SM α-actin because lipid loading with cyclodextrin-cholesterol complexes has been indicated to result in reduced expression of SM α-actin (202) and significant loss of SM α-actin expression has been indicated in apoE$^{-/-}$ mouse atheromas using a SMC lineage-tracing model (206). Although CD45 negativity does not confirm all cells to be SMCs, it has been reported that approximately 90% of the cells in the human atherosclerotic intima are SMCs (15, 16). Indicated are three regions of the intima (R1 to R3) where confocal microscopy images were acquired for LAL fluorescence analysis (**Figure 3.8 E i**). We found CD45+ macrophages within the intima and not the media, mostly close to the lumen (**R1 in Figure 3.8 E ii**) or middle of the intima (**R2 in Figure 3.8 E ii**). To control for experimental variability in LAL fluorescence intensity between images and also subjects, the fluorescence of LAL in CD45+ intimal macrophages or CD45- medial cells was normalized to the average LAL fluorescence in CD45- intimal cells within the same image. CD45- intimal cells were used for normalization as they were present in all microscopy images obtained. Consistent with our *in vitro* results indicating higher LAL levels in macrophages compared to SMCs we found that LAL expression, as evaluated by fluorescence intensity analysis, was significantly higher by ~3.2-fold in intimal CD45+ macrophages compared to CD45- intimal cells (SMCs) in human atherosclerotic coronary arteries (**Figure 3.8 E iii**). LAL fluorescence was significantly higher by ~1.9-fold in medial SMCs compared to intimal SMCs (**Figure 3.8 E iii**). Macrophage LAL fluorescence was significantly higher than both intimal and medial SMCs in atherosclerotic human coronary arteries ($p<0.0001$ and $p<0.01$ respectively). Lipid deposition was frequently found in the deeper portions of the intima as indicated by strong BODIPY staining (**R2 & R3 in Figure 3.8 E ii**). Both our *in vitro* and *in vivo* data indicate significantly higher levels of LAL in macrophages compared to SMCs, a striking phenotypic

difference associated with SMCs being inherently prone to accumulate CEs within lysosomal compartments due to this relative LAL deficiency.

3.4.5 SMC uptake of LAL leads to rescue of lysosomal CE accumulation

As LAL containing conditioned medium (CM) has been previously reported to reduce lysosomal CE accumulation in CESD fibroblasts (25, 233), we investigated whether CM from cultured macrophages would be able to rescue lysosomal CE sequestration observed in SMCs. After 24 hrs agLDL loading, HMMs and SMCs were treated with non-lipid loaded HMM CM for 24 hrs and LAL activity was measured in the cell lysates (**Figure 3.10 A i & ii**).

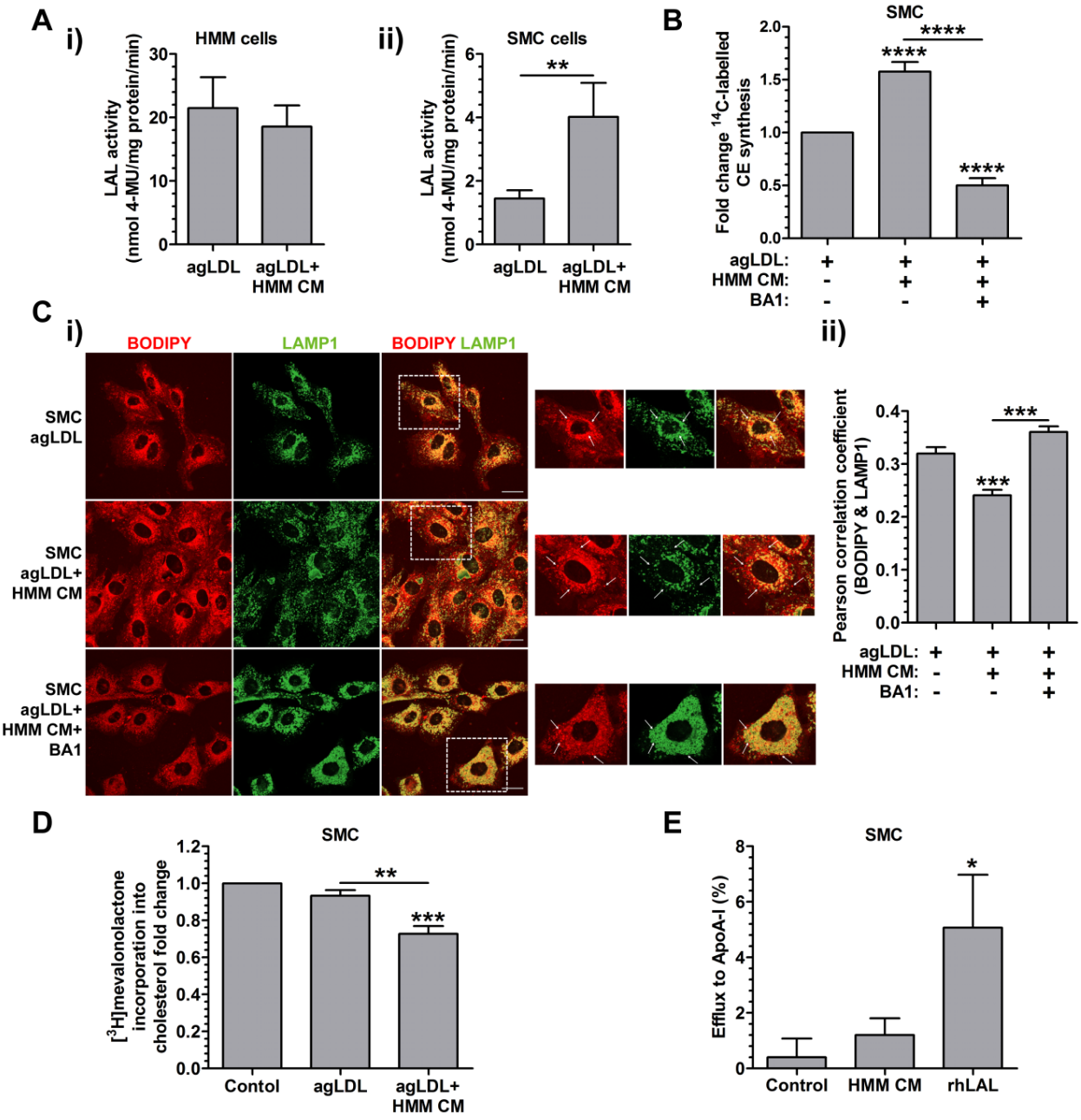

Figure 3.10 Treatment with LAL is able to reduce lysosomal lipid accumulation and increase cholesterol efflux in SMCs.

Figure 3.10 Treatment with LAL is able to reduce lysosomal lipid accumulation and increase cholesterol efflux in SMCs.
HMMs and SMCs were cultured as described in the Methods section and subsequently treated for 24 hrs with medium containing 10% LPDS. Cells were then extensively washed with PBS and fresh medium containing 2 mg/mL FAFA ± 100 µg/mL agLDL was applied for 24 hrs. (**A**) LAL enzyme activity – After lipid loading, cells were washed and equilibrated in medium alone containing 1 mg/mL FAFA with and without conditioned medium from non-lipid loaded HMMs (HMM CM) for 24 hours. Cells were collected in PBS and LAL enzyme activity was determined. (**B**) Cholesterol re-esterification – After lipid loading SMCs were washed and equilibrated 3.5 hrs in medium alone containing 1 mg/mL FAFA with and without HMM CM, or HMM CM containing 100 nM Bafilomycin A1 (BA1). Following extensive washes, cells were incubated with medium containing [^{14}C]oleate for 1 hr. Cell lipids were then extracted, separated by TLC, and the radioactivity of cholesteryl [^{14}C]oleate was determined by liquid scintillation counting. (**C**) Confocal microscopy – SMCs were grown on glass coverslips and after lipid loading cells were washed and equilibrated in medium alone containing 1 mg/mL FAFA with and without HMM CM, or HMM CM containing 100 nM BA1 to inhibit lysosomal acidification for 24 hrs. As described in the Methods section, cells were stained with (**C, i**) BODIPY (red) for neutral lipids and LAMP1 (green) antibody for lysosomal compartments. Images were obtained by confocal microscopy using a 63x/1.4 oil immersion objective and are representative of 3 experiments. Scale bars are 20 µm. (**C, ii**) Colocalization of BODIPY with LAMP1 was quantified by Pearson correlation. (**D**) New cholesterol synthesis – SMCs were treated for 24 hours with and without agLDL in medium containing 2 mg/mL FAFA and supplemented with 0.5 µCi/mL of [^{14}C]mevalonolactone; cells were also treated with and without HMM CM during lipid loading. After cell lipid extraction and TLC separation, the TC radioactivity was determined by liquid scintillation counting. (**E**) Efflux to ApoA-I – SMCs were loaded for 24 hours with [^{3}H]-CE labelled agLDL, washed, and treated with or without HMM CM or 5 µg/mL rhLAL for 4 hours. Cells were then washed and efflux to medium containing 1 mg/mL FAFA with and without 10 µg/mL apoA-I was performed for 24 hours. Radioactivity in medium and cells was determined by LSC. Efflux to apoA-I (%) is relative to total [^{3}H]-CE labelled agLDL taken up by cells. Results are mean±SEM (**A**, 2 experiments with n=2-4 replicates; **B**, 2 experiments with n=4 replicates; **C**, **ii** analysis of n>100 cells from 3 experiments; **D**, 3 experiments with n=3-6 replicates; **E**, 2 experiments with n=3 replicates). Statistical analysis was done using (**A**) Mann-Whitney test, (**B**) one-way ANOVA with Bonferonni corrections and (**C-E**) Kruskal-Wallis test with Dunn's Multiple Comparisons post-hoc test (*p<0.05, **p<0.01, ***p<0.001, ****p<0.0001, statistically different compared to corresponding control unless otherwise indicated).

LAL activity in SMCs treated with HMM CM was significantly increased by 2.8-fold.

Consistent with macrophages excreting higher levels of LAL compared to SMCs (**Figure 3.8 D ii**) and not lacking cellular LAL, we observed no appreciable increase in LAL activity after addition of non-lipid loaded HMM CM to agLDL loaded HMMs. We then investigated

lysosomal release of cholesterol in agLDL loaded SMCs following HMM CM treatment by evaluation of [^{14}C]oleic acid incorporation to form cholesteryl esters (**Figure 3.10 B**). Formation of new cholesteryl esters by SMCs was significantly increased following HMM CM treatment by 1.6-fold, an effect abolished with addition of the lysosomal v-ATPase inhibitor BA1, indicating the dependence of this effect on LAL in the conditioned medium. Compartmental changes in cellular CE lipid storage were corroborated by confocal microscopy after HMM CM exposure (**Figure 3.10 C**). By visual inspection some neutral lipids were released from lysosomal compartments in SMCs to cytosolic compartments with HMM CM treatment and remained in lysosomes with the addition of BA1 (**Figure 3.10 C i**). Quantitative analysis using the Pearson correlation coefficient indicated significantly lower colocalization of BODIPY with LAMP1 following HMM CM treatment and reversal with BA1 exposure (**Figure 3.10 C ii**). Release of cholesterol from the lysosome to the ER with HMM CM treatment resulted in significant reduction of new cholesterol synthesis by ~27% relative to non-lipid loaded SMCs or by ~22% compared to agLDL loaded cells (**Figure 3.10 D**). Efflux to apoA-I with exposure to LAL containing conditioned medium from HMMs (HMM CM) trended towards higher levels by ~3-fold but was not significantly increased (**Figure 3.10 E**). A significant increase in efflux by ~12.7-fold was observed with exposure of SMCs to acutely higher levels of LAL with rhLAL (5 µg/mL rhLAL had ~10,000-fold higher LAL enzyme activity then HMM CM). Collectively these results indicate that LAL treatment can reverse lysosomal CE accumulation in SMCs, correcting multiple cholesterol trafficking pathways, and enhance cholesterol efflux.

Interestingly, lysosomal release of cholesterol from LAL treatment with HMM CM for 24 hrs had no substantive effect on ABCA1 expression and was not increased with exogenous

addition of 27-OHC at 40 ng/mL (**Figure 3.11**), a concentration similar to what we found to be produced by macrophages as determined by mass spectrometry (calculated from **Figure 3.2 D**).

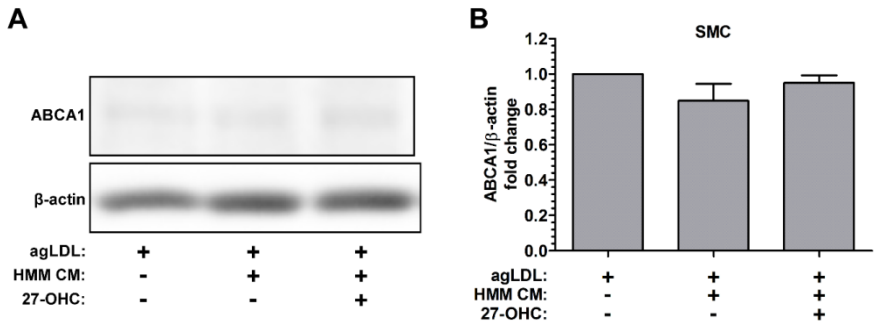

Figure 3.11 HMM conditioned medium and 27-OHC treatment does not up regulate ABCA1.
SMCs were lipid loaded with agLDL as described in the Methods section and subsequently treated with or without HMM CM medium for 24 hrs (± 40 ng/mL 27-OHC). (**A**) Cell proteins were separated by SDS-PAGE and visualized by Western blot using antibodies for ABCA1 and the loading control β-actin. (**B**) Western blots were analyzed by densitometry and the results expressed as the fold increase in ABCA1 relative to the agLDL loading control. Results are mean±SEM from 6 experiments. No statistically significant differences between conditions were found by one-way ANOVA with Bonferonni corrections.

Additionally, treatment of SMCs with higher concentrations of LAL (5 µg/mL rhLAL) for 24 hrs did not result in a robust increase in ABCA1 protein levels (data not shown). Increasing the exposure concentration of 27-OHC to 200 ng/mL also did not result in increased ABCA1 expression (data not shown). This data indicated possible defects in other sterol regulatory steps besides LAL in ABCA1 response, as both increasing LAL levels and bypassing the release of lysosomal cholesterol with addition of 27-OHC did not result in an increased expression of the LXR transcriptional target ABCA1. Our findings suggested that although SMCs may display a similar phenotype to CESD or Wolman Disease in regards to lysosomal sequestration of CEs being a result of low or absent LAL activity (25, 68), release of lysosomal cholesterol may not

have the anticipated robust effect on classic cholesterol metabolism markers like ABCA1. The reason for not finding robust effects on ABCA1 may be directly related to the fact that low LAL in SMCs relative to macrophages is a cell type specific difference and not a result of a genetic disorder. Differences in expression of sterol regulatory genes would be anticipated to be present between foam cell types as macrophages and SMCs have different functional roles in the arterial wall. We now investigate what differences may exist between macrophages and SMCs in genes involved in ABCA1 regulation and cholesterol metabolism.

3.4.6 SMCs display differences compared to macrophages in cholesterol metabolism gene expression

We screened a panel of genes directly involved with cholesterol synthesis & uptake, cholesterol removal, and lysosomal cholesterol processing for response to treatment with agLDL in HMMs and primary SMCs (**Figure 3.12**).

A

	Gene Symbol	HMM control 1	HMM control 2	HMM agLDL 1	HMM agLDL 2	Fold Change
Cholesterol synthesis & uptake	DHCR24	24.01	21.05	0.41	5.76	-7.30
	HMGCR	24.86	28.16	0.41	2.88	**-16.10**
	LDLR	14.88	23.85	0.41	2.88	**-11.76**
Cholesterol removal	CYP27A1	78.02	64.70	120.74	75.36	1.37
	LXRα	71.30	44.50	204.48	79.66	2.45
	ABCA1	10.60	18.97	46.71	39.55	**2.92**
	ABCG1	1.82	1.34	31.91	7.19	**12.35**
Lysosomal cholesterol processing	LIPA	2479.42	1647.18	4407.62	2514.03	1.68
	NPC1	52.19	51.83	73.81	46.07	1.15
	NPC2	466.52	291.18	946.06	489.71	1.89
	STARD3	13.60	13.42	56.33	14.88	2.64

B

	Gene Symbol	intimal SMC control 1	intimal SMC control 2	intimal SMC agLDL 1	intimal SMC agLDL 2	Fold Change
Cholesterol synthesis & uptake	DHCR24	5.64	6.90	6.13	5.64	-1.07
	HMGCR	10.38	13.70	10.97	10.90	**-1.10**
	LDLR	17.70	32.80	7.81	18.07	**-1.95**
Cholesterol removal	CYP27A1	2.05	0.65	5.08	0.69	2.14
	LXRα	1.41	2.29	1.38	1.29	-1.39
	ABCA1	67.92	59.54	75.36	34.67	**-1.16**
	ABCG1	23.36	1.81	24.01	1.69	**1.02**
Lysosomal cholesterol processing	LIPA	48.70	82.47	50.77	74.33	-1.05
	NPC1	94.08	33.73	108.07	39.01	1.15
	NPC2	607.10	339.15	668.96	285.19	1.01
	STARD3	24.01	17.70	25.03	15.09	-1.04

C

	Gene Symbol	medial SMC control 1	medial SMC control 2	medial SMC agLDL 1	medial SMC agLDL 2	Fold Change
Cholesterol synthesis & uptake	DHCR24	3.80	9.96	6.22	6.30	-1.10
	HMGCR	8.55	19.78	10.38	9.29	**-1.44**
	LDLR	15.73	38.21	33.73	15.84	**-1.09**
Cholesterol removal	CYP27A1	1.67	1.76	1.94	1.41	-1.02
	LXRα	3.22	1.93	2.56	1.58	-1.24
	ABCA1	89.62	41.81	36.91	34.92	**-1.83**
	ABCG1	3.38	2.51	1.67	1.80	**-1.70**
Lysosomal cholesterol processing	LIPA	31.47	43.28	36.91	37.16	-1.01
	NPC1	19.37	21.64	21.49	30.19	1.26
	NPC2	258.82	281.26	291.18	368.57	1.22
	STARD3	13.79	13.14	15.63	17.58	1.23

Figure 3.12 Primary intimal and medial SMCs display similar reduced response to agLDL treatment in comparison to HMMs in gene expression changes associated with lysosomal cholesterol processing, cholesterol synthesis & uptake, and cholesterol removal.

Figure 3.12 Primary intimal and medial SMCs display similar reduced response to agLDL treatment in comparison to HMMs in gene expression changes associated with lysosomal cholesterol processing, cholesterol synthesis & uptake, and cholesterol removal.
HMMs and primary human aortic SMCs isolated from the intima and media of the arterial wall were treated with and without agLDL for 24 hrs as indicated in the methods section and RNA extracted. RNA profiling was conducted using a custom CodeSet on the nCounter Analysis System (NanoString Technologies). (**A**, **B**, **C**) Fold change after agLDL treatment in each cell type is indicated. Intimal and medial SMCs were donor matched. Macrophage experiments were from two different donors, but were not from the same donors as SMCs.

In HMMs we found the expected downregulation of genes involved with cholesterol synthesis (*DHCR24* and *HMGCR*) & uptake (*LDLR*) and upregulation of genes involved with cholesterol removal (*CYP27A1, LXRα, ABCA1,* and *ABCG1*) following lipid loading. In both primary intimal SMCs and medial SMCs, genes involved with cholesterol synthesis & uptake were downregulated with agLDL treatment, but to a strikingly lesser extent than HMMs. This data is consistent with lysosomal CE sequestration leading to reduced FC trafficking to the endoplasmic reticulum resulting in lower suppression of SREBP mediated gene transcription in SMCs compared to macrophages. SREBP regulates the expression of *DHCR24* (287, 288) and *HMGCR* (65, 287), and *LDLR* (289). Interestingly, primary SMCs displayed negative or reduced response to agLDL loading in the genes *ABCA1* and *ABCG1*, which are known to be regulated via LXR through the generation of oxysterols (255, 264), notably 27-OHC which is generated by mono-oxygenation of cholesterol via CYP27A1 (263). ABCA1 has also been indicated to be negatively regulated by LXR antagonists, such as the non-sterol mevalonate products geranylgeranyl pyrophosphate (290) and geranylgeraniol (291). Reduced ABCA1 response in SMCs is supportive of our finding of lysosomal CE sequestration (**Figure 3.4**), factors that may antagonize LXR cannot not be discounted and might result in negative regulation with agLDL treatment. We also observed negative response with agLDL treatment in the expression of *LXRα*

in both primary intimal SMCs and medial SMCs. *LXRα* has been reported to upregulate its' own expression in the presence of LXR agonists in human macrophages (292), consistent with our results with agLDL treatment of HMMs (**Figure 3.12**). Regulation of CYP27A1 expression has been indicated to be weakly increased by treatment with the LXR ligand 27-OHC, but strongly by ligands for RXR and PPARγ in macrophages (293). The promoter of human *CYP27A1* has been reported to be a direct target of both RAR-RXR and PPARγ-RXR heterodimers (294). We found a modest 1.37-fold increase in *CYP27A1* expression in HMMs with agLDL treatment (**Figure 3.12**). It is unclear if the same regulation of *CYP27A1* in macrophages occurs in SMCs. Our results for agLDL induced expression of *CYP27A1* in SMCs were variable, suggesting perhaps both an influence of reduced lysosomal cholesterol release for generation of 27-OHC in SMCs compared to macrophages (**Figure 3.2 D**) and potential influence of other regulatory mechanisms. Overall, our results indicate reduced flux of lipoprotein-derived cholesterol out of lysosomes for downstream regulatory events in SMCs compared to macrophages.

We found modest upregulation of lysosomal cholesterol processing genes *LIPA, NPC1, NPC2,* and *STARD3* in macrophages with agLDL treatment (**Figure 3.12**). The direction of regulation of these genes in SMCs with agLDL treatment was more variable and the magnitude of change in expression was less than macrophages. In contrast, analysis of basal and agLDL stimulated levels between SMCs and macrophages in these important lysosomal processing genes was very informative. Our NanoString gene data indicated *LIPA* expression in SMCs was 31 to 93-times lower compared to macrophages (**Figure 3.13**).

Gene Symbol	Intimal SMC control vs HMM control (Fold change)	Intimal SMC agLDL vs HMM agLDL (Fold change)	Medial SMC control vs HMM control (Fold change)	Medial SMC agLDL vs HMM agLDL (Fold change)	Intimal SMC control vs Medial SMC control (Fold change)	Intimal SMC agLDL vs Medial SMC agLDL (Fold change)
LIPA	**-31.46**	**-55.33**	**-55.20**	**-93.45**	**1.75**	**1.69**
NPC1	1.23	1.23	-2.54	-2.32	3.12	2.85
NPC2	1.25	-1.50	-1.40	-2.18	1.75	1.45
STARD3	1.54	-1.77	-1.00	-2.14	1.55	1.21
CYP27A1	**-52.79**	**-33.96**	**-41.66**	**-58.54**	**-1.27**	**1.72**
LXRα	**-31.29**	**-106.43**	**-22.51**	**-68.72**	**-1.39**	**-1.55**

Figure 3.13 Primary intimal and medial SMCs display markedly reduced expression of several lysosomal and post-lysosomal genes important for ABCA1 regulation in comparison to macrophages.

This was consistent with our data indicating lysosomal CE sequestration (**Figure 3.4**) and other *in vitro* and *in vivo* data (**Figure 3.8**) indicating low *LIPA* in SMCs compared to macrophages. Expression of *NPC1*, *NPC2*, and *STARD3* genes, important for free cholesterol transport out of lysosomes, were similar between SMCs and macrophages. This data supports our finding that reduced lysosomal function causing CE sequestration in SMCs (**Figure 3.4**) was caused by relatively low expression of *LIPA* in SMCs compared to macrophages (**Figure 3.8**), and not accumulation of free cholesterol in lysosomes inhibiting lysosomal acidity in SMCs (**Figure 3.7**). Major differences in basal gene expression comparisons were between SMCs and macrophages, and not between intimal and medial type SMCs (**Figure 3.13**). Additionally, our gene analysis indicated acute differences in *CYP27A1* and also *LXRα*, which were 34 to 59-times and 23 to 106-times lower in SMCs compared to macrophages respectively (**Figure 3.13**). Low levels of *CYP27A1* were consisting with our findings of significantly reduced basal production of 27-OHC by 115-times ($p<0.0001$) in SMCs compared to macrophages (**Figure 3.2 D**). In addition to the presence of other factors that might antagonize LXR in SMCs, reduced response

to agLDL treatment in both *ABCA1* and *ABCG1* expression might be a combined result of markedly lower expression of *LIPA*, *CYP27A1*, and *LXR* in SMCs compared to macrophages. Despite this indication, SMCs do express ABCA1 (**Figure 3.2**) and ABCG1 (**Figure 3.3**), and LAL treatment does rescue lysosomal CE sequestration and promote cholesterol efflux (**Figure 3.10**).

As hydrolysis of lipoprotein-derived CE by LAL is the critical first step in cellular cholesterol processing, we evaluated the effect of chronic rhLAL (3 day) treatment on cholesterol metabolism genes in SMCs (**Figure 3.14**).

Gene Symbol	SMC 3 day agLDL 1 & 2 (log2)		SMC 3 day agLDL+rhLAL 1 & 2 (log2)		Fold Change
CYP27A1	4.45	4.15	3.95	4.11	-1.20
LXRα	6.16	6.54	5.86	6.50	-1.12
ABCA1	3.55	4.42	4.39	3.95	**1.14**
ABCG1	3.06	3.35	3.79	3.75	**1.48**
MVK	5.65	5.88	5.24	5.52	-1.30
DHCR7	3.89	4.95	4.40	4.11	-1.12
DHCR24	5.74	5.87	5.42	5.75	-1.16
HMGCR	5.66	5.03	5.20	5.12	**-1.13**
LDLR	4.68	4.31	4.01	4.44	**-1.20**

Figure 3.14 Effect of 3 day chronic LAL treatment on SMCs cholesterol metabolism genes. HMMs and SMCs (obtained from ATCC) were cultured and treated with 10% LPDS for 24 hrs with and without 5 µg/mL rhLAL. Cells were then washed and treated with and without 100 µg/mL agLDL ± 5 µg/mL rhLAL for 72 hrs. Medium was refreshed at 36 hrs. RNA profiling was conducted using the Clariom S Assay, Human on the Affymetrix microarray platform and analyzed using Transcriptome Analysis Console software. Results are from n=2 experiments. Fold change after rhLAL treatment is indicated.

Small reductions in cholesterol synthesis (*MVK*, *DHCR7*, *DHCR24*, and *HMGCR*) & uptake (*LDLR*) genes with rhLAL exposure relative to agLDL treatment alone were observed, but were consistently downregulated across multiple genes. Chronic rhLAL treatment increased

expression levels of *ABCG1* by 1.48-fold and *ABCA1* by 1.14-fold (**Figure 3.14**). Expression changes in both *ABCA1* and *ABCG1* with chronic rhLAL exposure in SMCs did not approach expression changes observed with agLDL loading in macrophages (**Figure 3.12 A**). Blunted changes in *ABCA1* and *ABCG1* expression with chronic rhLAL exposure are consistent with the influence of markedly reduced expression of *CYP27A1* and *LXR*. Despite not observing large changes in *ABCA1* or *ABCG1* with chronic rhLAL treatment (**Figure 3.14**), our other experimental data with 1 day LAL treatment indicated significant release of lysosomal cholesterol (**Figure 3.10 B&C**), reduced new cholesterol synthesis (**Figure 3.10 D**) consistent with trends observed in cholesterol synthesis genes (**Figure 3.14**), and enhanced cholesterol efflux (~12.7 fold, **Figure 3.10 E**). We cannot discount that there may be some additional cellular effects of LAL treatment with longer exposures beyond 24 hrs that may have influenced our chronic LAL incubation data. This remains to be explored further and what this might mean therapeutically for impact on formation and regression of SMC foam cells. Overall our results indicate that although additional sterol regulatory events downstream of lysosomal processing, including low levels of *CYP27A1* and *LXR*, also affect expression of *ABCA1* and *ABCG1*, enhanced hydrolysis and release of lipoprotein-derived CEs have a benefit for removal of cholesterol from SMC foam cells.

3.5 Discussion

Countless studies in both mouse and humans have indicated the very important role that macrophages play in both progression and regression of atherosclerosis (77, 91, 211, 295). As a result, much is already known about cholesterol metabolism in macrophages during atherosclerosis. Our previous findings that SMCs make up a significant quantitative proportion (>50%) of the foam cells found in atherosclerosis (24), a finding backed up by other reports on

the presence of SMC foam cells in atherosclerosis (17-22), has opened new areas of exploration for ischemic cardiovascular disease prevention and regression. Investigation of potential reason(s) why SMCs make up a significant fraction of the foam cells found in atheromas is therefore critically important, as very little is known about cholesterol metabolism in these cells in comparison to macrophages.

In our previous *in vivo* studies (24) we also found that ABCA1 levels were reduced in intimal SMCs compared to macrophages, hinting at the presence of important differences in cholesterol handling and removal between macrophage and SMCs. Also from our prior studies in CESD fibroblasts (25) and our studies with $lal^{-/-}$ mouse peritoneal macrophages, as indicated in Chapter 2 and published work (256), we know that genetic deficiency of LAL, the sole lysosomal cholesteryl ester hydrolase, results in reduced expression of ABCA1. Additionally we know that genetic deficiency in NPC1 and NPC2, proteins responsible for transport of free cholesterol out of lysosomes, results in reduced expression of ABCA1 (26, 27, 265). Interestingly, previous work by Jerome and colleagues has shown that prolonged exposure of macrophages to agLDL or oxLDL, modified forms of LDL, induces lysosomal lipid accumulation (80, 111, 267). This was determined to be a result of lysosomal accumulations of free cholesterol inhibiting vacuolar H^+-ATPase-mediated lysosomal acidification, leading to a loss of LAL activity and resulting in lysosomal cholesteryl ester accumulation (126, 128). Early reports have also indicated that lysosomal cholesteryl ester accumulation occurs in SMC foam cells (19, 142, 143, 296, 297), but the reasons for this were unknown. Based on our previous finding of low ABCA1 in SMCs compared to macrophages (24) and the direct association of lysosomal lipid release with regulation of ABCA1 (25-27, 265), we hypothesized that SMC foam

cell formation may be a result of reduced lysosomal function, either an increased tendency for loss of lysosomal acidity or a result of lysosomal enzyme deficiency.

Indeed, our results indicate a tendency for SMCs to sequester lipoprotein-derived CEs in lysosomal compartments compared to macrophages (**Figure 3.4** and **Figure 3.5**). Initially, based on extensive prior work in macrophages indicating a loss of lysosomal acidity with modified forms of LDL (126, 128), we suspected SMCs may exhibit a preferential loss of lysosomal acidity compared to macrophages after agLDL loading. Contrary to our hypothesis, SMCs did not display a loss of lysosomal acidity (**Figure 3.6 A&B**). Consistent with the previous reports (126, 128), macrophages did exhibit a loss of acidity after agLDL treatment. A loss of lysosomal acidity with agLDL treatment in macrophages but not SMCs (**Figure 3.6 A&B**) was consistent with higher colocalization of free cholesterol in lysosomal compartment of macrophages potentially resulting in inhibition of vacuolar H^+-ATPases (v-ATPases) relative to SMCs (**Figure 3.6 C** and **Figure 3.7**). The v-ATPase is the primary driver of endocytic acidification and is a rotary proton transport motor driven by the hydrolysis of adenosine triphosphate (ATP) consisting of a soluble V_1 subcomplex and a membrane embedded V_0 subcomplex (298, 299). Our gene analysis did not indicate obvious loss of v-ATPase V_1 or V_0 subcomplex expression in HMMs or SMCs with agLDL treatment (data not shown), consistent with previous analysis of v-ATPase H-subunit levels in macrophages following agLDL or oxLDL exposure in macrophages (126). The mechanism(s) by which free cholesterol accumulation in lysosomes inhibits the v-ATPases in macrophages is still unknown, but the presence of this induction in macrophages as previously reported (126, 128) is consistent with our results presented here. Although macrophages may lose lysosomal acidity by accumulation of free cholesterol in lysosomal compartments inhibiting v-ATPases activity, this does not seem to have an important effect on

the ability of macrophages to release enough cholesterol from lysosomal compartments for suppression of HMGCoA reductase and upregulation of ABCA1 expression. Under chronic agLDL exposure conditions (3 day), ABCA1 expression remained higher in HMMs relative to SMCs (**Figure 3.6 D**).

We next evaluated the expression and activity of LAL in macrophages and SMCs (**Figure 3.8 A-D**). Our data indicted significantly higher LAL expression and activity in macrophages compared to SMCs. Similarly, we found in human coronary arteries that macrophage expression of LAL was significantly higher than that of both intimal and medial SMCs (**Figure 3.8 E**). Our data is consistent with a recent report by Zhang, *et al*. (234) that indicated mRNA levels of *LIPA* in HMMs were significantly higher than both human coronary and aortic SMCs in culture. Interestingly, peripheral blood monocyte (PBMCs) mRNA expression of LAL was at a similar level to human SMCs, and increased with differentiation from monocytes to macrophages. Relatively small effects on LAL activity were indicated with macrophage polarization to inflammatory M1 phenotype with LPS+INFγ (LAL levels decreased) and anti-inflammatory M2 phenotype with IL-4 (LAL levels increased) (234). The variable stage of monocyte differentiation and macrophage polarization in tissue therefore may influence LAL expression levels. Despite this we found in human coronary atheromas a ~3.2-fold higher expression of LAL in macrophages (CD45+) compared to intimal SMCs (CD45-) in human coronary artery atheromas (**Figure 3.8 E**). This is consistent with the qualitative indication by Hakala *et al*. (97) of higher LAL levels in human coronary atherosclerotic lesions in areas of macrophage infiltration compared to normal. In addition to quantification of low levels of LAL in SMCs compared to macrophages from our *in vitro* and *in vivo* studies in Chapter 3, we also

report that lower expression of LAL in SMCs compared to macrophages results in preferential lysosomal CE accumulation, as also seen in the subtotal genetic LAL deficiency disorder CESD.

Our results are of great significance as they provide insight into some of the original inquiries about LAL levels in atherosclerosis that originated in the 1960-1980s following the initial discovery of the lysosome in 1955 by Christian de Duve and colleagues (300). Christian de Duve received the Nobel Prize Physiology or Medicine in 1974 for the discovery of the lysosome and peroxisome and is also credited with first coining the terms “endocytosis” and “autophagy” to designate pathways transferring substrates to the lysosome for degradation (301-303). In 1974 de Duve proposed that LAL deficiency was leading to accumulation of CEs in aortic cells in atherosclerosis (22). Opposing this hypothesis, a series of subsequent studies suggested increased levels of LAL in the arterial wall during atherosclerosis (60, 62-64), but were overall inconclusive due to not clearly identifying the cell types analyzed. These results were seemingly contradicted as other reports suggested lysosomal lipid accumulation was occurring in SMCs, but also did not clearly identify the cell types analyzed (19-21, 142, 143, 145). Our results presented here for the first time, now clearly indicate increases in LAL levels in atherosclerotic lesions to be a result of infiltrating macrophages expressing significantly higher levels of LAL (**Figure 3.8 E**) and not a response to LDL or agLDL loading causing increased LAL expression (**Figure 3.8 A-D**). We now report that SMCs have an enhanced tendency over macrophages for accumulation of CEs in lysosomal compartments, resulting from low LAL levels. Our data indicates that de Duve’s original proposal of LAL deficiency in atherosclerosis in 1974 to be true and additionally we show here for the first time that this results in tendency for lysosomal CE accumulation in SMCs compared to macrophages.

As lysosomal deficiency in LAL and not a loss of acidity leads to lysosomal CE accumulation in SMCs, treatment of arterial SMC foam cells with LAL as done for genetic deficiency of LAL in CESD (156) and Wolman Disease (155) may prove to be therapeutically beneficial for native atherosclerosis. One report has suggested a benefit of rhLAL treatment on reducing atheroma volume in an LDL receptor deficiency mouse model of atherosclerosis (161), but therapeutic usage of rhLAL in humans, outside of treating genetic deficiency, remains untested. Consistent with the initial hypothesis of de Duve in 1974 regarding a deficiency of LAL in atherosclerosis, our data now indicates that SMCs having relatively low LAL levels compared to macrophages, can be treated with LAL to enhance CE hydrolysis and FC release from lysosomes (**Figure 3.10 B&C**), reduce new cholesterol synthesis (**Figure 3.10 D**), and increase cholesterol efflux (**Figure 3.10 E**). Depending on the stage of atherosclerosis, therapeutic delivery of LAL to cells in the arterial wall may have a benefit for reducing cardiovascular events that are primarily driven by accumulation of cholesterol in the arterial wall.

Interestingly, although reduced lysosomal function in SMCs in the form of low LAL levels resulting in lysosomal CE accumulation is reversible with LAL treatment in SMCs (**Figure 3.10**), additional important sterol regulatory differences between macrophages and SMCs are present as indicated from our gene analysis studies. Specifically, our gene analysis studies indicate significantly lower expression of *CYP27A1* and *LXR* (**Figure 3.13**). Low *CYP27A1* expression levels in SMCs compared to macrophages is consistent with our results indicating low 27-OHC production relative to macrophages (**Figure 3.2 D**). A lack of significant increase in 27-OHC production after agLDL loading in SMCs is consistent with lysosomal CE sequestration as a result of low LAL expression. Our experimental results with 1 day LAL

treatment or 27-OHC supplementation not resulting in increased ABCA1 expression (**Figure 3.11**) were consistent with the combination of low *CYP27A1* and *LXR* levels in SMCS compared to macrophages. This was also consistent with chronic LAL treatment for 3 days resulting in smaller *ABCA1* and *ABCG1* expression increases (**Figure 3.14**) than observed with macrophages with agLDL loading (**Figure 3.12 A**). Despite differences between macrophages and SMCs in additional sterol regulatory genes, our results indicate that LAL treatment is able to promote the reversal of lysosomal CE accumulation and significantly increase cholesterol efflux from SMCs (**Figure 3.10**).

Chapter 4: Concluding remarks

4.1 Summary and conclusions

LAL is the sole lysosomal CE hydrolase and responsible for the initial metabolism of lipoprotein-derived CE by cells. Release of cholesterol from lysosomes is important for regulation of cellular cholesterol synthesis & uptake and also for generation of oxysterols that regulate proteins involved in cholesterol removal.

In Chapter 2 we investigated and defined the role of LAL in cholesterol metabolism using an LAL knockout mouse peritoneal macrophage model. We found reduced expression of ABCA1, which was partially corrected by treatment with rhLAL. Treatment with rhLAL in $lal^{-/-}$ macrophages resulted in increased production of the oxysterol 27-OHC and reduction in new cholesterol synthesis. Additionally restoration of LAL in $lal^{-/-}$ macrophages with rhLAL released lysosomal cholesterol for cytosolic re-esterification as has been previously indicated in CESD (233). Efflux to apoA-I in $lal^{-/-}$ macrophages was significantly increased with rhLAL treatment similar to our previous results with LAL from conditioned medium in CESD fibroblasts (25). A potential limitation of these studies may be the use of acLDL as this form of modified LDL is generated in the laboratory and not implicated *in vivo*. Further lipid metabolism insights perhaps may be gained in studying $lal^{-/-}$ macrophages using other forms of modified LDL that are found *in vivo*, such as agLDL as utilized in Chapter 3, or oxLDL.

In Chapter 3 we investigated the presence of reduced lysosomal function and cholesterol metabolism differences between human monocyte-derived macrophages (HMMs) and arterial SMCs in response to lipoprotein overload. Similar to our previous *in vivo* results indicating reduced ABCA1 expression in SMCs compared to macrophages in advanced human coronary atheromas (24), our *in vitro* results here now show a reduced response in ABCA1 and ABCG1 to

lipid loading by SMCs when compared to macrophages. Reduced ABCA1 and ABCG1 response to lipid loading were associated with reduced 27-hydroxycholesterol production, reduced cholesterol re-esterification, and a lack of decrease in new cholesterol synthesis. These findings strongly suggested a lysosomal cholesterol processing defect. Indeed, confocal microscopy revealed this to be true with SMCS displaying sequestration of CEs in lysosomes, while HMMs displayed mostly cytosolic lipid droplets. Initially we suspected that accumulation of free cholesterol in SMC lysosomes may be inhibiting lysosomal acidification via v-ATPases as has been previously reported in macrophages (126, 128). Contrary to our initial hypothesis, SMCs did not display a loss of lysosomal acidity with lipid overload, but consistent with previous reports we did observe a loss of lysosomal acidity in macrophages. Supporting this data, we found higher accumulation of free cholesterol in macrophage lysosomes compared to SMCs. We then investigated LAL expression and activity levels and found that they were markedly lower in SMCs compared to macrophages (LAL activity 23.4-times lower in agLDL loaded SMCs compared to HMMs, $p<0.001$). Our cell culture results were confirmed by confocal microscopy analysis of LAL levels in human coronary atherosclerosis. LAL levels were significantly higher in intimal macrophages compared to both intimal and medial SMCs. Additionally, we found that cultured mouse RAW 264.7 macrophages had significantly higher LAL than mouse SMCs and that mouse SMCs displayed increased lysosomal CE accumulations as in human SMCs. Treatment of SMCs with LAL containing medium decreased lysosomal lipid accumulation, decreased new cholesterol synthesis, and increased cholesterol efflux. Interestingly, we found a lack of robust increase in ABCA1 expression in response to LAL treatment in SMCs, potentially attributable to low expression of CYP27A1 and LXR relative to macrophages. Despite this LAL treatment was able to restore lysosomal lipid release and increase cholesterol efflux from arterial

SMCs. This suggests that enhancement of lysososomal CE hydrolysis by LAL treatment allows release of FC from lysosomes and an increase in the substrate pool of FC for efflux by the existing level of ABCA1 expression in SMCs. Regardless of other cholesterol regulatory differences between macrophages and SMCs, this raises the strong possibility that supplementing LAL to arterial SMCs could have a major effect on arterial cholesterol accumulation and overall plaque volume.

Some limitations of the studies presented in Chapter 3 include: (1) *In vitro* lipid loading of SMCs and macrophages was conducted over the course of days, whereas in human atherosclerosis prone arteries lipid accumulation occurs over decades; (2) We utilized agLDL in our studies, but in the arterial wall oxidized and enzymatically modified LDL may also exist as discussed in Chapter 1. ApoB containing chylomicron and VLDL remnant particles and their modified forms may influence foam cell foramation in atherosclerosis prone arteries (304, 305); (3) In addition to low levels of *LIPA* in SMCs relative to macrophages, the influence of genetic variations in *LIPA* (306) could also influence both SMC and macrophage foam cell formation and RCT; (4) The impact of aging on LAL levels in SMCs and macrophages was not investigated in these studies and could be a additional risk factor *in vivo* for lipid accumulation; (5) We did not investigate the influence of inflammatory cytokines or presence of other signaling molecules in the arterial wall, which might also effect LAL levels and lipid accumulation in SMCs.

Overall, we find that arterial SMCs have a relative deficiency in LAL expression and associated defects in downstream sterol regulatory events compared to macrophages. Our results indicate low levels of LAL in SMCs as a novel reason for foam cell formation and a potential target to reduce atherosclerosis development and promote regression therapeutically. Research

into novel therapeutic agents is needed to reduce the global burden of cardiovascular disease in the years to come. Targeting cholesterol removal at the lesional level specifically in SMCs may prove to be a viable therapeutic option for atherosclerosis prevention and regression.

4.2 Future directions

Our studies presented here open up many interesting avenues of future investigations for SMC lipid biology in relation to cardiovascular disease. Several lines of further exploration might involve:

1) A previous study has suggested that LAL treatment in vivo may initiate atherosclerosis regression (161). Whether or not a specifically targeted LAL therapy to SMCs and not other cell types such as macrophages in the arterial wall will reduce progression and induce regression of atherosclerosis needs further investigation. We aim to investigate this in an atherosclerosis mouse progression and regression model using a TetON -Tet OFF system to specifically and conditionally express LAL in arterial SMCs in response to doxycycline treatment, similar to what has been done in a prior inducible macrophage LAL overexpression study in $lal^{-/-}$ mice (307). Further studies will be needed to evaluate if LAL treatment conditionally needs to be specific to SMCs or if general exposure to all arterial cells is enough for therapeutic benefit.
2) A previous report by Davies, *et al* (308) has suggested that in vascular SMCs, 27-OHC might act as an antagonist of LXR in the presence of other LXR agonists (oxysterols or TO901317). Other reports have indicated that non-sterol mevalonate products can also act as LXR antagonists (290, 291), leading to reduced ABCA1 expression. Is reduced ABCA1 response in SMCs to agLDL or 27-OHC exposure as we have found, indicative of a protective or causative mechanism(s) for cardiovascular disease in the vascular wall

beyond simply cholesterol flux? Why are levels of 27-OHC and associated CYP27A1 levels so much lower in arterial SMCs compared to macrophages? Along the same lines, why are LXR levels reduced in SMCs compared to macrophages? A report by Riendeau, *et al* (309) has indicated that 27-OHC induced apoptosis in SMCs but induced increased cell viability in macrophages. Does a combination of low CYP27A1 and LXR have protective effects for SMCs in the arterial wall? This remains an interesting area of further inquiry.

3) Apoptosis of arterial SMCs (310) and macrophages (311) is associated with plaque destabilization in atherosclerosis. What is the role of LAL in these processes, specifically if LAL is relatively low in vascular SMCs compared to macrophages? Is necrosis and apoptosis a feature of enhanced lysosomal lipid accumulation in SMCs and is cell death an overriding factor that would significantly inhibit the viability of a therapy targeting LAL? Alternatively, would LAL treatment have a beneficial affect on SMC survival and plaque stabilization? Further studies are needed to evaluate these questions.

References

1. Murray CJ, Vos T, Lozano R, Naghavi M, Flaxman AD, Michaud C, Ezzati M, Shibuya K, Salomon JA, Abdalla S, et al. Disability-adjusted life years (DALYs) for 291 diseases and injuries in 21 regions, 1990-2010: a systematic analysis for the Global Burden of Disease Study 2010. *Lancet.* 2012;380(9859):2197-223.

2. Roth GA, Forouzanfar MH, Moran AE, Barber R, Nguyen G, Feigin VL, Naghavi M, Mensah GA, and Murray CJ. Demographic and epidemiologic drivers of global cardiovascular mortality. *The New England journal of medicine.* 2015;372(14):1333-41.

3. Mortality GBD, and Causes of Death C. Global, regional, and national age-sex specific all-cause and cause-specific mortality for 240 causes of death, 1990-2013: a systematic analysis for the Global Burden of Disease Study 2013. *Lancet.* 2015;385(9963):117-71.

4. Roth GA, Huffman MD, Moran AE, Feigin V, Mensah GA, Naghavi M, and Murray CJ. Global and regional patterns in cardiovascular mortality from 1990 to 2013. *Circulation.* 2015;132(17):1667-78.

5. Benjamin EJ, Blaha MJ, Chiuve SE, Cushman M, Das SR, Deo R, de Ferranti SD, Floyd J, Fornage M, Gillespie C, et al. Heart Disease and Stroke Statistics-2017 Update: A Report From the American Heart Association. *Circulation.* 2017;135(10):e146-e603.

6. Bloom DE, Cafiero, E.T., Jané-Llopis, E., Abrahams-Gessel, S., Bloom, L.R., Fathima, S., Feigl, A.B., Gaziano, T., Mowafi, M., Pandya, A., Prettner, K., Rosenberg, L., Seligman, B., Stein, A., & Weinstein, C. The Global Economic Burden of Non-communicable Diseases. Geneva: World Economic Forum. 2011.

7. Thomas GS, Wann LS, Allam AH, Thompson RC, Michalik DE, Sutherland ML, Sutherland JD, Lombardi GP, Watson L, Cox SL, et al. Why did ancient people have atherosclerosis?: from autopsies to computed tomography to potential causes. *Global heart.* 2014;9(2):229-37.

8. Clarke EM, Thompson RC, Allam AH, Wann LS, Lombardi GP, Sutherland ML, Sutherland JD, Cox SL, Soliman MA, Abd el-Maksoud G, et al. Is atherosclerosis fundamental to human aging? Lessons from ancient mummies. *Journal of cardiology.* 2014;63(5):329-34.

9. Windaus A. Ueber den Gehalt normaler und atheromatoeser Aorten an Cholesterol and Cholesterinester. *Zeitschrift Physiol Chem.* 1910;67(174–6.

10. Mayerl C, Lukasser M, Sedivy R, Niederegger H, Seiler R, and Wick G. Atherosclerosis research from past to present--on the track of two pathologists with opposing views, Carl von Rokitansky and Rudolf Virchow. *Virchows Archiv : an international journal of pathology.* 2006;449(1):96-103.

11. Anitschkow N, and Chalatow S. Ueber experimentelle Cholesterinsteatose und ihre Bedeutung fuer die Entstehung einiger pathologischer Prozesse. *Zentrbl Allg Pathol Pathol Anat.* 1913;24(1-9.

12. Mehta NJ, and Khan IA. Cardiology's 10 greatest discoveries of the 20th century. *Texas Heart Institute journal.* 2002;29(3):164-71.

13. Friedman M, and Friedland GW. *Medicine's 10 greatest discoveries.* New Haven, (CT): Yale University Press; 1998.

14. Konstantinov IE, Mejevoi N, and Anichkov NM. Nikolai N. Anichkov and his theory of atherosclerosis. *Texas Heart Institute journal.* 2006;33(4):417-23.

15. Orekhov AN, Andreeva ER, Mikhailova IA, and Gordon D. Cell proliferation in normal and atherosclerotic human aorta: proliferative splash in lipid-rich lesions. *Atherosclerosis.* 1998;139(1):41-8.

16. Orekhov AN, Andreeva ER, Krushinsky AV, Novikov ID, Tertov VV, Nestaiko GV, Khashimov Kh A, Repin VS, and Smirnov VN. Intimal cells and atherosclerosis. Relationship between the number of intimal cells and major manifestations of atherosclerosis in the human aorta. *The American journal of pathology.* 1986;125(2):402-15.

17. Stary HC. Macrophages, macrophage foam cells, and eccentric intimal thickening in the coronary arteries of young children. *Atherosclerosis.* 1987;64(2-3):91-108.

18. Katsuda S, Boyd HC, Fligner C, Ross R, and Gown AM. Human atherosclerosis. III. Immunocytochemical analysis of the cell composition of lesions of young adults. *The American journal of pathology.* 1992;140(4):907-14.

19. Goldfischer S, Schiller B, and Wolinsky H. Lipid accumulation in smooth muscle cell lysosomes im primate atherosclerosis. *The American journal of pathology.* 1975;78(3):497-504.

20. Fowler S, Berberian PA, Shio H, Goldfischer S, and Wolinsky H. Characterization of cell populations isolated from aortas of rhesus monkeys with experimental atherosclerosis. *Circulation research.* 1980;46(4):520-30.

21. Jerome WG, and Lewis JC. Early atherogenesis in White Carneau pigeons. II. Ultrastructural and cytochemical observations. *The American journal of pathology.* 1985;119(2):210-22.

22. de Duve C. The participation of lysosomes in the transformation of smooth muscle cells to foamy cells in the aorta of cholesterol-fed rabbits. *Acta cardiologica.* 1974;Suppl 20(9-25.

23. Choi HY, Rahmani M, Wong BW, Allahverdian S, McManus BM, Pickering JG, Chan T, and Francis GA. ATP-binding cassette transporter A1 expression and apolipoprotein A-I binding are impaired in intima-type arterial smooth muscle cells. *Circulation.* 2009;119(25):3223-31.

24. Allahverdian S, Chehroudi AC, McManus BM, Abraham T, and Francis GA. Contribution of intimal smooth muscle cells to cholesterol accumulation and macrophage-like cells in human atherosclerosis. *Circulation.* 2014;129(15):1551-9.

25. Bowden KL, Bilbey NJ, Bilawchuk LM, Boadu E, Sidhu R, Ory DS, Du H, Chan T, and Francis GA. Lysosomal acid lipase deficiency impairs regulation of ABCA1 gene and formation of high density lipoproteins in cholesteryl ester storage disease. *The Journal of biological chemistry.* 2011;286(35):30624-35.

26. Boadu E, Choi HY, Lee DW, Waddington EI, Chan T, Asztalos B, Vance JE, Chan A, Castro G, and Francis GA. Correction of apolipoprotein A-I-mediated lipid efflux and high density lipoprotein particle formation in human Niemann-Pick type C disease fibroblasts. *The Journal of biological chemistry.* 2006;281(48):37081-90.

27. Choi HY, Karten B, Chan T, Vance JE, Greer WL, Heidenreich RA, Garver WS, and Francis GA. Impaired ABCA1-dependent lipid efflux and hypoalphalipoproteinemia in human Niemann-Pick type C disease. *The Journal of biological chemistry.* 2003;278(35):32569-77.

28. Oncley JL, Gurd FRN, and Melin M. Preparation and Properties of Serum and Plasma Proteins .25. Composition and Properties of Human Serum Beta-Lipoprotein. *J Am Chem Soc.* 1950;72(1):458-64.

29. Valle D, Beaudet A, Vogelstein B, Kinzler K, Antonarakis S, Ballabio A, Gibson K, and Mitchell G. *The Online Metabolic and Molecular Bases of Inherited Disease - Chapter 114, Table 114-3*. New York, NY: McGraw-Hill; 2014.

30. Muller C. Xanthomata, hypercholesterolemia, angina pectoris. *Acta Med Scand.* 1938:75-84.

31. Goldstein JL, and Brown MS. Binding and degradation of low density lipoproteins by cultured human fibroblasts. Comparison of cells from a normal subject and from a patient with homozygous familial hypercholesterolemia. *The Journal of biological chemistry.* 1974;249(16):5153-62.

32. Goldstein JL, and Brown MS. Familial hypercholesterolemia: identification of a defect in the regulation of 3-hydroxy-3-methylglutaryl coenzyme A reductase activity associated with overproduction of cholesterol. *Proceedings of the National Academy of Sciences of the United States of America.* 1973;70(10):2804-8.

33. Brown MS, Dana SE, and Goldstein JL. Receptor-dependent hydrolysis of cholesteryl esters contained in plasma low density lipoprotein. *Proceedings of the National Academy of Sciences of the United States of America.* 1975;72(8):2925-9.

34. Goldstein JL, and Brown MS. The LDL receptor. *Arteriosclerosis, thrombosis, and vascular biology.* 2009;29(4):431-8.

35. Tabas I, Williams KJ, and Boren J. Subendothelial lipoprotein retention as the initiating process in atherosclerosis: update and therapeutic implications. *Circulation.* 2007;116(16):1832-44.

36. Jerome WG. Advanced atherosclerotic foam cell formation has features of an acquired lysosomal storage disorder. *Rejuvenation research.* 2006;9(2):245-55.

37. Anderson RA, Rao N, Byrum RS, Rothschild CB, Bowden DW, Hayworth R, and Pettenati M. In situ localization of the genetic locus encoding the lysosomal acid lipase/cholesteryl esterase (LIPA) deficient in Wolman disease to chromosome 10q23.2-q23.3. *Genomics.* 1993;15(1):245-7.

38. Ameis D, Merkel M, Eckerskorn C, and Greten H. Purification, characterization and molecular cloning of human hepatic lysosomal acid lipase. *European journal of biochemistry / FEBS.* 1994;219(3):905-14.

39. Sando GN, and Henke VL. Recognition and receptor-mediated endocytosis of the lysosomal acid lipase secreted by cultured human fibroblasts. *Journal of lipid research.* 1982;23(1):114-23.

40. Sheriff S, Du H, and Grabowski GA. Characterization of lysosomal acid lipase by site-directed mutagenesis and heterologous expression. *The Journal of biological chemistry.* 1995;270(46):27766-72.

41. Scott SA, Liu B, Nazarenko I, Martis S, Kozlitina J, Yang Y, Ramirez C, Kasai Y, Hyatt T, Peter I, et al. Frequency of the cholesteryl ester storage disease common LIPA E8SJM mutation (c.894G>A) in various racial and ethnic groups. *Hepatology.* 2013;58(3):958-65.

42. Stitziel NO, Fouchier SW, Sjouke B, Peloso GM, Moscoso AM, Auer PL, Goel A, Gigante B, Barnes TA, Melander O, et al. Exome sequencing and directed clinical phenotyping diagnose cholesterol ester storage disease presenting as autosomal recessive hypercholesterolemia. *Arteriosclerosis, thrombosis, and vascular biology.* 2013;33(12):2909-14.

43. Bernstein DL, Hulkova H, Bialer MG, and Desnick RJ. Cholesteryl ester storage disease: review of the findings in 135 reported patients with an underdiagnosed disease. *Journal of hepatology.* 2013;58(6):1230-43.

44. Grabowski GA, Du H, and Charnas L. In: Beaudet AL, Vogelstein B, Kinzler KW, Antonarakis SE, Ballabio A, Gibson KM, and Mitchell G eds. *The Online Metabolic and Molecular Bases of Inherited Disease*. New York, NY: The McGraw-Hill Companies, Inc.; 2014.

45. Ries S, Buchler C, Langmann T, Fehringer P, Aslanidis C, and Schmitz G. Transcriptional regulation of lysosomal acid lipase in differentiating monocytes is mediated by transcription factors Sp1 and AP-2. *Journal of lipid research.* 1998;39(11):2125-34.

46. Lettieri Barbato D, Tatulli G, Aquilano K, and Ciriolo MR. FoxO1 controls lysosomal acid lipase in adipocytes: implication of lipophagy during nutrient restriction and metformin treatment. *Cell death & disease.* 2013;4(e861.

47. Sardiello M, Palmieri M, di Ronza A, Medina DL, Valenza M, Gennarino VA, Di Malta C, Donaudy F, Embrione V, Polishchuk RS, et al. A gene network regulating lysosomal biogenesis and function. *Science.* 2009;325(5939):473-7.

48. Settembre C, Zoncu R, Medina DL, Vetrini F, Erdin S, Erdin S, Huynh T, Ferron M, Karsenty G, Vellard MC, et al. A lysosome-to-nucleus signalling mechanism senses and regulates the lysosome via mTOR and TFEB. *The EMBO journal.* 2012;31(5):1095-108.

49. Efeyan A, Zoncu R, and Sabatini DM. Amino acids and mTORC1: from lysosomes to disease. *Trends in molecular medicine.* 2012;18(9):524-33.

50. Shanware NP, Bray K, and Abraham RT. The PI3K, metabolic, and autophagy networks: interactive partners in cellular health and disease. *Annual review of pharmacology and toxicology.* 2013;53(89-106.

51. He C, and Klionsky DJ. Regulation mechanisms and signaling pathways of autophagy. *Annual review of genetics.* 2009;43(67-93.

52. Sergin I, and Razani B. Self-eating in the plaque: what macrophage autophagy reveals about atherosclerosis. *Trends in endocrinology and metabolism: TEM.* 2014;25(5):225-34.

53. Settembre C, De Cegli R, Mansueto G, Saha PK, Vetrini F, Visvikis O, Huynh T, Carissimo A, Palmer D, Klisch TJ, et al. TFEB controls cellular lipid metabolism through a starvation-induced autoregulatory loop. *Nature cell biology.* 2013;15(6):647-58.

54. Emanuel R, Sergin I, Bhattacharya S, Turner J, Epelman S, Settembre C, Diwan A, Ballabio A, and Razani B. Induction of lysosomal biogenesis in atherosclerotic macrophages can rescue lipid-induced lysosomal dysfunction and downstream sequelae. *Arteriosclerosis, thrombosis, and vascular biology.* 2014;34(9):1942-52.

55. Emanuel R, Sergin I, Bhattacharya S, Turner JN, Epelman S, Settembre C, Diwan A, Ballabio A, and Razani B. Induction of lysosomal biogenesis in atherosclerotic

macrophages can rescue lipid-induced lysosomal dysfunction and downstream sequelae. *Arteriosclerosis, thrombosis, and vascular biology.* 2014;34(9):1942-52.

56. Heltianu C, Robciuc A, Botez G, Musina C, Stancu C, Sima AV, and Simionescu M. Modified low density lipoproteins decrease the activity and expression of lysosomal acid lipase in human endothelial and smooth muscle cells. *Cell biochemistry and biophysics.* 2011;61(1):209-16.

57. Patrick AD, and Lake BD. Deficiency of an acid lipase in Wolman's disease. *Nature.* 1969;222(5198):1067-8.

58. Lake BD, and Patrick AD. Wolman's disease: deficiency of E600-resistant acid esterase activity with storage of lipids in lysosomes. *The Journal of pediatrics.* 1970;76(2):262-6.

59. Sloan HR, and Fredrickson DS. Enzyme deficiency in cholesteryl ester storage idisease. *The Journal of clinical investigation.* 1972;51(7):1923-6.

60. Brecher P, Pyun HY, and Chobanian AV. Effect of atherosclerosis on lysosomal cholesterol esterase activity in rabbit aorta. *Journal of lipid research.* 1977;18(2):154-63.

61. Takano TI, T. Lysosomal acid cholesteryl esterase and atherosclerosis in cholesterol-fed rabbits. *Acta Histochem Cytochem.* 1978;11(3):323-36.

62. Subbiah MT. Significance of various cholesterol, ester hydrolases in aorta. *Steroids.* 1979;33(3):305-15.

63. Haley NJ, Fowler S, and de Duve C. Lysosomal acid cholesteryl esterase activity in normal and lipid-laden aortic cells. *Journal of lipid research.* 1980;21(8):961-9.

64. Davis HR, Glagov S, and Zarins CK. Role of acid lipase in cholesteryl ester accumulation during atherogenesis. Correlation of enzyme activity with acid lipase-containing macrophages in rabbit and human lesions. *Atherosclerosis.* 1985;55(2):205-15.

65. Brown MS, and Goldstein JL. The SREBP pathway: regulation of cholesterol metabolism by proteolysis of a membrane-bound transcription factor. *Cell.* 1997;89(3):331-40.

66. Venkateswaran A, McFarlan SC, Ghosal D, Minton KW, Vasilenko A, Makarova K, Wackett LP, and Daly MJ. Physiologic determinants of radiation resistance in Deinococcus radiodurans. *Applied and environmental microbiology.* 2000;66(6):2620-6.

67. Oram JF, and Heinecke JW. ATP-binding cassette transporter A1: a cell cholesterol exporter that protects against cardiovascular disease. *Physiological reviews.* 2005;85(4):1343-72.

68. Goldstein JL, Dana SE, Faust JR, Beaudet AL, and Brown MS. Role of lysosomal acid lipase in the metabolism of plasma low density lipoprotein. Observations in cultured

fibroblasts from a patient with cholesteryl ester storage disease. *The Journal of biological chemistry.* 1975;250(21):8487-95.

69. Liscum L, and Faust JR. Low density lipoprotein (LDL)-mediated suppression of cholesterol synthesis and LDL uptake is defective in Niemann-Pick type C fibroblasts. *The Journal of biological chemistry.* 1987;262(35):17002-8.

70. Garver WS, Jelinek D, Meaney FJ, Flynn J, Pettit KM, Shepherd G, Heidenreich RA, Vockley CM, Castro G, and Francis GA. The National Niemann-Pick Type C1 Disease Database: correlation of lipid profiles, mutations, and biochemical phenotypes. *Journal of lipid research.* 2010;51(2):406-15.

71. Goldstein JL, and Brown MS. The low-density lipoprotein pathway and its relation to atherosclerosis. *Annual review of biochemistry.* 1977;46(897-930.

72. Chisolm GM, and Steinberg D. The oxidative modification hypothesis of atherogenesis: an overview. *Free radical biology & medicine.* 2000;28(12):1815-26.

73. Torzewski M, and Lackner KJ. Initiation and progression of atherosclerosis--enzymatic or oxidative modification of low-density lipoprotein? *Clinical chemistry and laboratory medicine : CCLM / FESCC.* 2006;44(12):1389-94.

74. Aviram M. Modified forms of low density lipoprotein and atherosclerosis. *Atherosclerosis.* 1993;98(1):1-9.

75. Hoff HF, and Hoppe G. Structure of cholesterol-containing particles accumulating in atherosclerotic lesions and the mechanisms of their derivation. *Current opinion in lipidology.* 1995;6(5):317-25.

76. Bhakdi S, Dorweiler B, Kirchmann R, Torzewski J, Weise E, Tranum-Jensen J, Walev I, and Wieland E. On the pathogenesis of atherosclerosis: enzymatic transformation of human low density lipoprotein to an atherogenic moiety. *The Journal of experimental medicine.* 1995;182(6):1959-71.

77. Brown MS, and Goldstein JL. Lipoprotein metabolism in the macrophage: implications for cholesterol deposition in atherosclerosis. *Annual review of biochemistry.* 1983;52(223-61.

78. Brown MS, Goldstein JL, Krieger M, Ho YK, and Anderson RG. Reversible accumulation of cholesteryl esters in macrophages incubated with acetylated lipoproteins. *The Journal of cell biology.* 1979;82(3):597-613.

79. Moore KJ, and Freeman MW. Scavenger receptors in atherosclerosis: beyond lipid uptake. *Arteriosclerosis, thrombosis, and vascular biology.* 2006;26(8):1702-11.

80. Griffin EE, Ullery JC, Cox BE, and Jerome WG. Aggregated LDL and lipid dispersions induce lysosomal cholesteryl ester accumulation in macrophage foam cells. *Journal of lipid research.* 2005;46(10):2052-60.

81. Yancey PG, and Jerome WG. Lysosomal cholesterol derived from mildly oxidized low density lipoprotein is resistant to efflux. *Journal of lipid research.* 2001;42(3):317-27.

82. Dhaliwal BS, and Steinbrecher UP. Cholesterol delivered to macrophages by oxidized low density lipoprotein is sequestered in lysosomes and fails to efflux normally. *Journal of lipid research.* 2000;41(10):1658-65.

83. Takano T, Black WJ, Peters TJ, and de Duve C. Assay, kinetics, and lysosomal localization of an acid cholesteryl esterase in rabbit aortic smooth muscle cells. *The Journal of biological chemistry.* 1974;249(21):6732-7.

84. Kwon HJ, Abi-Mosleh L, Wang ML, Deisenhofer J, Goldstein JL, Brown MS, and Infante RE. Structure of N-terminal domain of NPC1 reveals distinct subdomains for binding and transfer of cholesterol. *Cell.* 2009;137(7):1213-24.

85. Tabas I. Consequences of cellular cholesterol accumulation: basic concepts and physiological implications. *The Journal of clinical investigation.* 2002;110(7):905-11.

86. Singh R, Kaushik S, Wang Y, Xiang Y, Novak I, Komatsu M, Tanaka K, Cuervo AM, and Czaja MJ. Autophagy regulates lipid metabolism. *Nature.* 2009;458(7242):1131-5.

87. Ouimet M, Franklin V, Mak E, Liao X, Tabas I, and Marcel YL. Autophagy regulates cholesterol efflux from macrophage foam cells via lysosomal acid lipase. *Cell metabolism.* 2011;13(6):655-67.

88. Haust MD. The morphogenesis and fate of potential and early atherosclerotic lesions in man. *Human pathology.* 1971;2(1):1-29.

89. Li H, Freeman MW, and Libby P. Regulation of smooth muscle cell scavenger receptor expression in vivo by atherogenic diets and in vitro by cytokines. *The Journal of clinical investigation.* 1995;95(1):122-33.

90. Doran AC, Meller N, and McNamara CA. Role of smooth muscle cells in the initiation and early progression of atherosclerosis. *Arteriosclerosis, thrombosis, and vascular biology.* 2008;28(5):812-9.

91. Williams KJ, and Tabas I. The response-to-retention hypothesis of early atherogenesis. *Arteriosclerosis, thrombosis, and vascular biology.* 1995;15(5):551-61.

92. Williams KJ, and Tabas I. Lipoprotein retention--and clues for atheroma regression. *Arteriosclerosis, thrombosis, and vascular biology.* 2005;25(8):1536-40.

93. Stocker R, and Keaney JF, Jr. Role of oxidative modifications in atherosclerosis. *Physiological reviews.* 2004;84(4):1381-478.

94. Steinberg D, and Witztum JL. Is the oxidative modification hypothesis relevant to human atherosclerosis? Do the antioxidant trials conducted to date refute the hypothesis? *Circulation.* 2002;105(17):2107-11.

95. Wen Y, and Leake DS. Low density lipoprotein undergoes oxidation within lysosomes in cells. *Circulation research.* 2007;100(9):1337-43.

96. Torzewski M, Klouche M, Hock J, Messner M, Dorweiler B, Torzewski J, Gabbert HE, and Bhakdi S. Immunohistochemical demonstration of enzymatically modified human LDL and its colocalization with the terminal complement complex in the early atherosclerotic lesion. *Arteriosclerosis, thrombosis, and vascular biology.* 1998;18(3):369-78.

97. Hakala JK, Oksjoki R, Laine P, Du H, Grabowski GA, Kovanen PT, and Pentikainen MO. Lysosomal enzymes are released from cultured human macrophages, hydrolyze LDL in vitro, and are present extracellularly in human atherosclerotic lesions. *Arteriosclerosis, thrombosis, and vascular biology.* 2003;23(8):1430-6.

98. Schnyder J, and Baggiolini M. Secretion of lysosomal hydrolases by stimulated and nonstimulated macrophages. *The Journal of experimental medicine.* 1978;148(2):435-50.

99. Naghavi M, John R, Naguib S, Siadaty MS, Grasu R, Kurian KC, van Winkle WB, Soller B, Litovsky S, Madjid M, et al. pH Heterogeneity of human and rabbit atherosclerotic plaques; a new insight into detection of vulnerable plaque. *Atherosclerosis.* 2002;164(1):27-35.

100. Tapper H, and Sundler R. Cytosolic pH regulation in mouse macrophages. Proton extrusion by plasma-membrane-localized H(+)-ATPase. *The Biochemical journal.* 1992;281 (Pt 1)(245-50.

101. Newsholme P, Gordon S, and Newsholme EA. Rates of utilization and fates of glucose, glutamine, pyruvate, fatty acids and ketone bodies by mouse macrophages. *The Biochemical journal.* 1987;242(3):631-6.

102. Buton X, Mamdouh Z, Ghosh R, Du H, Kuriakose G, Beatini N, Grabowski GA, Maxfield FR, and Tabas I. Unique cellular events occurring during the initial interaction of macrophages with matrix-retained or methylated aggregated low density lipoprotein (LDL). Prolonged cell-surface contact during which ldl-cholesteryl ester hydrolysis exceeds ldl protein degradation. *The Journal of biological chemistry.* 1999;274(45):32112-21.

103. Mehrabi MR, Sinzinger H, Ekmekcioglu C, Tamaddon F, Plesch K, Glogar HD, Maurer G, Stefenelli T, and Lang IM. Accumulation of oxidized LDL in human semilunar valves correlates with coronary atherosclerosis. *Cardiovascular research.* 2000;45(4):874-82.

104. Gaut JP, and Heinecke JW. Mechanisms for oxidizing low-density lipoprotein. Insights from patterns of oxidation products in the artery wall and from mouse models of atherosclerosis. *Trends in cardiovascular medicine.* 2001;11(3-4):103-12.

105. Yoshida H, and Kisugi R. Mechanisms of LDL oxidation. *Clinica chimica acta; international journal of clinical chemistry.* 2010;411(23-24):1875-82.

106. Parthasarathy S, Raghavamenon A, Garelnabi MO, and Santanam N. Oxidized low-density lipoprotein. *Methods in molecular biology.* 2010;610(403-17.

107. Steinbrecher UP, and Lougheed M. Scavenger receptor-independent stimulation of cholesterol esterification in macrophages by low density lipoprotein extracted from human aortic intima. *Arteriosclerosis and thrombosis : a journal of vascular biology.* 1992;12(5):608-25.

108. Brown AJ, and Jessup W. Oxysterols and atherosclerosis. *Atherosclerosis.* 1999;142(1):1-28.

109. Orso E, Grandl M, and Schmitz G. Oxidized LDL-induced endolysosomal phospholipidosis and enzymatically modified LDL-induced foam cell formation determine specific lipid species modulation in human macrophages. *Chemistry and physics of lipids.* 2011;164(6):479-87.

110. Jessup W, and Kritharides L. Metabolism of oxidized LDL by macrophages. *Current opinion in lipidology.* 2000;11(5):473-81.

111. Yancey PG, and Jerome WG. Lysosomal sequestration of free and esterified cholesterol from oxidized low density lipoprotein in macrophages of different species. *Journal of lipid research.* 1998;39(7):1349-61.

112. Brown AJ, Mander EL, Gelissen IC, Kritharides L, Dean RT, and Jessup W. Cholesterol and oxysterol metabolism and subcellular distribution in macrophage foam cells. Accumulation of oxidized esters in lysosomes. *Journal of lipid research.* 2000;41(2):226-37.

113. Niu X, Zammit V, Upston JM, Dean RT, and Stocker R. Coexistence of oxidized lipids and alpha-tocopherol in all lipoprotein density fractions isolated from advanced human atherosclerotic plaques. *Arteriosclerosis, thrombosis, and vascular biology.* 1999;19(7):1708-18.

114. Goldstein JL, Hoff HF, Ho YK, Basu SK, and Brown MS. Stimulation of cholesteryl ester synthesis in macrophages by extracts of atherosclerotic human aortas and complexes of albumin/cholesteryl esters. *Arteriosclerosis.* 1981;1(3):210-26.

115. Hoff HF, and Morton RE. Lipoproteins containing apo B extracted from human aortas. Structure and function. *Annals of the New York Academy of Sciences.* 1985;454(183-94.

116. Guyton JR, and Klemp KF. Transitional features in human atherosclerosis. Intimal thickening, cholesterol clefts, and cell loss in human aortic fatty streaks. *The American journal of pathology.* 1993;143(5):1444-57.

117. Kruth HS. Sequestration of aggregated low-density lipoproteins by macrophages. *Current opinion in lipidology.* 2002;13(5):483-8.

118. Suits AG, Chait A, Aviram M, and Heinecke JW. Phagocytosis of aggregated lipoprotein by macrophages: low density lipoprotein receptor-dependent foam-cell formation. *Proceedings of the National Academy of Sciences of the United States of America.* 1989;86(8):2713-7.

119. Tertov VV, Orekhov AN, Sobenin IA, Gabbasov ZA, Popov EG, Yaroslavov AA, and Smirnov VN. Three types of naturally occurring modified lipoproteins induce intracellular lipid accumulation due to lipoprotein aggregation. *Circulation research.* 1992;71(1):218-28.

120. Xu XX, and Tabas I. Sphingomyelinase enhances low density lipoprotein uptake and ability to induce cholesteryl ester accumulation in macrophages. *The Journal of biological chemistry.* 1991;266(36):24849-58.

121. Maor I, and Aviram M. Macrophage released proteoglycans are involved in cell-mediated aggregation of LDL. *Atherosclerosis.* 1999;142(1):57-66.

122. Hoff HF, O'Neil J, Pepin JM, and Cole TB. Macrophage uptake of cholesterol-containing particles derived from LDL and isolated from atherosclerotic lesions. *European heart journal.* 1990;11 Suppl E(105-15.

123. Xu S, and Lin B. The mechanism of oxidation-induced low-density lipoprotein aggregation: an analogy to colloidal aggregation and beyond? *Biophysical journal.* 2001;81(4):2403-13.

124. Falcone DJ, and Salisbury BG. Fibronectin stimulates macrophage uptake of low density lipoprotein-heparin-collagen complexes. *Arteriosclerosis.* 1988;8(3):263-73.

125. Maor I, and Aviram M. Oxidized low density lipoprotein leads to macrophage accumulation of unesterified cholesterol as a result of lysosomal trapping of the lipoprotein hydrolyzed cholesteryl ester. *Journal of lipid research.* 1994;35(5):803-19.

126. Cox BE, Griffin EE, Ullery JC, and Jerome WG. Effects of cellular cholesterol loading on macrophage foam cell lysosome acidification. *Journal of lipid research.* 2007;48(5):1012-21.

127. Burton BK, Emery D, and Mueller HW. Lysosomal acid lipase in cultivated fibroblasts: characterization of enzyme activity in normal and enzymatically deficient cell lines. *Clinica chimica acta; international journal of clinical chemistry.* 1980;101(1):25-32.

128. Jerome WG, Cox BE, Griffin EE, and Ullery JC. Lysosomal cholesterol accumulation inhibits subsequent hydrolysis of lipoprotein cholesteryl ester. *Microsc Microanal.* 2008;14(2):138-49.

129. Ullery-Ricewick JC, Cox BE, Griffin EE, and Jerome WG. Triglyceride alters lysosomal cholesterol ester metabolism in cholesteryl ester-laden macrophage foam cells. *Journal of lipid research.* 2009;50(10):2014-26.

130. Li W, Yuan XM, Olsson AG, and Brunk UT. Uptake of oxidized LDL by macrophages results in partial lysosomal enzyme inactivation and relocation. *Arteriosclerosis, thrombosis, and vascular biology.* 1998;18(2):177-84.

131. Yuan XM, Li W, Brunk UT, Dalen H, Chang YH, and Sevanian A. Lysosomal destabilization during macrophage damage induced by cholesterol oxidation products. *Free radical biology & medicine.* 2000;28(2):208-18.

132. Tangirala RK, Jerome WG, Jones NL, Small DM, Johnson WJ, Glick JM, Mahlberg FH, and Rothblat GH. Formation of cholesterol monohydrate crystals in macrophage-derived foam cells. *Journal of lipid research.* 1994;35(1):93-104.

133. Tapper H, and Sundler R. Role of lysosomal and cytosolic pH in the regulation of macrophage lysosomal enzyme secretion. *The Biochemical journal.* 1990;272(2):407-14.

134. Lougheed M, Zhang HF, and Steinbrecher UP. Oxidized low density lipoprotein is resistant to cathepsins and accumulates within macrophages. *The Journal of biological chemistry.* 1991;266(22):14519-25.

135. Mander EL, Dean RT, Stanley KK, and Jessup W. Apolipoprotein B of oxidized LDL accumulates in the lysosomes of macrophages. *Biochimica et biophysica acta.* 1994;1212(1):80-92.

136. Jessup W, Mander EL, and Dean RT. The intracellular storage and turnover of apolipoprotein B of oxidized LDL in macrophages. *Biochimica et biophysica acta.* 1992;1126(2):167-77.

137. Roma P, Bernini F, Fogliatto R, Bertulli SM, Negri S, Fumagalli R, and Catapano AL. Defective catabolism of oxidized LDL by J774 murine macrophages. *Journal of lipid research.* 1992;33(6):819-29.

138. Hoppe G, O'Neil J, and Hoff HF. Inactivation of lysosomal proteases by oxidized low density lipoprotein is partially responsible for its poor degradation by mouse peritoneal macrophages. *The Journal of clinical investigation.* 1994;94(4):1506-12.

139. O'Neil J, Hoppe G, and Hoff HF. Phospholipids in oxidized low density lipoproteins perturb the ability of macrophages to degrade internalized macromolecules and reduce intracellular cathepsin B activity. *Atherosclerosis.* 2003;169(2):215-24.

140. Itabe H, Suzuki K, Tsukamoto Y, Komatsu R, Ueda M, Mori M, Higashi Y, and Takano T. Lysosomal accumulation of oxidized phosphatidylcholine-apolipoprotein B complex in macrophages: intracellular fate of oxidized low density lipoprotein. *Biochimica et biophysica acta.* 2000;1487(2-3):233-45.

141. Jerome WG, and Yancey PG. The role of microscopy in understanding atherosclerotic lysosomal lipid metabolism. *Microsc Microanal.* 2003;9(1):54-67.

142. Coltoff-Schiller B, Goldfischer S, Wolinsky H, and Factor SM. Lipid accumulation in human aortic smooth muscle cell lysosomes. *The American journal of pathology.* 1976;83(1):39-44.

143. Shio H, Farquhar MG, and de Duve C. Lysosomes of the arterial wall. IV. Cytochemical localization of acid phosphatase and catalase in smooth muscle cells and foam cells from rabbit atheromatous aorta. *The American journal of pathology.* 1974;76(1):1-16.

144. Peters TJ, Muller M, and De Duve C. Lysosomes of the arterial wall. I. Isolation and subcellular fractionation of cells from normal rabbit aorta. *The Journal of experimental medicine.* 1972;136(5):1117-39.

145. Shio H, Haley NJ, and Fowler S. Characterization of lipid-laden aortic cells from cholesterol-fed rabbits. III. Intracellular localization of cholesterol and cholesteryl ester. *Laboratory investigation; a journal of technical methods and pathology.* 1979;41(2):160-7.

146. Peters TJ, and De Duve C. Lysosomes of the arterial wall. II. Subcellular fractionation of aortic cells from rabbits with experimantal atheroma. *Experimental and molecular pathology.* 1974;20(2):228-56.

147. Miller BF, and Kothari HV. Increased activity of lysosomal enzymes in human atherosclerotic aortas. *Experimental and molecular pathology.* 1969;10(3):288-94.

148. Garver WS, Jelinek D, Francis GA, and Murphy BD. The Niemann-Pick C1 gene is downregulated by feedback inhibition of the SREBP pathway in human fibroblasts. *Journal of lipid research.* 2008;49(5):1090-102.

149. Jelinek D, Patrick SM, Kitt KN, Chan T, Francis GA, and Garver WS. Physiological and coordinate downregulation of the NPC1 and NPC2 genes are associated with the sequestration of LDL-derived cholesterol within endocytic compartments. *Journal of cellular biochemistry.* 2009;108(5):1102-16.

150. Jelinek D, Castillo JJ, Richardson LM, Luo L, Heidenreich RA, and Garver WS. The Niemann-Pick C1 gene is downregulated in livers of C57BL/6J mice by dietary fatty

acids, but not dietary cholesterol, through feedback inhibition of the SREBP pathway. *The Journal of nutrition.* 2012;142(11):1935-42.

151. Jerome WGC, B.; Vaughan, J. B. The distribution of NPC-1 protein in macrophages is altered after oxidized LDL lyososomal accumulation. *Microsc Microanal.* 2002;8(Suppl. 2):894-5.

152. Rigamonti E, Helin L, Lestavel S, Mutka AL, Lepore M, Fontaine C, Bouhlel MA, Bultel S, Fruchart JC, Ikonen E, et al. Liver X receptor activation controls intracellular cholesterol trafficking and esterification in human macrophages. *Circulation research.* 2005;97(7):682-9.

153. Chinetti-Gbaguidi G, Rigamonti E, Helin L, Mutka AL, Lepore M, Fruchart JC, Clavey V, Ikonen E, Lestavel S, and Staels B. Peroxisome proliferator-activated receptor alpha controls cellular cholesterol trafficking in macrophages. *Journal of lipid research.* 2005;46(12):2717-25.

154. Yu X, Li X, Zhao G, Xiao J, Mo Z, Yin K, Jiang Z, Fu Y, Zha X, and Tang C. OxLDL up-regulates Niemann-Pick type C1 expression through ERK1/2/COX-2/PPARalpha-signaling pathway in macrophages. *Acta biochimica et biophysica Sinica.* 2012;44(2):119-28.

155. Jones SA, Rojas-Caro S, Quinn AG, Friedman M, Marulkar S, Ezgu F, Zaki O, Gargus JJ, Hughes J, Plantaz D, et al. Survival in infants treated with sebelipase Alfa for lysosomal acid lipase deficiency: an open-label, multicenter, dose-escalation study. *Orphanet journal of rare diseases.* 2017;12(1):25.

156. Burton BK, Balwani M, Feillet F, Baric I, Burrow TA, Camarena Grande C, Coker M, Consuelo-Sanchez A, Deegan P, Di Rocco M, et al. A Phase 3 Trial of Sebelipase Alfa in Lysosomal Acid Lipase Deficiency. *The New England journal of medicine.* 2015;373(11):1010-20.

157. Balwani M, Breen C, Enns GM, Deegan PB, Honzik T, Jones S, Kane JP, Malinova V, Sharma R, Stock EO, et al. Clinical effect and safety profile of recombinant human lysosomal acid lipase in patients with cholesteryl ester storage disease. *Hepatology.* 2013;58(3):950-7.

158. Valayannopoulos V, Malinova V, Honzik T, Balwani M, Breen C, Deegan PB, Enns GM, Jones SA, Kane JP, Stock EO, et al. Sebelipase alfa over 52 weeks reduces serum transaminases, liver volume and improves serum lipids in patients with lysosomal acid lipase deficiency. *Journal of hepatology.* 2014;61(5):1135-42.

159. Du H, Schiavi S, Levine M, Mishra J, Heur M, and Grabowski GA. Enzyme therapy for lysosomal acid lipase deficiency in the mouse. *Human molecular genetics.* 2001;10(16):1639-48.

160. Sun Y, Xu YH, Du H, Quinn B, Liou B, Stanton L, Inskeep V, Ran H, Jakubowitz P, Grilliot N, et al. Reversal of advanced disease in lysosomal acid lipase deficient mice: A model for lysosomal acid lipase deficiency disease. *Molecular genetics and metabolism.* 2014.

161. Du H, Schiavi S, Wan N, Levine M, Witte DP, and Grabowski GA. Reduction of atherosclerotic plaques by lysosomal acid lipase supplementation. *Arteriosclerosis, thrombosis, and vascular biology.* 2004;24(1):147-54.

162. Coronary Artery Disease Genetics C. A genome-wide association study in Europeans and South Asians identifies five new loci for coronary artery disease. *Nature genetics.* 2011;43(4):339-44.

163. Wild PS, Zeller T, Schillert A, Szymczak S, Sinning CR, Deiseroth A, Schnabel RB, Lubos E, Keller T, Eleftheriadis MS, et al. A genome-wide association study identifies LIPA as a susceptibility gene for coronary artery disease. *Circulation Cardiovascular genetics.* 2011;4(4):403-12.

164. Consortium IKC. Large-scale gene-centric analysis identifies novel variants for coronary artery disease. *PLoS genetics.* 2011;7(9):e1002260.

165. Yusuf S, Hawken S, Ounpuu S, Dans T, Avezum A, Lanas F, McQueen M, Budaj A, Pais P, Varigos J, et al. Effect of potentially modifiable risk factors associated with myocardial infarction in 52 countries (the INTERHEART study): case-control study. *Lancet.* 2004;364(9438):937-52.

166. Weber C, and Noels H. Atherosclerosis: current pathogenesis and therapeutic options. *Nature medicine.* 2011;17(11):1410-22.

167. Hegele RA, Gidding SS, Ginsberg HN, McPherson R, Raal FJ, Rader DJ, Robinson JG, and Welty FK. Nonstatin Low-Density Lipoprotein-Lowering Therapy and Cardiovascular Risk Reduction-Statement From ATVB Council. *Arteriosclerosis, thrombosis, and vascular biology.* 2015;35(11):2269-80.

168. Wissler RW, Vesselinovitch D, and Komatsu A. The contribution of studies of atherosclerotic lesions in young people to future research. *Annals of the New York Academy of Sciences.* 1990;598(418-34.

169. Nakashima Y, Wight TN, and Sueishi K. Early atherosclerosis in humans: role of diffuse intimal thickening and extracellular matrix proteoglycans. *Cardiovascular research.* 2008;79(1):14-23.

170. Ikari Y, McManus BM, Kenyon J, and Schwartz SM. Neonatal intima formation in the human coronary artery. *Arteriosclerosis, thrombosis, and vascular biology.* 1999;19(9):2036-40.

171. Bonert M, Leask RL, Butany J, Ethier CR, Myers JG, Johnston KW, and Ojha M. The relationship between wall shear stress distributions and intimal thickening in the human abdominal aorta. *Biomedical engineering online.* 2003;2(18.

172. Stary HC, Blankenhorn DH, Chandler AB, Glagov S, Insull W, Jr., Richardson M, Rosenfeld ME, Schaffer SA, Schwartz CJ, Wagner WD, et al. A definition of the intima of human arteries and of its atherosclerosis-prone regions. A report from the Committee on Vascular Lesions of the Council on Arteriosclerosis, American Heart Association. *Circulation.* 1992;85(1):391-405.

173. Nakashima Y, Chen YX, Kinukawa N, and Sueishi K. Distributions of diffuse intimal thickening in human arteries: preferential expression in atherosclerosis-prone arteries from an early age. *Virchows Archiv : an international journal of pathology.* 2002;441(3):279-88.

174. Napoli C, D'Armiento FP, Mancini FP, Postiglione A, Witztum JL, Palumbo G, and Palinski W. Fatty streak formation occurs in human fetal aortas and is greatly enhanced by maternal hypercholesterolemia. Intimal accumulation of low density lipoprotein and its oxidation precede monocyte recruitment into early atherosclerotic lesions. *The Journal of clinical investigation.* 1997;100(11):2680-90.

175. Nakashima Y, Fujii H, Sumiyoshi S, Wight TN, and Sueishi K. Early human atherosclerosis: accumulation of lipid and proteoglycans in intimal thickenings followed by macrophage infiltration. *Arteriosclerosis, thrombosis, and vascular biology.* 2007;27(5):1159-65.

176. Virmani R, Kolodgie FD, Burke AP, Farb A, and Schwartz SM. Lessons from sudden coronary death: a comprehensive morphological classification scheme for atherosclerotic lesions. *Arteriosclerosis, thrombosis, and vascular biology.* 2000;20(5):1262-75.

177. Murry CE, Gipaya CT, Bartosek T, Benditt EP, and Schwartz SM. Monoclonality of smooth muscle cells in human atherosclerosis. *The American journal of pathology.* 1997;151(3):697-705.

178. Chung IM, Schwartz SM, and Murry CE. Clonal architecture of normal and atherosclerotic aorta: implications for atherogenesis and vascular development. *The American journal of pathology.* 1998;152(4):913-23.

179. Aikawa M, Sivam PN, Kuro-o M, Kimura K, Nakahara K, Takewaki S, Ueda M, Yamaguchi H, Yazaki Y, Periasamy M, et al. Human smooth muscle myosin heavy chain isoforms as molecular markers for vascular development and atherosclerosis. *Circulation research.* 1993;73(6):1000-12.

180. Hoshiga M, Alpers CE, Smith LL, Giachelli CM, and Schwartz SM. Alpha-v beta-3 integrin expression in normal and atherosclerotic artery. *Circulation research.* 1995;77(6):1129-35.

181. Nakata A, Miyagawa J, Yamashita S, Nishida M, Tamura R, Yamamori K, Nakamura T, Nozaki S, Kameda-Takemura K, Kawata S, et al. Localization of heparin-binding epidermal growth factor-like growth factor in human coronary arteries. Possible roles of HB-EGF in the formation of coronary atherosclerosis. *Circulation.* 1996;94(11):2778-86.

182. Merrilees MJ, and Beaumont B. Structural heterogeneity of the diffuse intimal thickening and correlation with distribution of TGF-beta 1. *Journal of vascular research.* 1993;30(5):293-302.

183. Kaprio J, Norio R, Pesonen E, and Sarna S. Intimal thickening of the coronary arteries in infants in relation to family history of coronary artery disease. *Circulation.* 1993;87(6):1960-8.

184. Velican C, and Velican D. Some particular aspects of the microarchitecture of human coronary arteries. *Atherosclerosis.* 1979;33(2):191-200.

185. Coleman R, Hayek T, Keidar S, and Aviram M. A mouse model for human atherosclerosis: long-term histopathological study of lesion development in the aortic arch of apolipoprotein E-deficient (E0) mice. *Acta histochemica.* 2006;108(6):415-24.

186. Stary HC. Evolution and progression of atherosclerotic lesions in coronary arteries of children and young adults. *Arteriosclerosis.* 1989;9(1 Suppl):I19-32.

187. Fukuchi M, Watanabe J, Kumagai K, Baba S, Shinozaki T, Miura M, Kagaya Y, and Shirato K. Normal and oxidized low density lipoproteins accumulate deep in physiologically thickened intima of human coronary arteries. *Laboratory investigation; a journal of technical methods and pathology.* 2002;82(10):1437-47.

188. Edwards IJ, Goldberg IJ, Parks JS, Xu H, and Wagner WD. Lipoprotein lipase enhances the interaction of low density lipoproteins with artery-derived extracellular matrix proteoglycans. *Journal of lipid research.* 1993;34(7):1155-63.

189. Camejo G, Hurt-Camejo E, Wiklund O, and Bondjers G. Association of apo B lipoproteins with arterial proteoglycans: pathological significance and molecular basis. *Atherosclerosis.* 1998;139(2):205-22.

190. Schonherr E, Jarvelainen HT, Sandell LJ, and Wight TN. Effects of platelet-derived growth factor and transforming growth factor-beta 1 on the synthesis of a large versican-like chondroitin sulfate proteoglycan by arterial smooth muscle cells. *The Journal of biological chemistry.* 1991;266(26):17640-7.

191. Little PJ, Tannock L, Olin KL, Chait A, and Wight TN. Proteoglycans synthesized by arterial smooth muscle cells in the presence of transforming growth factor-beta1 exhibit increased binding to LDLs. *Arteriosclerosis, thrombosis, and vascular biology.* 2002;22(1):55-60.

192. Chang MY, Potter-Perigo S, Tsoi C, Chait A, and Wight TN. Oxidized low density lipoproteins regulate synthesis of monkey aortic smooth muscle cell proteoglycans that have enhanced native low density lipoprotein binding properties. *The Journal of biological chemistry.* 2000;275(7):4766-73.

193. Gomez D, and Owens GK. Smooth muscle cell phenotypic switching in atherosclerosis. *Cardiovascular research.* 2012;95(2):156-64.

194. Louis SF, and Zahradka P. Vascular smooth muscle cell motility: From migration to invasion. *Experimental and clinical cardiology.* 2010;15(4):e75-85.

195. Geng YJ, and Libby P. Progression of atheroma: a struggle between death and procreation. *Arteriosclerosis, thrombosis, and vascular biology.* 2002;22(9):1370-80.

196. Owens GK, Kumar MS, and Wamhoff BR. Molecular regulation of vascular smooth muscle cell differentiation in development and disease. *Physiological reviews.* 2004;84(3):767-801.

197. Barrett TB, and Benditt EP. Platelet-derived growth factor gene expression in human atherosclerotic plaques and normal artery wall. *Proceedings of the National Academy of Sciences of the United States of America.* 1988;85(8):2810-4.

198. Holycross BJ, Blank RS, Thompson MM, Peach MJ, and Owens GK. Platelet-derived growth factor-BB-induced suppression of smooth muscle cell differentiation. *Circulation research.* 1992;71(6):1525-32.

199. Gong Q, and Pitas RE. Synergistic effects of growth factors on the regulation of smooth muscle cell scavenger receptor activity. *The Journal of biological chemistry.* 1995;270(37):21672-8.

200. Glukhova MA, Kabakov AE, Frid MG, Ornatsky OI, Belkin AM, Mukhin DN, Orekhov AN, Koteliansky VE, and Smirnov VN. Modulation of human aorta smooth muscle cell phenotype: a study of muscle-specific variants of vinculin, caldesmon, and actin expression. *Proceedings of the National Academy of Sciences of the United States of America.* 1988;85(24):9542-6.

201. Rong JX, Shapiro M, Trogan E, and Fisher EA. Transdifferentiation of mouse aortic smooth muscle cells to a macrophage-like state after cholesterol loading. *Proceedings of the National Academy of Sciences of the United States of America.* 2003;100(23):13531-6.

202. Vengrenyuk Y, Nishi H, Long X, Ouimet M, Savji N, Martinez FO, Cassella CP, Moore KJ, Ramsey SA, Miano JM, et al. Cholesterol loading reprograms the microRNA-143/145-myocardin axis to convert aortic smooth muscle cells to a dysfunctional macrophage-like phenotype. *Arteriosclerosis, thrombosis, and vascular biology.* 2015;35(3):535-46.

203. Klouche M, Rose-John S, Schmiedt W, and Bhakdi S. Enzymatically degraded, nonoxidized LDL induces human vascular smooth muscle cell activation, foam cell transformation, and proliferation. *Circulation.* 2000;101(15):1799-805.

204. Huff MW, and Pickering JG. Can a vascular smooth muscle-derived foam-cell really change its spots? *Arteriosclerosis, thrombosis, and vascular biology.* 2015;35(3):492-5.

205. Feil S, Fehrenbacher B, Lukowski R, Essmann F, Schulze-Osthoff K, Schaller M, and Feil R. Transdifferentiation of vascular smooth muscle cells to macrophage-like cells during atherogenesis. *Circulation research.* 2014;115(7):662-7.

206. Shankman LS, Gomez D, Cherepanova OA, Salmon M, Alencar GF, Haskins RM, Swiatlowska P, Newman AA, Greene ES, Straub AC, et al. KLF4-dependent phenotypic modulation of smooth muscle cells has a key role in atherosclerotic plaque pathogenesis. *Nature medicine.* 2015;21(6):628-37.

207. Deaton RA, Gan Q, and Owens GK. Sp1-dependent activation of KLF4 is required for PDGF-BB-induced phenotypic modulation of smooth muscle. *American journal of physiology Heart and circulatory physiology.* 2009;296(4):H1027-37.

208. Pidkovka NA, Cherepanova OA, Yoshida T, Alexander MR, Deaton RA, Thomas JA, Leitinger N, and Owens GK. Oxidized phospholipids induce phenotypic switching of vascular smooth muscle cells in vivo and in vitro. *Circulation research.* 2007;101(8):792-801.

209. Caplice NM, Bunch TJ, Stalboerger PG, Wang S, Simper D, Miller DV, Russell SJ, Litzow MR, and Edwards WD. Smooth muscle cells in human coronary atherosclerosis can originate from cells administered at marrow transplantation. *Proceedings of the National Academy of Sciences of the United States of America.* 2003;100(8):4754-9.

210. Iwata H, Manabe I, Fujiu K, Yamamoto T, Takeda N, Eguchi K, Furuya A, Kuro-o M, Sata M, and Nagai R. Bone marrow-derived cells contribute to vascular inflammation but do not differentiate into smooth muscle cell lineages. *Circulation.* 2010;122(20):2048-57.

211. Moore KJ, Sheedy FJ, and Fisher EA. Macrophages in atherosclerosis: a dynamic balance. *Nature reviews Immunology.* 2013;13(10):709-21.

212. Dhaliwal BS, and Steinbrecher UP. Scavenger receptors and oxidized low density lipoproteins. *Clinica chimica acta; international journal of clinical chemistry.* 1999;286(1-2):191-205.

213. Stephen SL, Freestone K, Dunn S, Twigg MW, Homer-Vanniasinkam S, Walker JH, Wheatcroft SB, and Ponnambalam S. Scavenger receptors and their potential as therapeutic targets in the treatment of cardiovascular disease. *International journal of hypertension.* 2010;2010(646929.

214. Platt N, Haworth R, Darley L, and Gordon S. The many roles of the class A macrophage scavenger receptor. *International review of cytology.* 2002;212(1-40.

215. Gough PJ, Greaves DR, Suzuki H, Hakkinen T, Hiltunen MO, Turunen M, Herttuala SY, Kodama T, and Gordon S. Analysis of macrophage scavenger receptor (SR-A) expression in human aortic atherosclerotic lesions. *Arteriosclerosis, thrombosis, and vascular biology.* 1999;19(3):461-71.

216. Mietus-Snyder M, Gowri MS, and Pitas RE. Class A scavenger receptor up-regulation in smooth muscle cells by oxidized low density lipoprotein. Enhancement by calcium flux and concurrent cyclooxygenase-2 up-regulation. *The Journal of biological chemistry.* 2000;275(23):17661-70.

217. Tomokiyo R, Jinnouchi K, Honda M, Wada Y, Hanada N, Hiraoka T, Suzuki H, Kodama T, Takahashi K, and Takeya M. Production, characterization, and interspecies reactivities of monoclonal antibodies against human class A macrophage scavenger receptors. *Atherosclerosis.* 2002;161(1):123-32.

218. Luechtenborg B, Hofnagel O, Weissen-Plenz G, Severs NJ, and Robenek H. Function of scavenger receptor class A type I/II is not important for smooth muscle foam cell formation. *European journal of cell biology.* 2008;87(2):91-9.

219. Ma S, Yang D, Li D, Tang B, and Yang Y. Oleic acid induces smooth muscle foam cell formation and enhances atherosclerotic lesion development via CD36. *Lipids in health and disease.* 2011;10(53.

220. Rivera J, Walduck A, Thomas S, Glaros E, Hooker E, Guida E, Sobey C, and Drummond G. Accumulation of serum lipids by vascular smooth muscle cells involves a macropinocytosis-like uptake pathway and is associated with the downregulation of the ATP-binding cassette transporter A1. *Naunyn-Schmiedeberg's Arch Pharmacol.* 2013;386(12):1081-93.

221. Haka AS, Grosheva I, Chiang E, Buxbaum AR, Baird BA, Pierini LM, and Maxfield FR. Macrophages create an acidic extracellular hydrolytic compartment to digest aggregated lipoproteins. *Molecular biology of the cell.* 2009;20(23):4932-40.

222. Haka AS, Singh RK, Grosheva I, Hoffner H, Capetillo-Zarate E, Chin HF, Anandasabapathy N, and Maxfield FR. Monocyte-Derived Dendritic Cells Upregulate Extracellular Catabolism of Aggregated Low-Density Lipoprotein on Maturation, Leading to Foam Cell Formation. *Arteriosclerosis, thrombosis, and vascular biology.* 2015;35(10):2092-103.

223. Costales P, Fuentes-Prior P, Castellano J, Revuelta-Lopez E, Corral-Rodriguez MA, Nasarre L, Badimon L, and Llorente-Cortes V. K Domain CR9 of Low Density Lipoprotein (LDL) Receptor-related Protein 1 (LRP1) Is Critical for Aggregated LDL-

induced Foam Cell Formation from Human Vascular Smooth Muscle Cells. *The Journal of biological chemistry.* 2015;290(24):14852-65.

224. Llorente-Cortes V, Otero-Vinas M, Camino-Lopez S, Costales P, and Badimon L. Cholesteryl esters of aggregated LDL are internalized by selective uptake in human vascular smooth muscle cells. *Arteriosclerosis, thrombosis, and vascular biology.* 2006;26(1):117-23.

225. Francis GA. In: McLeod NDRS ed. *Biochemistry of Lipids, Lipoproteins and Membranes (Sixth Edition).* Boston: Elsevier; 2016:437-57.

226. Nagao S, Murao K, Imachi H, Cao WM, Yu X, Li J, Matsumoto K, Nishiuchi T, Ahmed RA, Wong NC, et al. Platelet derived growth factor regulates ABCA1 expression in vascular smooth muscle cells. *FEBS letters.* 2006;580(18):4371-6.

227. Dubland JA, and Francis GA. Lysosomal acid lipase: at the crossroads of normal and atherogenic cholesterol metabolism. *Frontiers in cell and developmental biology.* 2015;3(3.

228. Frontini MJ, O'Neil C, Sawyez C, Chan BM, Huff MW, and Pickering JG. Lipid incorporation inhibits Src-dependent assembly of fibronectin and type I collagen by vascular smooth muscle cells. *Circulation research.* 2009;104(7):832-41.

229. Beyea MM, Reaume S, Sawyez CG, Edwards JY, O'Neil C, Hegele RA, Pickering JG, and Huff MW. The oxysterol 24(s),25-epoxycholesterol attenuates human smooth muscle-derived foam cell formation via reduced low-density lipoprotein uptake and enhanced cholesterol efflux. *Journal of the American Heart Association.* 2012;1(3):e000810.

230. Feig JE, Hewing B, Smith JD, Hazen SL, and Fisher EA. High-density lipoprotein and atherosclerosis regression: evidence from preclinical and clinical studies. *Circulation research.* 2014;114(1):205-13.

231. Grabowski GA, Du H, and Charnas L. In: Valle D, and Beaudet AL eds. *The Online Metabolic and Molecular Bases of Inherited Disease* McGraw-Hill; 2016.

232. Du H, Levine M, Ganesa C, Witte DP, Cole ES, and Grabowski GA. The role of mannosylated enzyme and the mannose receptor in enzyme replacement therapy. *American journal of human genetics.* 2005;77(6):1061-74.

233. Brown MS, Sobhani MK, Brunschede GY, and Goldstein JL. Restoration of a regulatory response to low density lipoprotein in acid lipase-deficient human fibroblasts. *The Journal of biological chemistry.* 1976;251(11):3277-86.

234. Zhang H, Shi J, Hachet MA, Xue C, Bauer RC, Jiang H, Li W, Tohyama J, Millar J, Billheimer J, et al. CRISPR/Cas9-Mediated Gene Editing in Human iPSC-Derived

Macrophage Reveals Lysosomal Acid Lipase Function in Human Macrophages-Brief Report. *Arteriosclerosis, thrombosis, and vascular biology.* 2017;37(11):2156-60.

235. Chung BH, Wilkinson T, Geer JC, and Segrest JP. Preparative and quantitative isolation of plasma lipoproteins: rapid, single discontinuous density gradient ultracentrifugation in a vertical rotor. *Journal of lipid research.* 1980;21(3):284-91.

236. Sattler W, and Stocker R. Greater selective uptake by Hep G2 cells of high-density lipoprotein cholesteryl ester hydroperoxides than of unoxidized cholesteryl esters. *Biochem J.* 1993;294 (Pt 3)(771-8.

237. Basu SK, Goldstein JL, Anderson GW, and Brown MS. Degradation of cationized low density lipoprotein and regulation of cholesterol metabolism in homozygous familial hypercholesterolemia fibroblasts. *Proc Natl Acad Sci U S A.* 1976;73(9):3178-82.

238. Boadu E, Bilbey NJ, and Francis GA. Cellular cholesterol substrate pools for adenosine-triphosphate cassette transporter A1-dependent high-density lipoprotein formation. *Current opinion in lipidology.* 2008;19(3):270-6.

239. Castoreno AB, Wang Y, Stockinger W, Jarzylo LA, Du H, Pagnon JC, Shieh EC, and Nohturfft A. Transcriptional regulation of phagocytosis-induced membrane biogenesis by sterol regulatory element binding proteins. *Proc Natl Acad Sci U S A.* 2005;102(37):13129-34.

240. Folch J, Lees M, and Sloane Stanley GH. A simple method for the isolation and purification of total lipides from animal tissues. *The Journal of biological chemistry.* 1957;226(1):497-509.

241. von Trotha KT, Heun R, Schmitz S, Lutjohann D, Maier W, and Kolsch H. Influence of lysosomal acid lipase polymorphisms on chromosome 10 on the risk of Alzheimer's disease and cholesterol metabolism. *Neuroscience letters.* 2006;402(3):262-6.

242. Francis GA, Oram JF, Heinecke JW, and Bierman EL. Oxidative tyrosylation of HDL enhances the depletion of cellular cholesteryl esters by a mechanism independent of passive sterol desorption. *Biochemistry.* 1996;35(48):15188-97.

243. Burkard I, Rentsch KM, and von Eckardstein A. Determination of 24S- and 27-hydroxycholesterol in plasma by high-performance liquid chromatography-mass spectrometry. *Journal of lipid research.* 2004;45(4):776-81.

244. Choi HY, Karten B, Chan T, Vance JE, Greer WL, Heidenreich RA, Garver WS, and Francis GA. Impaired ABCA1-dependent lipid efflux and hypoalphalipoproteinemia in human Niemann-Pick type C disease. *The Journal of biological chemistry.* 2003;278(32569-77.

245. Lowry OH, Rosebrough NJ, Farr AL, and Randall RJ. Protein measurement with the Folin phenol reagent. *The Journal of biological chemistry.* 1951;193(1):265-75.

246. Wang WQ, Merriam DL, Moses AS, and Francis GA. Enhanced cholesterol efflux by tyrosyl radical-oxidized high density lipoprotein is mediated by apolipoprotein AI-AII heterodimers. *The Journal of biological chemistry.* 1998;273(28):17391-8.

247. Hara A, and Radin NS. Lipid extraction of tissues with a low-toxicity solvent. *Analytical biochemistry.* 1978;90(1):420-6.

248. Zhu X, Lee JY, Timmins JM, Brown JM, Boudyguina E, Mulya A, Gebre AK, Willingham MC, Hiltbold EM, Mishra N, et al. Increased cellular free cholesterol in macrophage-specific Abca1 knock-out mice enhances pro-inflammatory response of macrophages. *The Journal of biological chemistry.* 2008;283(34):22930-41.

249. Cortner JA, Coates PM, Swoboda E, and Schnatz JD. Genetic variation of lysosomal acid lipase. *Pediatric research.* 1976;10(11):927-32.

250. Schlager S, Vujic N, Korbelius M, Duta-Mare M, Dorow J, Leopold C, Rainer S, Wegscheider M, Reicher H, Ceglarek U, et al. Lysosomal lipid hydrolysis provides substrates for lipid mediator synthesis in murine macrophages. *Oncotarget.* 2017;8(25):40037-51.

251. Zhang WY, Gaynor PM, and Kruth HS. Apolipoprotein E produced by human monocyte-derived macrophages mediates cholesterol efflux that occurs in the absence of added cholesterol acceptors. *The Journal of biological chemistry.* 1996;271(45):28641-6.

252. Smith JD, Miyata M, Ginsberg M, Grigaux C, Shmookler E, and Plump AS. Cyclic AMP induces apolipoprotein E binding activity and promotes cholesterol efflux from a macrophage cell line to apolipoprotein acceptors. *The Journal of biological chemistry.* 1996;271(48):30647-55.

253. Huang ZH, Fitzgerald ML, and Mazzone T. Distinct cellular loci for the ABCA1-dependent and ABCA1-independent lipid efflux mediated by endogenous apolipoprotein E expression. *Arteriosclerosis, thrombosis, and vascular biology.* 2006;26(1):157-62.

254. Bjorkhem I, Andersson O, Diczfalusy U, Sevastik B, Xiu RJ, Duan C, and Lund E. Atherosclerosis and sterol 27-hydroxylase: evidence for a role of this enzyme in elimination of cholesterol from human macrophages. *Proc Natl Acad Sci U S A.* 1994;91(18):8592-6.

255. Fu X, Menke JG, Chen Y, Zhou G, MacNaul KL, Wright SD, Sparrow CP, and Lund EG. 27-hydroxycholesterol is an endogenous ligand for liver X receptor in cholesterol-loaded cells. *The Journal of biological chemistry.* 2001;276(42):38378-87.

256. Bowden KL, Dubland JA, Chan T, Xu YH, Grabowski GA, Du H, and Francis GA. LAL (Lysosomal Acid Lipase) Promotes Reverse Cholesterol Transport In Vitro and In Vivo. *Arteriosclerosis, thrombosis, and vascular biology.* 2018;38(5):1191-201.

257. Repa JJ, Berge KE, Pomajzl C, Richardson JA, Hobbs H, and Mangelsdorf DJ. Regulation of ATP-binding cassette sterol transporters ABCG5 and ABCG8 by the liver X receptors alpha and beta. *The Journal of biological chemistry.* 2002;277(21):18793-800.

258. Yu L, Hammer RE, Li-Hawkins J, Von Bergmann K, Lutjohann D, Cohen JC, and Hobbs HH. Disruption of Abcg5 and Abcg8 in mice reveals their crucial role in biliary cholesterol secretion. *Proceedings of the National Academy of Sciences of the United States of America.* 2002;99(25):16237-42.

259. Stary HC, Chandler AB, Glagov S, Guyton JR, Insull W, Jr., Rosenfeld ME, Schaffer SA, Schwartz CJ, Wagner WD, and Wissler RW. A definition of initial, fatty streak, and intermediate lesions of atherosclerosis. A report from the Committee on Vascular Lesions of the Council on Arteriosclerosis, American Heart Association. *Circulation.* 1994;89(5):2462-78.

260. Dubland JA, and Francis GA. So Much Cholesterol: the unrecognized importance of smooth muscle cells in atherosclerotic foam cell formation. *Current opinion in lipidology.* 2016;27(2):155-61.

261. Basu SK, Brown MS, Ho YK, Havel RJ, and Goldstein JL. Mouse macrophages synthesize and secrete a protein resembling apolipoprotein E. *Proceedings of the National Academy of Sciences of the United States of America.* 1981;78(12):7545-9.

262. Lucic D, Huang ZH, Gu de S, Altenburg MK, Maeda N, and Mazzone T. Regulation of macrophage apoE secretion and sterol efflux by the LDL receptor. *Journal of lipid research.* 2007;48(2):366-72.

263. Pannu PS, Allahverdian S, and Francis GA. Oxysterol generation and liver X receptor-dependent reverse cholesterol transport: not all roads lead to Rome. *Molecular and cellular endocrinology.* 2013;368(1-2):99-107.

264. Venkateswaran A, Laffitte BA, Joseph SB, Mak PA, Wilpitz DC, Edwards PA, and Tontonoz P. Control of cellular cholesterol efflux by the nuclear oxysterol receptor LXR alpha. *Proceedings of the National Academy of Sciences of the United States of America.* 2000;97(22):12097-102.

265. Boadu E, Nelson RC, and Francis GA. ABCA1-dependent mobilization of lysosomal cholesterol requires functional Niemann-Pick C2 but not Niemann-Pick C1 protein. *Biochimica et biophysica acta.* 2012;1821(3):396-404.

266. Langer C, Huang Y, Cullen P, Wiesenhutter B, Mahley RW, Assmann G, and von Eckardstein A. Endogenous apolipoprotein E modulates cholesterol efflux and cholesteryl ester hydrolysis mediated by high-density lipoprotein-3 and lipid-free apolipoproteins in mouse peritoneal macrophages. *Journal of molecular medicine.* 2000;78(4):217-27.

267. Jerome WG, Cash C, Webber R, Horton R, and Yancey PG. Lysosomal lipid accumulation from oxidized low density lipoprotein is correlated with hypertrophy of the Golgi apparatus and trans-Golgi network. *Journal of lipid research.* 1998;39(7):1362-71.

268. Khoo JC, Miller E, McLoughlin P, and Steinberg D. Enhanced macrophage uptake of low density lipoprotein after self-aggregation. *Arteriosclerosis.* 1988;8(4):348-58.

269. Pena OM, Afacan N, Pistolic J, Chen C, Madera L, Falsafi R, Fjell CD, and Hancock RE. Synthetic cationic peptide IDR-1018 modulates human macrophage differentiation. *PloS one.* 2013;8(1):e52449.

270. Manley S, Ni HM, Kong B, Apte U, Guo G, and Ding WX. Suppression of autophagic flux by bile acids in hepatocytes. *Toxicological sciences : an official journal of the Society of Toxicology.* 2014;137(2):478-90.

271. Sakr SW, Eddy RJ, Barth H, Wang F, Greenberg S, Maxfield FR, and Tabas I. The uptake and degradation of matrix-bound lipoproteins by macrophages require an intact actin Cytoskeleton, Rho family GTPases, and myosin ATPase activity. *The Journal of biological chemistry.* 2001;276(40):37649-58.

272. Llorente-Cortes V, Martinez-Gonzalez J, and Badimon L. LDL receptor-related protein mediates uptake of aggregated LDL in human vascular smooth muscle cells. *Arteriosclerosis, thrombosis, and vascular biology.* 2000;20(6):1572-9.

273. Yoshimori T, Yamamoto A, Moriyama Y, Futai M, and Tashiro Y. Bafilomycin A1, a specific inhibitor of vacuolar-type H(+)-ATPase, inhibits acidification and protein degradation in lysosomes of cultured cells. *The Journal of biological chemistry.* 1991;266(26):17707-12.

274. Campbell JH, Reardon MF, Campbell GR, and Nestel PJ. Metabolism of atherogenic lipoproteins by smooth muscle cells of different phenotype in culture. *Arteriosclerosis.* 1985;5(4):318-28.

275. Sakashita N, Chang CC, Lei X, Fujiwara Y, Takeya M, and Chang TY. Cholesterol loading in macrophages stimulates formation of ER-derived vesicles with elevated ACAT1 activity. *Journal of lipid research.* 2010;51(6):1263-72.

276. Vaya J, Aviram M, Mahmood S, Hayek T, Grenadir E, Hoffman A, and Milo S. Selective distribution of oxysterols in atherosclerotic lesions and human plasma lipoproteins. *Free radical research.* 2001;34(5):485-97.

277. Garcia-Cruset S, Carpenter KL, Guardiola F, Stein BK, and Mitchinson MJ. Oxysterol profiles of normal human arteries, fatty streaks and advanced lesions. *Free radical research.* 2001;35(1):31-41.

278. Hulten LM, Lindmark H, Diczfalusy U, Bjorkhem I, Ottosson M, Liu Y, Bondjers G, and Wiklund O. Oxysterols present in atherosclerotic tissue decrease the expression of

lipoprotein lipase messenger RNA in human monocyte-derived macrophages. *The Journal of clinical investigation.* 1996;97(2):461-8.

279. Crisby M, Nilsson J, Kostulas V, Bjorkhem I, and Diczfalusy U. Localization of sterol 27-hydroxylase immuno-reactivity in human atherosclerotic plaques. *Biochimica et biophysica acta.* 1997;1344(3):278-85.

280. Shanahan CM, Carpenter KL, and Cary NR. A potential role for sterol 27-hydroxylase in atherogenesis. *Atherosclerosis.* 2001;154(2):269-76.

281. Chang TY, Chang CC, and Cheng D. Acyl-coenzyme A:cholesterol acyltransferase. *Annual review of biochemistry.* 1997;66(613-38.

282. Hermiston ML, Xu Z, and Weiss A. CD45: a critical regulator of signaling thresholds in immune cells. *Annual review of immunology.* 2003;21(107-37.

283. Frid MG, Li M, Gnanasekharan M, Burke DL, Fragoso M, Strassheim D, Sylman JL, and Stenmark KR. Sustained hypoxia leads to the emergence of cells with enhanced growth, migratory, and promitogenic potentials within the distal pulmonary artery wall. *American journal of physiology Lung cellular and molecular physiology.* 2009;297(6):L1059-72.

284. Yu J, Li Y, Li M, Qu Z, and Ruan Q. Oxidized low density lipoprotein-induced transdifferentiation of bone marrow-derived smooth muscle-like cells into foam-like cells in vitro. *International journal of experimental pathology.* 2010;91(1):24-33.

285. Chang L, Noseda M, Higginson M, Ly M, Patenaude A, Fuller M, Kyle AH, Minchinton AI, Puri MC, Dumont DJ, et al. Differentiation of vascular smooth muscle cells from local precursors during embryonic and adult arteriogenesis requires Notch signaling. *Proceedings of the National Academy of Sciences of the United States of America.* 2012;109(18):6993-8.

286. Paez-Cortez J, Krishnan R, Arno A, Aven L, Ram-Mohan S, Patel KR, Lu J, King OD, Ai X, and Fine A. A new approach for the study of lung smooth muscle phenotypes and its application in a murine model of allergic airway inflammation. *PloS one.* 2013;8(9):e74469.

287. Horton JD, Shah NA, Warrington JA, Anderson NN, Park SW, Brown MS, and Goldstein JL. Combined analysis of oligonucleotide microarray data from transgenic and knockout mice identifies direct SREBP target genes. *Proceedings of the National Academy of Sciences of the United States of America.* 2003;100(21):12027-32.

288. Daimiel LA, Fernandez-Suarez ME, Rodriguez-Acebes S, Crespo L, Lasuncion MA, Gomez-Coronado D, and Martinez-Botas J. Promoter analysis of the DHCR24 (3beta-hydroxysterol Delta(24)-reductase) gene: characterization of SREBP (sterol-regulatory-element-binding protein)-mediated activation. *Bioscience reports.* 2012;33(1):57-69.

289. Horton JD, Goldstein JL, and Brown MS. SREBPs: activators of the complete program of cholesterol and fatty acid synthesis in the liver. *The Journal of clinical investigation.* 2002;109(9):1125-31.

290. Gan X, Kaplan R, Menke JG, MacNaul K, Chen Y, Sparrow CP, Zhou G, Wright SD, and Cai TQ. Dual mechanisms of ABCA1 regulation by geranylgeranyl pyrophosphate. *The Journal of biological chemistry.* 2001;276(52):48702-8.

291. Forman BM, Ruan B, Chen J, Schroepfer GJ, Jr., and Evans RM. The orphan nuclear receptor LXRalpha is positively and negatively regulated by distinct products of mevalonate metabolism. *Proceedings of the National Academy of Sciences of the United States of America.* 1997;94(20):10588-93.

292. Whitney KD, Watson MA, Goodwin B, Galardi CM, Maglich JM, Wilson JG, Willson TM, Collins JL, and Kliewer SA. Liver X receptor (LXR) regulation of the LXRalpha gene in human macrophages. *The Journal of biological chemistry.* 2001;276(47):43509-15.

293. Quinn CM, Jessup W, Wong J, Kritharides L, and Brown AJ. Expression and regulation of sterol 27-hydroxylase (CYP27A1) in human macrophages: a role for RXR and PPARgamma ligands. *The Biochemical journal.* 2005;385(Pt 3):823-30.

294. Szanto A, Benko S, Szatmari I, Balint BL, Furtos I, Ruhl R, Molnar S, Csiba L, Garuti R, Calandra S, et al. Transcriptional regulation of human CYP27 integrates retinoid, peroxisome proliferator-activated receptor, and liver X receptor signaling in macrophages. *Molecular and cellular biology.* 2004;24(18):8154-66.

295. Bobryshev YV, Ivanova EA, Chistiakov DA, Nikiforov NG, and Orekhov AN. Macrophages and Their Role in Atherosclerosis: Pathophysiology and Transcriptome Analysis. *BioMed research international.* 2016;2016(9582430.

296. Minor LK, Mahlberg FH, Jerome WG, Lewis JC, Rothblat GH, and Glick JM. Lysosomal hydrolysis of lipids in a cell culture model of smooth muscle foam cells. *Experimental and molecular pathology.* 1991;54(2):159-71.

297. Jerome WG, Minor LK, Glick JM, Rothblat GH, and Lewis JC. Lysosomal lipid accumulation in vascular smooth muscle cells. *Experimental and molecular pathology.* 1991;54(2):144-58.

298. Mindell JA. Lysosomal acidification mechanisms. *Annual review of physiology.* 2012;74(69-86.

299. Forgac M. Vacuolar ATPases: rotary proton pumps in physiology and pathophysiology. *Nature reviews Molecular cell biology.* 2007;8(11):917-29.

300. De Duve C, Pressman BC, Gianetto R, Wattiaux R, and Appelmans F. Tissue fractionation studies. 6. Intracellular distribution patterns of enzymes in rat-liver tissue. *The Biochemical journal.* 1955;60(4):604-17.

301. de Reuck AVS, and Cameron MP. *Ciba Foundation Symposium on Lysosomes*. London: J.A. Churchill Ltd.; 1963.

302. Klionsky DJ. Autophagy revisited: a conversation with Christian de Duve. *Autophagy.* 2008;4(6):740-3.

303. De Duve C, and Wattiaux R. Functions of lysosomes. *Annual review of physiology.* 1966;28(435-92.

304. Botham KM, Moore EH, De Pascale C, and Bejta F. The induction of macrophage foam cell formation by chylomicron remnants. *Biochemical Society transactions.* 2007;35(Pt 3):454-8.

305. Kosaka S, Takahashi S, Masamura K, Kanehara H, Sakai J, Tohda G, Okada E, Oida K, Iwasaki T, Hattori H, et al. Evidence of macrophage foam cell formation by very low-density lipoprotein receptor: interferon-gamma inhibition of very low-density lipoprotein receptor expression and foam cell formation in macrophages. *Circulation.* 2001;103(8):1142-7.

306. Morris GE, Braund PS, Moore JS, Samani NJ, Codd V, and Webb TR. Coronary Artery Disease-Associated LIPA Coding Variant rs1051338 Reduces Lysosomal Acid Lipase Levels and Activity in Lysosomes. *Arteriosclerosis, thrombosis, and vascular biology.* 2017;37(6):1050-7.

307. Yan C, Lian X, Li Y, Dai Y, White A, Qin Y, Li H, Hume DA, and Du H. Macrophage-specific expression of human lysosomal acid lipase corrects inflammation and pathogenic phenotypes in lal-/- mice. *The American journal of pathology.* 2006;169(3):916-26.

308. Davies JD, Carpenter KL, Challis IR, Figg NL, McNair R, Proudfoot D, Weissberg PL, and Shanahan CM. Adipocytic differentiation and liver x receptor pathways regulate the accumulation of triacylglycerols in human vascular smooth muscle cells. *The Journal of biological chemistry.* 2005;280(5):3911-9.

309. Riendeau V, and Garenc C. Effect of 27-hydroxycholesterol on survival and death of human macrophages and vascular smooth muscle cells. *Free radical research.* 2009;43(10):1019-28.

310. Clarke MC, Figg N, Maguire JJ, Davenport AP, Goddard M, Littlewood TD, and Bennett MR. Apoptosis of vascular smooth muscle cells induces features of plaque vulnerability in atherosclerosis. *Nature medicine.* 2006;12(9):1075-80.

311. Tabas I. Apoptosis and plaque destabilization in atherosclerosis: the role of macrophage apoptosis induced by cholesterol. *Cell death and differentiation.* 2004;11 Suppl 1(S12-6).